University of Potsdam

Master Thesis

Introduction to the Glauber Dynamics for the Curie-Weiss Potts Model

by

Paul Tschisgale

Supervisor:	Alexander Zass
First Examiner:	Prof. Dr. Sylvie Roelly
Second Examiner:	Alexander Zass
Submission Date:	30.09.2020

Faculty of Science
Institute for Mathematics
Probability Theory

Published online on the
Publication Server of the University of Potsdam:
https://doi.org/10.25932/publishup-48676
https://nbn-resolving.org/urn:nbn:de:kobv:517-opus4-486769

Abstract

This thesis aims at presenting in an organized fashion the required basics to understand the Glauber dynamics as a way of simulating configurations according to the Gibbs distribution of the Curie-Weiss Potts model. Therefore, essential aspects of discrete-time Markov chains on a finite state space are examined, especially their convergence behavior and related mixing times. Furthermore, special emphasis is placed on a consistent and comprehensive presentation of the Curie-Weiss Potts model and its analysis. Finally, the Glauber dynamics is studied in general and applied afterwards in an exemplary way to the Curie-Weiss model as well as the Curie-Weiss Potts model. The associated considerations are supplemented with two computer simulations aiming to show the cutoff phenomenon and the temperature dependence of the convergence behavior.

Zusammenfassung

Die vorliegende Arbeit verfolgt das Ziel, die erforderlichen Grundlagen für das Verständnis der Glauber Dynamik auf organisierte Art und Weise darzustellen. Die Glauber Dynamik stellt eine Möglichkeit der Simulation von Konfigurationen der Gibbs Verteilung des Curie-Weiss Potts Modells dar. Es werden zunächst die zum Verständnis notwendigen Grundlagen von endlichen Markov-Ketten in diskreter Zeit beleuchtet, insbesondere ihr Konvergenzverhalten und die damit verbundene Mischzeit. Darüber hinaus legt diese Arbeit einen Schwerpunkt auf eine konsistente sowie verständliche Darbietung und Analyse des Curie-Weiss Potts Modells. Schließlich wird explizit die Glauber Dynamik betrachtet und anschließend exemplarisch auf das Curie-Weiss Modell und auf das Curie-Weiss Potts Modell angewandt. Die dazugehörigen Betrachtungen werden durch zwei Computersimulationen ergänzt, welche darauf abzielen, das Cutoff-Phänomen sowie die Temperaturabhängigkeit des Konvergenzverhaltens darzustellen bzw. zu verdeutlichen.

Contents

1 Introduction

The *Potts model* was introduced by Renfrey Potts in the context of statistical mechanics in 1952. It was meant as a generalization of the well-known Ising model for more than two possible spin values. Both the Potts and the Ising model aim to describe the interaction of magnetic moments of atoms in a lattice. These magnetic moments are referred to as spins and the lattice is decribed by a graph. In the case of the Ising model, there are $q = 2$ possible spin values, as opposed to the $q > 2$ potential spin values found in the Potts model. [Wu82]

In the context of statistical mechanics, for these systems of interacting particles there are only few exact solutions found, and these are often quite complicated. The same is true for the q-state Potts model. Therefore it is convenient to examine this model using the *mean-field approximation* which is used in various areas of physics. In other words, the q-state Potts model is approximated by a simpler model which, in physics contexts, is called *q-state Curie-Weiss Potts model*. [BH19]

To understand the model at hand, we study phenomena regarding arrangements of spins, so-called configurations. Since we consider systems at thermodynamic equilibrium, we use the *Gibbs distribution* to describe these configurations probabilistically. Unfortunately, the computation of the complete distribution is not easily done when the corresponding graphs become quite large. Therefore, we want to simulate this Gibbs distribution for the q-state Curie-Weiss Potts model using a special kind of Markov chain – the *Glauber dynamics*.

This thesis aims to provide a detailed introduction to the Glauber dynamics, especially for the Curie-Weiss Potts model. The reader should have prior knowledge of linear algebra, basic analysis and probability theory. Additionally helpful might be some basics of statistical physics, but they do not represent a necessary condition in order to understand this thesis.

Since the Glauber dynamics is a special kind of Markov chain, we adress *finite, discrete-time Markov chains* first. In the course of this, we primarily stick to the explanations of Levin et al. [LPW09]. We talk about and discuss the prop-

erties of *irreducibility*, *aperiodicity* and *reversibility* of such chains. After this, we define an appropriate distance between two probability measures using the *total variation distance* and prove, on this basis, the *Convergence Theorem* for finite, discrete-time Markov chains. Knowing that many Markov chains converge towards a *stationary distribution*, we want to measure the rate of convergence. In this context, we introduce the notion of *mixing time*. This quantity tells us when the *distance to stationarity* of a Markov chain falls below a certain threshold. We then use *Spectral Theory* to prove theorems that provide upper and lower bounds for the mixing time. At the end of this chapter, we introduce an interesting phenomenon regarding the rate of convergence – the *cutoff phenomenon* which describes a sharp drop in the distance to stationarity.

The following chapter gives an overview of many important and interesting aspects of the Curie-Weiss Potts model. We start with a description of the Potts model and introduce the mean-field approximation for the purpose of deriving the Curie-Weiss Potts model. Afterwards, we define the Gibbs distribution of this model and examine its *zero-temperature limit* as well as its *infinite-temperature limit*. We then introduce the *proportions vector* of a configuration. On this basis, we define the *energy density* and the *entropy density* of a configuration. The interplay of this two quantities is described by the *free energy function* which helps us understand *phase transition* for the model at hand. By introducing an *order parameter*, we are able to derive the exact critical temperature at which this phase transition occurs. We also examine two other interesting temperatures – the *first and the second spinodal temperature* – that will help us in the understanding of the Glauber dynamics for this model. Finally, we consider the model in the *thermodynamic limit* and state the results regarding the distribution of the proportions vector.

In the final chapter, we combine the results of chapters before to understand the Glauber dynamics for the Curie-Weiss Potts model. After giving an introduction to *Markov Chain Monte Carlo (MCMC)*, we define the Glauber dynamics in an appropriate mathematical way and prove selected properties. Afterwards, we apply our newly acquired knowledge of mixing times to the Glauber dynamics of the *Curie-Weiss model*, the mean-field version of the Ising model. Having done this, we examine the Glauber dynamics for the Curie-Weiss Potts model. Here we give

a summary of a mixing time analysis accomplished by Cuff et al. in [CDL12]. Finally, we present and discuss two simulations regarding the Glauber dynamics for our model of interest.

Although we concentrate on this aspect, the Potts model is not only used in statistical mechanics to model ferromagnets and other spin systems. Indeed, over the years, the Potts model has found its way into various areas, one famous example being computational biology. In this field, the so-called Cellular Potts model was first introduced by F. Graner and J. Glazier to simulate cell sorting in 1992 [GG92]. In 1996, N. J. Savill and P. Hogeweg adapted this model in order to model morphogenesis for simple cellular systems [SH96]. These days, the Cellular Potts model is also used to model cellular processes in tumor development [SM13]. Additionally, the Potts model is used in signal and image processing [Geo15], as well as in the analysis of the properties of complex networks [DGM04]. Further research regarding the Potts model is therefore essential, since it is acquiring more and more significance in various applications.

2 Markov Chains and Mixing Times

In this chapter we discuss the essential aspects concerning discrete-time Markov chains on a finite state space. Despite their simplicity, they are interesting mathematical objects that can be used to describe systems evolving in time. A main goal of this chapter is the proof of the Convergence Theorem which states that certain kinds of Markov chains converge to their stationary distributions. Based on this theorem, we will derive statements regarding the time a chain needs to reach equilibrium. This contemplation will finally lead us to the concept of mixing times. From this point onward, we will use arguments from linear algebra to arrive at conclusions about bounds on mixing times and the rate of convergence to stationarity. The following aspects are primarily orientated on the book "Markov Chains and Mixing Times" by Levin et al. [LPW09, chapter $1, 4, 12, 18$].

2.1 Basic Properties

We start by summarizing elementary characteristics of finite, discrete-time Markov chains. In the course of this we will see that the so-called transition matrix plays a key role in describing such processes.

2.1.1 Definitions

We focus on processes on a finite set Ω. Each element $\omega \in \Omega$ is called a *state* and Ω is called the *state space*. In the course of this thesis, we will be confronted with a certain class of real square matrices of $\mathbb{R}^{|\Omega|\times|\Omega|}$, the so-called *stochastic* matrices.

Definition 2.1. *Let P be an $|\Omega| \times |\Omega|$ matrix. We say that P is* stochastic *if every row of P is a probability distribution, i.e. all entries are non-negative and*

$$\sum_{\omega' \in \Omega} P(\omega, \omega') = 1 \qquad \text{for all } \omega \in \Omega.$$

Let us denote the set of all probability distributions on the measurable space $\big(\Omega, \mathscr{P}(\Omega)\big)$ by $\mathscr{M}_1(\Omega)$, whereby the σ-algebra $\mathscr{P}(\Omega)$ represents the power set on Ω. Thus, for each $\pi \in \mathscr{M}_1(\Omega)$, the triple $\big(\Omega, \mathscr{P}(\Omega), \pi\big)$ defines a probability space.

Lemma 2.2. *Let $\pi \in \mathscr{M}_1(\Omega)$ and $\Pi \in \mathbb{R}^{|\Omega|\times|\Omega|}$ be the matrix with identical rows π. For all $M, M' \in \mathbb{R}^{|\Omega|\times|\Omega|}$ the following holds:*

(i) If M is stochastic, then $M\Pi = \Pi$.

(ii) If $\pi M = \pi$, then $\Pi M = \Pi$.

(iii) If M and M' are stochastic, then MM' is stochastic.

Proof.

(i) $\Big(M\Pi\Big)(\omega,\omega') = \sum_{\zeta\in\Omega} M(\omega,\zeta)\Pi(\zeta,\omega') = \pi(\omega')\sum_{\zeta\in\Omega} M(\omega,\zeta) = \pi(\omega')\,.$

(ii) This is a consequence of the definition of matrix multiplication.

(iii) $$\sum_{\omega'\in\Omega}\Big(MM'\Big)(\omega,\omega') = \sum_{\omega'\in\Omega}\sum_{\zeta\in\Omega} M(\omega,\zeta)M'(\zeta,\omega') = \sum_{\zeta\in\Omega} M(\omega,\zeta)\sum_{\omega'\in\Omega} M'(\zeta,\omega')$$
$$= \sum_{\zeta\in\Omega} M(\omega,\zeta) = 1\,.$$

□

The best known class of processes that can be described by stochastic matrices are discrete-time Markov chains on a finite state space Ω. This kind of stochastic process moves among the elements of Ω such that the probability of the next state only depends on the current state. This leads to the following definition:

Definition 2.3. *A sequence of random variables $(X_t)_{t\geq 0}$ is called a* discrete-time Markov chain *with finite state space Ω if for all $\omega, \omega' \in \Omega$, all $t \geq 1$, and all events $E_{t-1} := \bigcap_{i=0}^{t-1}\{X_i = \omega^{(i)}\}$ that satisfy $\mathbb{P}(E_{t-1} \cap \{X_t = \omega\}) > 0$, we have*

$$\mathbb{P}(X_{t+1} = \omega' \mid E_{t-1} \cap \{X_t = \omega\}) = \mathbb{P}(X_{t+1} = \omega' \mid X_t = \omega)\,. \tag{2.1}$$

Equation (2.1) is often referred to as *Markov property*. Due to the fact that the probability of moving from ω to ω' does not depend on the past, i.e. on the sequence of states $\omega^{(0)}, ..., \omega^{(t-1)}$, an $|\Omega| \times |\Omega|$ matrix suffices to describe the transitions of the process. The entries are given by the probabilities of the new state $\omega' \in \Omega$ conditioned on the current state $\omega \in \Omega$.

Definition 2.4. *Let $(X_t)_{t\geq 0}$ be a discrete-time Markov chain with finite state space Ω. Then the matrix $P \in \mathbb{R}^{|\Omega|\times|\Omega|}$ with entries*

$$P(\omega, \omega') := \mathbb{P}(X_{t+1} = \omega' \mid X_t = \omega)$$

is called transition matrix *and its entries are called* transition probabilities.

Remark 2.5. Let $P \in \mathbb{R}^{|\Omega|\times|\Omega|}$ be a transition matrix.

1. Then the transition matrix P is obviously stochastic.
2. According to our definition of P, we are forced to consider probability distributions as row vectors. Therefore the ω-th row of P must be a distribution.
3. Hence, when at $\omega \in \Omega$, the distribution of the next state is given by $P(\omega, \cdot)$.

Now let the row vector $\mu_0 \in \mathscr{M}_1(\Omega)$ be the distribution of X_0 (in short form we write $X_0 \sim \mu_0$). Given this *initial distribution*, the distribution at time $t \geq 1$ can be obtained by simple matrix multiplication as can be seen from the proof of the following theorem.

Theorem 2.6. *Let $(X_t)_{t\geq 0}$ be a discrete-time Markov chain with finite state space Ω and transition matrix P. Let X_t be distributed according to μ_t (i.e. $X_t \sim \mu_t$) for all $t \geq 0$. Then*

$$\mu_t = \mu_0 P^t \quad \text{for } t \geq 1. \tag{2.2}$$

Proof. Let $t \geq 1$. Consider the distribution of the chain at time $t+1$. For all $\omega' \in \Omega$, using the law of total probability, we obtain

$$\begin{aligned}
\mu_{t+1}(\omega') &= \mathbb{P}(X_{t+1} = \omega') \\
&= \sum_{\omega\in\Omega} \mathbb{P}(X_t = \omega)\, \mathbb{P}(X_{t+1} = \omega' \mid X_t = \omega) \\
&= \sum_{\omega\in\Omega} \mu_t(\omega) P(\omega, \omega').
\end{aligned}$$

Using the definition of matrix multiplication, this is equivalent to $\mu_{t+1} = \mu_t P$ and inductively $\mu_t = \mu_0 P^t$.

□

Remark 2.7. Let $P \in \mathbb{R}^{|\Omega|\times|\Omega|}$ be a transition matrix.

1. Since P is an element of the matrix ring $\mathbb{R}^{|\Omega|\times|\Omega|}$, P to the power of zero is given by the identity matrix, i.e. $P^0 = \mathrm{I}_{|\Omega|}$. Hence (2.2) is also true for $t = 0$.

2. Corollary 2.2 (iii) implies that P^t is also stochastic, since P is stochastic.

To summarize, a discrete-time Markov chain is completely described by a finite state space Ω, a transition matrix P and an initial distribution μ_0 (or an initial state). For the sake of simplicity, when talking about discrete-time Markov chains with finite state space in the following chapters, we will often refer to them only as Markov chains

2.1.2 Irreducibility and Aperiodicity

In the following, we turn to some important properties that lots of Markov chains have, namely irreducibility and aperiodicity.

Definition 2.8. *A transition matrix P of a Markov chain is called* irreducible *if for all $\omega, \omega' \in \Omega$ there exists $t \in \mathbb{N}$ such that $P^t(\omega, \omega') > 0$.*

Intuitively, this definition means that it is possible to get from any state $\omega \in \Omega$ to any other state $\omega' \in \Omega$ in a finite amount of time steps. Equivalently, there exists a sequence of states $\omega = \omega^{(0)}, \omega^{(1)}, \ldots, \omega^{(t-1)}, \omega^{(t)} = \omega'$ in Ω such that the chain starts in ω and arrives in ω'. We call such a sequence of states a trajectory of the chain in the state space Ω. Instead of saying a Markov chain has an irreducible transition matrix, we will simply say that the Markov chain is irreducible.

Definition 2.9. *Define $\mathscr{T}(\omega) := \{t \in \mathbb{N} \mid P^t(\omega, \omega) > 0\}$ as the set of all times for which the Markov chain with transition matrix P can return to its starting state ω. Then the period of the state ω is given by* $\gcd \mathscr{T}(\omega)$.

Lemma 2.10. *If a Markov chain with transition matrix P is irreducible, then all states have the same period, i.e.* $\gcd \mathscr{T}(\omega) = \gcd \mathscr{T}(\omega')$ *for all $\omega, \omega' \in \Omega$.*

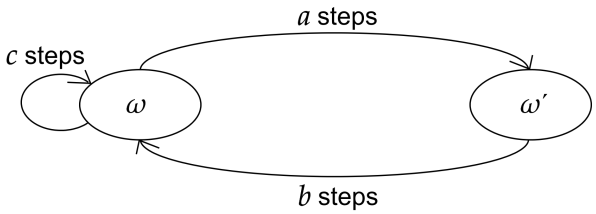

Fig. 1: Irreducibility implies that we can get from ω to ω' in a steps, from ω' to ω in b steps and from ω to itself in $c \in \mathscr{T}(\omega)$ steps.

Proof. Fixing $\omega, \omega' \in \Omega$, irreducibility implies that there exist $a, b \in \mathbb{N}$ such that $P^a(\omega, \omega') > 0$ and $P^b(\omega', \omega) > 0$ (see Figure 1). Define $m := a + b$, then we have $m \in \mathscr{T}(\omega) \cap \mathscr{T}(\omega')$. For $c \in \mathscr{T}(\omega)$, we have $c + m \in \mathscr{T}(\omega')$ and hence $c \in \{n - m \mid n \in \mathscr{T}(\omega')\}$. Since $m, n \in \mathscr{T}(\omega')$, we have $\gcd \mathscr{T}(\omega') \,|\, m$ and $\gcd \mathscr{T}(\omega') \,|\, n$. Therefore, we have $\gcd \mathscr{T}(\omega') \,|\, n - m$ and consequently $\gcd \mathscr{T}(\omega')$ divides all $c \in \mathscr{T}(\omega)$. Thus, we obtain $\gcd \mathscr{T}(\omega') \mid \gcd \mathscr{T}(\omega)$.
Switching the roles of ω and ω', we can deduce by an entire parallel argument that $\gcd \mathscr{T}(\omega) \mid \gcd \mathscr{T}(\omega')$ and therefore $\gcd \mathscr{T}(\omega) = \gcd \mathscr{T}(\omega')$ for all $\omega, \omega' \in \Omega$. □

Lemma 2.10 shows that an irreducible Markov chain has a period common to all of its states. Therefore, we can make the following definition:

Definition 2.11. *An irreducible Markov chain $(X_t)_{t \geq 0}$ with state space Ω is called* aperiodic *if $\gcd \mathscr{T}(\omega) = 1$ for all $\omega \in \Omega$. Otherwise, the chain will be called* periodic.

Lemma 2.12. *Let $(X_t)_{t \geq 0}$ be an irreducible Markov chain with transition matrix P that has at least one positive diagonal entry. Then the chain is also aperiodic.*

Proof. We assume that $P(\omega', \omega') > 0$ for one $\omega' \in \Omega$. Then we have $1 \in \mathscr{T}(\omega')$ and hence $\gcd \mathscr{T}(\omega') = 1$. Since the chain is also irreducible, all states $\omega \in \Omega$ share the same period according to Lemma 2.10. Therefore, we have $\gcd \mathscr{T}(\omega) = 1$ for all $\omega \in \Omega$ and hence the chain is aperiodic. □

In order to prove the Convergence Theorem later, we need a result regarding aperiodic Markov chains and the following number-theoretic lemma to prove it.

Lemma 2.13. *Let $M \subset \mathbb{N}$ with $\gcd M = m$. Then there exists $N_M \in \mathbb{N}$ such that for all $n \geq N_M$ we have*

$$nm = \sum_{\tilde{m} \in M} s_{\tilde{m}} \tilde{m}$$

with coefficients $\{s_{\tilde{m}}\}_{\tilde{m} \in \mathbb{N}} \subset \mathbb{N}$.

Proof. See for instance [LPW09, p. 20]. □

Remark 2.14. Let M be closed under addition with $\gcd M = 1$, then we obtain $n \in M$ for all $n \geq N_M$. Therefore, M must contain all but finitely many positive integers.

Proposition 2.15. *If a Markov chain $(X_t)_{t \geq 0}$ with transition matrix P is irreducible and aperiodic, then there exists $r \in \mathbb{N}$ such that $P^r(\omega, \omega') > 0$ for all $\omega, \omega' \in \Omega$.*

Proof. Let $a, b \in \mathscr{T}(\omega)$, then

$$P^{a+b}(\omega, \omega) = \sum_{\omega' \in \Omega} P^a(\omega, \omega') P^b(\omega', \omega) \geq P^a(\omega, \omega) P^b(\omega, \omega) > 0\,,$$

hence $a + b \in \mathscr{T}(\omega)$ which means that the set $\mathscr{T}(\omega)$ is closed under addition. Since P is aperiodic, we have $\gcd \mathscr{T}(\omega) = 1$ for all $\omega \in \Omega$. Now Remark 2.14 implies there exists $T(\omega) \in \mathscr{T}(\omega)$ such that $t \in \mathscr{T}(\omega)$ for all $t \geq T(\omega)$. Since P is also irreducible, there exists $\tau = \tau(\omega, \omega') \in \mathbb{N}$ such that $P^\tau(\omega, \omega') > 0$. Thus, for $t \geq T(\omega) + \tau(\omega, \omega')$, we have

$$P^t(\omega, \omega') = \sum_{\zeta \in \Omega} P^{t-\tau}(\omega, \zeta) P^\tau(\zeta, \omega') \geq P^{t-\tau}(\omega, \omega) P^\tau(\omega, \omega') > 0\,.$$

Finally, if we choose $t \geq \bar{t} := \max_{\omega \in \Omega} T(\omega) + \max_{\omega, \omega' \in \Omega} \tau(\omega, \omega')$, we have $P^t(\omega, \omega') > 0$ for all $\omega, \omega' \in \Omega$. □

Proposition 2.15 implies that for two arbitrary states $\omega, \omega' \in \Omega$, it is always possible to get from ω to ω' in a finite number of time steps if the chain is irreducible and aperiodic.

2.1.3 Stationary Distributions

In this section we introduce special distributions of Markov chains. We will see that these so-called *stationary distributions* have interesting and useful properties.

Definition 2.16. *Let $(X_t)_{t\geq 0}$ be a Markov chain with state space Ω and transition matrix P. Then $\pi \in \mathscr{M}_1(\Omega)$ is called* stationary distribution *for P if*

$$\pi = \pi P\,. \tag{2.3}$$

Let us consider a Markov chain with stationary distribution π. If we start the chain in π, i.e. we choose initial distribution $\mu_0 = \pi$, then we have $\mu_t = \pi P^t = \pi$ for all $t \geq 0$. This is the reason why we call π stationary.

Corollary 2.17. *The condition for stationarity* (2.3) *is obviously equivalent to*

$$\pi(\omega') = \sum_{\omega\in\Omega} \pi(\omega)P(\omega,\omega') \quad \textit{for all} \quad \omega' \in \Omega\,.$$

Proposition 2.18. *Let $(X_t)_{t\geq 0}$ be an irreducible Markov chain with state space Ω and transition matrix P. Then there exists a unique stationary distribution $\pi \in \mathscr{M}_1(\Omega)$ for P.*

Proof. Proofs for the existence and the uniqueness of the stationary distribution are given in [LPW09, p. 12 f., p. 14]. □

Lemma 2.19. *The stationary distribution $\pi \in \mathscr{M}_1(\Omega)$ of an irreducible Markov chain $(X_t)_{t\geq 0}$ with transition matrix P is strictly positive.*

Proof. Let $\omega' \in \Omega$ be an arbitrary state. Since π is a probability distribution, there must exist a state $\omega \in \Omega$ with $\pi(\omega) > 0$. Irreducibility also implies that there exists a time $t \geq 0$ such that $P^t(\omega,\omega') > 0$. Since π is stationary for P, we have $\pi = \pi P^t$. Therefore, for all $\omega' \in \Omega$, we have

$$\pi(\omega') = \sum_{\zeta\in\Omega} \pi(\zeta)P^t(\zeta,\omega') \geq \pi(\omega)P^t(\omega,\omega') > 0\,,$$

since $\pi(\omega) > 0$ and $P^t(\omega,\omega') > 0$. Hence $\pi(\omega') > 0$ for all $\omega' \in \Omega$. □

Proposition 2.20. *Let $(X_t)_{t\geq 0}$ be an irreducible Markov chain with state space Ω and transition matrix P. If $\pi \in \mathscr{M}_1(\Omega)$ satisfies the* detailed balance equations

$$\pi(\omega)P(\omega,\omega') = \pi(\omega')P(\omega',\omega) \quad \textit{for all} \quad \omega,\omega' \in \Omega\,, \tag{2.4}$$

then π is stationary for P.

Proof. By taking the sum over all $\omega' \in \Omega$ on both sides of (2.4), we obtain

$$\sum_{\omega'\in\Omega} \pi(\omega')P(\omega',\omega) = \sum_{\omega'\in\Omega} \pi(\omega)P(\omega,\omega') = \pi(\omega) \sum_{\omega'\in\Omega} P(\omega,\omega') = \pi(\omega)\,,$$

where we used the fact that P is stochastic. According to Corollary 2.17, this is equivalent to $\pi P = \pi$ and hence π is stationary for P. □

The detailed balance equations represent an easy way to show that a given distribution is stationary. We will take use of it in the upcoming chapters. At last, we introduce another term that is often used in the context of stationary distributions, the so-called *reversibility* of a Markov chain.

Definition 2.21. *A Markov chain $(X_t)_{t\geq 0}$ with state space Ω and transition matrix P that satisfies the detailed balance equations is called* reversible *with respect to $\pi \in \mathscr{M}_1(\Omega)$.*

2.2 Distance to Stationarity

In this section we discuss the long-term behavior of Markov chains. We will see that an irreducible and aperiodic Markov chain converges to its unique stationary distribution. In this case, we intend to quantify the speed of convergence and therefore need to measure the distance between the chain at a certain time and its stationary distribution.

2.2.1 Total Variation Distance

In order to measure the distance between two probability measures, we first need to define an appropriate metric. Therefore, we make the following definition:

Definition 2.22. *Let $\mu, \nu \in \mathscr{M}_1(\Omega)$. Then the* total variation distance *between μ and ν is defined by*

$$\|\mu - \nu\|_{\mathrm{TV}} := \max_{A \subset \Omega} |\mu(A) - \nu(A)| .$$

Remark 2.23. Since μ and ν are two probability distributions, the definition implies that $\|\mu - \nu\|_{\mathrm{TV}} \in [0, 1]$.

We see that the total variation distance is obtained by looking at the maximum over all $2^{|\Omega|}$ subsets of our state space Ω. If Ω contains many elements, then this definition is not always the best way to compute this distance. We will now prove another characterization of the total variation distance, where we only have to take a sum over all elements in Ω.

Proposition 2.24. *Let $\mu, \nu \in \mathscr{M}_1(\Omega)$. Then the total variation distance between μ and ν is given by*

$$\|\mu - \nu\|_{\mathrm{TV}} = \frac{1}{2} \sum_{\omega \in \Omega} |\mu(\omega) - \nu(\omega)| . \tag{2.5}$$

Proof. Let $A \subset \Omega$ and $B := \{\omega \in \Omega \mid \mu(\omega) \geq \nu(\omega)\}$. Then we have

$$\begin{aligned} \mu(A) - \nu(A) &= \mu(A \cap B) - \nu(A \cap B) + \mu(A \cap B^C) - \nu(A \cap B^C) \\ &< \mu(A \cap B) - \nu(A \cap B) \\ &\leq \mu(A \cap B) - \nu(A \cap B) + \mu(A^C \cap B) - \nu(A^C \cap B) \\ &= \mu(B) - \nu(B)\,. \end{aligned} \tag{2.6}$$

The first inequality holds because $\mu(\omega') - \nu(\omega') < 0$ for any $\omega' \in A \cap B^C \subset B^C$ and the second inequality is true because $\mu(\omega) - \nu(\omega) \geq 0$ for all $\omega \in A^C \cap B \subset B$. Analogously, we have

$$\begin{aligned} \nu(A) - \mu(A) &\leq \nu(B^C) - \mu(B^C) \\ &= 1 - \nu(B) - \Big(1 - \mu(B)\Big) \\ &= \mu(B) - \nu(B)\,. \end{aligned} \tag{2.7}$$

Combining (2.6) and (2.7), we get $|\mu(A) - \nu(A)| \leq \mu(B) - \nu(B)$. By taking $A = B$, the left-hand side equals the upper bound on the right-hand side. Therefore, we obtain

$$\begin{aligned} \max_{A \subset \Omega} |\mu(A) - \nu(A)| &= \mu(B) - \nu(B) \\ &= \frac{1}{2}\Big[\mu(B) - \nu(B) + \nu(B^C) - \mu(B^C)\Big] \\ &= \frac{1}{2}\Big(\sum_{\omega \in B}\Big(\mu(\omega) - \nu(\omega)\Big) + \sum_{\omega' \in B^C}\Big(\nu(\omega') - \mu(\omega')\Big)\Big) \\ &= \frac{1}{2}\sum_{\omega \in \Omega} |\mu(\omega) - \nu(\omega)|\,. \end{aligned}$$

□

We mentioned that we want to define an appropriate metric. Hence, we prove that the total variation distance satisfies the properties of a metric, namely identity of indiscernibles, symmetry and the triangle inequality.

Proposition 2.25. *The total variation distance defines a metric on* $\mathscr{M}_1(\Omega)$.

Proof. Let $\mu, \nu, \eta \in \mathscr{M}_1(\Omega)$.

(i) *Identity of indiscernibles* holds because

$$\begin{aligned} \|\mu - \nu\|_{\mathrm{TV}} = 0 \quad &\Leftrightarrow \quad \frac{1}{2}\sum_{\omega\in\Omega} |\mu(\omega) - \nu(\omega)| = 0 \\ &\Leftrightarrow \quad |\mu(\omega) - \nu(\omega)| = 0 \quad \text{for all } \omega \in \Omega \\ &\Leftrightarrow \quad \mu(\omega) = \nu(\omega) \quad \text{for all } \omega \in \Omega \\ &\Leftrightarrow \quad \mu = \nu\,. \end{aligned}$$

(ii) *Symmetry* is obviously true. We have

$$\|\mu - \nu\|_{\mathrm{TV}} = \frac{1}{2}\sum_{\omega\in\Omega} |\mu(\omega) - \nu(\omega)| = \frac{1}{2}\sum_{\omega\in\Omega} |\nu(\omega) - \mu(\omega)| = \|\nu - \mu\|_{\mathrm{TV}}\,.$$

(iii) Using the triangle inequality for real numbers, we easily see that the total variation distance satisfies the *triangle inequality*,

$$\begin{aligned} \|\mu - \nu\|_{\mathrm{TV}} &= \frac{1}{2}\sum_{\omega\in\Omega} |\mu(\omega) - \nu(\omega)| \\ &\le \frac{1}{2}\sum_{\omega\in\Omega} \Big(|\mu(\omega) - \eta(\omega)| + |\eta(\omega) - \nu(\omega)|\Big) \\ &= \frac{1}{2}\sum_{\omega\in\Omega} |\mu(\omega) - \eta(\omega)| + \frac{1}{2}\sum_{\omega\in\Omega} |\eta(\omega) - \nu(\omega)| \\ &= \|\mu - \eta\|_{\mathrm{TV}} + \|\eta - \nu\|_{\mathrm{TV}}\,. \end{aligned}$$

□

2.2.2 Convergence Theorem

Knowing the total variation distance is an appropriate metric to measure the distance between two probability measures, we want to define the distance between a Markov chain $(X_t)_{t\geq 0}$ at time $t \geq 0$ and its stationary distribution π. Having this done, we will prove the Convergence Theorem for irreducible and aperiodic Markov chains.

The aforementioned distance obviously depends on the initial distribution $\mu_0 \in \mathscr{M}_1(\Omega)$. Since we normally speak of an initial state $\omega_0 \in \Omega$ instead of an initial distribution, we use the Kronecker delta notation and set $\mu_0 = \delta_{\omega_0}$ defined by

$$\delta_\omega(\omega') := \delta(\omega, \omega') = \begin{cases} 1 & \text{if } \omega' = \omega, \\ 0 & \text{if } \omega' \neq \omega, \end{cases} \tag{2.8}$$

for $\omega, \omega' \in \Omega$. In this case, the initial distribution is completely concentrated at a single state $\omega_0 \in \Omega$. Hence, we obtain the distribution of the chain $(X_t)_{t\geq 0}$ with transition matrix P at time $t \geq 1$ by $\delta_{\omega_0} P^t = P^t(\omega_0, \cdot)$. Therefore, we can define the distance to stationary in the following way:

Definition 2.26. *Let $(X_t)_{t\geq 0}$ be a Markov chain with transition matrix P and stationary distribution $\pi \in \mathscr{M}_1(\Omega)$. Then the distance to stationarity at time $t \geq 1$ is given by*

$$d(t) := \max_{\omega \in \Omega} \left\| P^t(\omega, \cdot) - \pi \right\|_{\mathrm{TV}}. \tag{2.9}$$

Remark 2.27. In the more general case, the *distance to stationarity* is given by

$$d(t) = \sup_{\mu \in \mathscr{M}_1(\Omega)} \left\| \mu P^t - \pi \right\|_{\mathrm{TV}}.$$

A proof can be found, for example, in [LPW09, p. 329 f.].

Finally, we give a formulation and a proof of the *Convergence Theorem* for Markov chains. We will see that irreducibility and aperiodicity are indeed needed to prove this theorem.

Theorem 2.28. *Let $(X_t)_{t\geq 0}$ be an irreducible and aperiodic Markov chain with transition matrix P and stationary distribution $\pi \in \mathscr{M}_1(\Omega)$. Then there exist constants $A > 0$ and $\gamma \in (0,1)$ such that the distance to stationarity is bounded by*

$$d(t) \leq A\gamma^t \,.$$

Proof. Since P is irreducible and aperiodic, Proposition 2.15 tells us there exists an $r \in \mathbb{N}$ such that $P^r(\omega,\omega') > 0$ for all $\omega,\omega' \in \Omega$. Let $\Pi \in \mathbb{R}^{|\Omega|\times|\Omega|}$ be the matrix with identical rows π. Define

$$\tilde{\delta} := \min_{\omega,\omega'\in\Omega} \frac{P^r(\omega,\omega')}{\pi(\omega')} \,,$$

then $P^r(\omega,\omega') \geq \tilde{\delta}\pi(\omega')$ for all $\omega,\omega' \in \Omega$. For any $a \in (0,1)$, this inequality also holds for $\delta := \min(\tilde{\delta}, a) \in (0,1)$. Let $\varphi := 1-\delta \in (0,1)$, then define

$$Q := \varphi^{-1}P^r + (1-\varphi^{-1}\Pi) \,.$$

Obviously, Q is stochastic because P^t and Π are stochastic. Rewriting this equation, we obtain

$$P^r = (1-\varphi)\Pi + \varphi Q \,.$$

We will now prove by induction over $k \in \mathbb{N}_0$ that

$$P^{rk} = (1-\varphi^k)\Pi + \varphi^k Q^k \tag{2.10}$$

holds. The case $k = 0$ is trivial. Now assume (2.10) is true for $k = n$ (induction hypothesis), then we have

$$\begin{aligned}
P^{r(n+1)} &= P^{rn}P^r \\
&= \Big((1-\varphi^n)\Pi + \varphi^n Q^n\Big)P^r \\
&= (1-\varphi^n)\Pi P^r + \varphi^n Q^n\Big((1-\varphi)\Pi + \varphi Q\Big) \\
&= (1-\varphi^n)\underbrace{\Pi P^r}_{=\Pi} + \varphi^n(1-\varphi)\underbrace{Q^n\Pi}_{=\Pi} + \varphi^{n+1}Q^{n+1} \\
&= (1-\varphi^{n+1})\Pi + \varphi^{n+1}Q^{n+1} \,.
\end{aligned}$$

Therefore, equation (2.10) holds for $k = n+1$ under the assumption that it holds for $k = n$ and hence it is true for all $k \in \mathbb{N}_0$.
Next we multiply (2.10) by P^j ($j \in \mathbb{N}_0$) which yields

$$P^{rk+j} = (1-\varphi^k)\underbrace{\Pi P^j}_{=\Pi} + \varphi^k Q^k P^j = \Pi + \varphi^k\Big(Q^k P^j - \Pi\Big)\,,$$

or equivalently $P^{rk+j} - \Pi = \varphi^k(Q^k P^j - \Pi)$. Fixing $\omega \in \Omega$ and examining the ω-th row on both sides of this equation, we have

$$P^{rk+j}(\omega,\cdot) - \pi = \varphi^k\Big(Q^k P^j(\omega,\cdot) - \pi\Big)\,.$$

Thus, using the total variation distance, we obtain

$$\begin{aligned}\Big\|P^{rk+j}(\omega,\cdot) - \pi\Big\|_{\mathrm{TV}} &= \Big\|\varphi^k\Big(Q^k P^j(\omega,\cdot) - \pi\Big)\Big\|_{\mathrm{TV}} \\ &= \varphi^k\Big\|Q^k P^j(\omega,\cdot) - \pi\Big\|_{\mathrm{TV}} \\ &\le \varphi^k\,.\end{aligned}$$

We used the fact that $Q^k P^j(\omega,\cdot)$ is a probability distribution according to Corollary 2.2 (iii) and hence the total variation distance is bounded by 1. Now we define $\gamma := \sqrt[r]{\varphi} \in (0,1)$ and $A := \gamma^{-r} > 0$. Representing $t \ge 0$ using Euclidean division yields $t = rk + j$ for $0 \le j < r$. Then we have

$$\Big\|P^t(\omega,\cdot) - \pi\Big\|_{\mathrm{TV}} = \Big\|P^{rk+j}(\omega,\cdot) - \pi\Big\|_{\mathrm{TV}} \le \varphi^k = \gamma^{rk} \le \gamma^{rk}\gamma^{j-r} = \gamma^{-r}\gamma^{rk+j} = A\gamma^t$$

which holds for any $\omega \in \Omega$. Therefore, for all $t \ge 0$, we finally obtain

$$\max_{\omega\in\Omega}\Big\|P^t(\omega,\cdot) - \pi\Big\|_{\mathrm{TV}} \le A\gamma^t\,.$$

□

Remark 2.29. Since $\gamma \in (0,1)$, we have $d(t) \to 0$ as $t \to \infty$. Therefore, every irreducible and aperiodic Markov chain converges to its unique stationary distribution π which is also called *equilibrium distribution*.

2.2.3 Properties of the Distance

We proved that the distance to stationarity goes to 0 as the time t goes to infinity. In this section, we will prove and mention some properties regarding the distance to stationarity which might be helpful in the course of the next sections.

Proposition 2.30. *The distance to stationarity $d(t)$ is monotonically decreasing in t, i.e. $d(t+1) \leq d(t)$ for all $t \geq 1$.*

Proof. Using Proposition 2.5 and the triangle inequality, we can write

$$\begin{aligned}
d(t+1) &= \max_{\omega\in\Omega} \frac{1}{2} \sum_{\omega'\in\Omega} \left| P^{t+1}(\omega,\omega') - \pi(\omega') \right| \\
&= \max_{\omega\in\Omega} \frac{1}{2} \sum_{\omega'\in\Omega} \left| \sum_{\zeta\in\Omega} P^t(\omega,\zeta)P(\zeta,\omega') - \sum_{\zeta\in\Omega} \pi(\zeta)P(\zeta,\omega') \right| \\
&= \max_{\omega\in\Omega} \frac{1}{2} \sum_{\omega'\in\Omega} \left| \sum_{\zeta\in\Omega} \Big(P^t(\omega,\zeta) - \pi(\zeta) \Big) P(\zeta,\omega') \right| \\
&\leq \max_{\omega\in\Omega} \frac{1}{2} \sum_{\omega'\in\Omega} \sum_{\zeta\in\Omega} \left| P^t(\omega,\zeta) - \pi(\zeta) \right| P(\zeta,\omega') \\
&= \max_{\omega\in\Omega} \frac{1}{2} \sum_{\zeta\in\Omega} \left| P^t(\omega,\zeta) - \pi(\zeta) \right| \sum_{\omega'\in\Omega} P(\zeta,\omega') \\
&= d(t)\,.
\end{aligned}$$

□

In other situations, it will be convenient to define another distance, i.e.

$$\bar{d}(t) := \max_{\omega,\omega'\in\Omega} \left\| P^t(\omega,\cdot) - P^t(\omega',\cdot) \right\|_{\mathrm{TV}}\,. \tag{2.11}$$

Proposition 2.31. *Let $(X_t)_{t\geq 0}$ be an irreducible and aperiodic Markov chain with transition matrix P and stationary distribution $\pi \in \mathscr{M}_1(\Omega)$. Let d and $\bar{d}$ be the distances defined in (2.9) and (2.11). Then the following identities hold:*

(i) $d(t) \leq \bar{d}(t) \leq 2d(t)$ *for all* $t \in \mathbb{N}$,

(ii) $\bar{d}(s+t) \leq \bar{d}(s)\bar{d}(t)$ *for all* $s,t \in \mathbb{N}$,

(iii) $d(ct) \leq \bar{d}(ct) \leq \bar{d}(t)^c$ *for all* $c,t \in \mathbb{N}$.

Proof. See for instance [LPW09, p. 53 ff]. □

2.2.4 Mixing Times

In order to say something about the speed of convergence, we introduce the concept of mixing times. The mixing time is a parameter that measures the time a Markov chain needs for its distance to stationarity to be small (at most ε) in the worst case. This leads us to make the following definition:

Definition 2.32. *Let $\varepsilon \in (0,1)$. Then the* ε-mixing time *equals the number of time steps until the distance to stationarity d is at most ε, i.e.*

$$t_{\text{mix}}(\varepsilon) := \min\{t \in \mathbb{N} \mid d(t) \leq \varepsilon\}\,.$$

By convention, we additionally set

$$t_{\text{mix}} := t_{\text{mix}}(\tfrac{1}{4})\,.$$

Lemma 2.33. *Let $l \in \mathbb{N}$ and $\varepsilon \in (0,1)$, then*

$$d\Big(l\, t_{\text{mix}}(\varepsilon)\Big) \leq (2\varepsilon)^l \tag{2.12}$$

and in particular

$$t_{\text{mix}}(\varepsilon) \leq \Big\lceil \log_2(\varepsilon^{-1})\Big\rceil t_{\text{mix}}\,. \tag{2.13}$$

Proof. Proposition 2.31 and the definition of the mixing time allow us to write

$$d\Big(l\, t_{\text{mix}}(\varepsilon)\Big) \leq \bar{d}\Big(l\, t_{\text{mix}}(\varepsilon)\Big) \leq \bar{d}\Big(t_{\text{mix}}(\varepsilon)\Big)^l \leq \Big(2d(t_{\text{mix}}(\varepsilon))\Big)^l \leq (2\varepsilon)^l.$$

Taking $\varepsilon = 1/4$, we obtain $d(l\, t_{\text{mix}}) \leq 2^{-l}$. Now let $\tilde{\varepsilon} := 2^{-l}$, then $d(l\, t_{\text{mix}}) \leq \tilde{\varepsilon}$. Since $t_{\text{mix}}(\tilde{\varepsilon}) = \min\{t \in \mathbb{N} \mid d(t) \leq \tilde{\varepsilon}\}$, we achieve the inequality $t_{\text{mix}}(\tilde{\varepsilon}) \leq l\, t_{\text{mix}}$. Rewriting $\tilde{\varepsilon} = 2^{-l}$, we get $l = \log_2(\varepsilon^{-1})$. Since we are interested in an upper bound for $t_{\text{mix}}(\tilde{\varepsilon}) \in \mathbb{N}$, we set $\tilde{l} := \Big\lceil \log_2(\tilde{\varepsilon}^{-1})\Big\rceil \in \mathbb{N}$ which also satisfies our inequality and hence completes the proof. □

Remark 2.34. The choice of $\varepsilon = 1/4$ in the definition of t_{mix} may seem arbitrary, but choosing $\varepsilon < 1/2$ is essential in order to make inequality (2.12) non-trivial and achieve the upper bound in (2.13).

2.3 Spectral Theory

In this section, we focus on the eigenvalues and eigenvectors of transition matrices of Markov chains. On the one hand we will see that the speed of convergence depends primarily on the biggest eigenvalues. On the other hand, we will be able to achieve a lower and an upper bound for the ε-mixing time of an irreducible and reversible Markov chain.

2.3.1 Eigenvalues of the transition Matrix

Since we consider the elements of $\mathbb{R}^\Omega$ as functions from Ω to $\mathbb{R}$, we will sometimes use the term eigenfunctions when talking about eigenvectors of the transition matrix P. Firstly, we want to prove some basic facts considering eigenvalues of transition matrices.

Lemma 2.35. *Let $(X_t)_{t\geq 0}$ be a Markov chain with transition matrix P.*
(i) If $\lambda \in \mathbb{R}$ is an eigenvalue of the stochastic matrix P, then $|\lambda| \leq 1$.
(ii) The matrix P has the eigenvalue 1 corresponding to the eigenvector $(1, \dots, 1)^T$.

Proof. (i) Let $\|f\|_\infty := \max_{\omega\in\Omega} |f(\omega)|$ be the maximum norm. We first show that $\|Pf\|_\infty \leq \|f\|_\infty$. We have

$$\begin{aligned}
\|Pf\|_\infty &= \max_{\omega\in\Omega} \Big| \sum_{\omega'\in\Omega} P(\omega,\omega') f(\omega') \Big| \\
&\leq \max_{\omega\in\Omega} \Big(\sum_{\omega'\in\Omega} |P(\omega,\omega')|\, |f(\omega')| \Big) \\
&\leq \max_{\omega\in\Omega} \Big(\max_{\omega'\in\Omega} |f(\omega')| \sum_{\omega'\in\Omega} P(\omega,\omega') \Big) \\
&= \max_{\omega'\in\Omega} |f(\omega')| \\
&= \|f\|_\infty ,
\end{aligned}$$

where we used the triangle inequality for real numbers and the fact that P is stochastic. Now let φ be an eigenfunction with the corresponding eigenvalue λ, i.e. $P\varphi = \lambda\varphi$. Then we obtain

$$\|P\varphi\|_\infty = \|\lambda\varphi\|_\infty = |\lambda|\, \|\varphi\|_\infty \leq \|\varphi\|_\infty$$

and hence $|\lambda| \leq 1$.

(ii) Since P is stochastic, we have $P \cdot (1, \dots, 1)^T = (1, \dots, 1)^T$ which proves the statement. □

Let $\langle \cdot, \cdot \rangle$ be the inner product on $\mathbb{R}^\Omega$ defined by $\langle f, g \rangle := \sum_{\omega \in \Omega} f(\omega) g(\omega)$. Additionally, we define another inner product on $\mathbb{R}^\Omega$ in the following way:

Definition 2.36. *For $\pi \in \mathbb{R}^\Omega$, the inner product $\langle \cdot, \cdot \rangle_\pi : \mathbb{R}^\Omega \times \mathbb{R}^\Omega \to \mathbb{R}$ is defined by*

$$\langle f, g \rangle_\pi := \sum_{\omega \in \Omega} f(\omega) g(\omega) \pi(\omega) \qquad \text{for } f, g \in \mathbb{R}^\Omega.$$

Lemma 2.37. *Let $(X_t)_{t \geq 0}$ be an irreducible Markov chain with transition matrix P and stationary distribution $\pi \in \mathscr{M}_1(\Omega)$.*

(i) The pre-Hilbert space $(\mathbb{R}^\Omega, \langle \cdot, \cdot \rangle_\pi)$ has an orthonormal basis of real-valued eigenfunctions $\{\varphi_i\}_{i=1}^{|\Omega|}$ corresponding to real eigenvalues $\{\lambda_i\}_{i=1}^{|\Omega|}$.

(ii) For $t \geq 1$, the matrix P^t can be decomposed as

$$\frac{P^t(\omega, \omega')}{\pi(\omega')} = \sum_{i=1}^{|\Omega|} \varphi_i(\omega) \varphi_i(\omega') \lambda_i^t = 1 + \sum_{i=2}^{|\Omega|} \varphi_i(\omega) \varphi_i(\omega') \lambda_i^t \,. \tag{2.14}$$

Proof. (i) Since π is a stationary distribution of an irreducible Markov chain, we have $\pi(\omega) > 0$ for all $\omega \in \Omega$. Therefore, we can define the matrix $A \in \mathbb{R}^{|\Omega| \times |\Omega|}$ by $A(\omega, \omega') := \pi(\omega)^{\frac{1}{2}} \pi(\omega')^{-\frac{1}{2}} P(\omega, \omega')$. Using the reversibility of P with respect to π, we obtain

$$A(\omega, \omega') = \pi(\omega)^{\frac{1}{2}} \pi(\omega')^{\frac{1}{2}} \pi(\omega) P(\omega, \omega') = \pi(\omega')^{\frac{1}{2}} \pi(\omega)^{\frac{1}{2}} \pi(\omega') P(\omega', \omega) = A(\omega', \omega) \,.$$

Therefore, A is symmetric and hence there exists an orthonormal basis for the inner product space $(\mathbb{R}^\Omega, \langle \cdot, \cdot \rangle)$. This basis consists of eigenfunctions $\{\xi_i\}_{i=1}^{|\Omega|}$ with corresponding real eigenvalues $\{\lambda_i\}_{i=1}^{|\Omega|}$. Now we define the set of diagonal matrices $\{D_\pi^r\}_{r \in \mathbb{R}}$ by $D_\pi^r(\omega, \omega') := \delta_{\omega'}(\omega) \pi(\omega')^r$. Then, we can write $A = D_\pi^{1/2} P D_\pi^{-1/2}$

because

$$\begin{aligned}
A(\omega,\omega') &= \sum_{\zeta\in\Omega}\Big(D_\pi^{1/2}P\Big)(\omega,\zeta)D_\pi^{-1/2}(\zeta,\omega') \\
&= \sum_{\zeta\in\Omega}\Big(D_\pi^{1/2}P\Big)(\omega,\zeta)\,\delta_{\omega'}(\zeta)\pi(\omega')^{-\frac{1}{2}} \\
&= \Big(D_\pi^{1/2}P\Big)(\omega,\omega')\pi(\omega')^{-\frac{1}{2}} \\
&= \sum_{\tilde\zeta\in\Omega} D_\pi^{1/2}(\omega,\tilde\zeta)P(\tilde\zeta,\omega')\pi(\omega')^{-\frac{1}{2}} \\
&= \sum_{\tilde\zeta\in\Omega} \delta_{\tilde\zeta}(\omega)\pi(\tilde\zeta)^{\frac{1}{2}}P(\tilde\zeta,\omega')\pi(\omega')^{-\frac{1}{2}} \\
&= \pi(\omega)^{\frac{1}{2}}P(\omega,\omega')\pi(\omega')^{-\frac{1}{2}}.
\end{aligned}$$

Let $\varphi_i := D_\pi^{-1/2}\xi_i$ for $i \in \{1,\dots,|\Omega|\}$, then we have

$$P\varphi_i = PD_\pi^{-1/2}\xi_i = D_\pi^{-1/2}\Big(D_\pi^{1/2}PD_\pi^{-1/2}\Big)\xi_i = D_\pi^{-1/2}A\xi_i = D_\pi^{-1/2}\lambda_i\xi_i = \lambda_i\varphi_i\,.$$

Therefore, φ_i is a real-valued eigenfunction of P with corresponding eigenvalue λ_i for all $i \in \{1,\dots,|\Omega|\}$. Now we want to show the orthonormality of the set $\{\varphi_i\}_{i=1}^{|\Omega|}$. Since $\{\xi_i\}_{i=1}^{|\Omega|}$ is orthonormal with respect to the inner product $\langle\cdot,\cdot\rangle$, we can write

$$\delta_i(j) = \langle\xi_i,\xi_j\rangle = \langle D_\pi^{1/2}\varphi_i, D_\pi^{1/2}\varphi_j\rangle = \langle D_\pi^1\,\varphi_i,\varphi_j\rangle = \sum_{\omega\in\Omega}(D_\pi^1\,\varphi_i)(\omega)\,\varphi_j(\omega)\,.$$

Expanding the matrix multiplication yields

$$\begin{aligned}
\delta_i(j) &= \sum_{\omega\in\Omega}\Big(\sum_{\omega'\in\Omega}D_\pi^1(\omega,\omega')\varphi_i(\omega')\Big)\varphi_j(\omega) \\
&= \sum_{\omega\in\Omega}\Big(\sum_{\omega'\in\Omega}\delta_{\omega'}(\omega)\pi(\omega')\varphi_i(\omega')\Big)\varphi_j(\omega) \\
&= \sum_{\omega\in\Omega}\pi(\omega)\varphi_i(\omega)\varphi_j(\omega) \\
&= \langle\varphi_i,\varphi_j\rangle\,.
\end{aligned}$$

Hence, the set $\{\varphi_i\}_{i=1}^{|\Omega|}$ is an orthonormal basis of the pre-Hilbert space $(\mathbb{R}^\Omega,\langle\cdot,\cdot\rangle_\pi)$.

(ii) Firstly, we decompose the function $\delta_{\omega'}$ in the the basis $\{\varphi_i\}_{i=1}^{|\Omega|}$. Thus, we obtain

$$\begin{aligned}\delta_{\omega'} = \sum_{i=1}^{|\Omega|} \langle \delta_{\omega'}, \varphi_i \rangle_\pi \varphi_i &= \sum_{i=1}^{|\Omega|} \Big(\sum_{\omega \in \Omega} \delta_{\omega'}(\omega) \varphi_i(\omega) \pi(\omega) \Big) \varphi_i \\ &= \sum_{i=1}^{|\Omega|} \varphi_i(\omega') \pi(\omega') \varphi_i \,.\end{aligned} \tag{2.15}$$

Using this and the fact that $P^t \varphi_i = \lambda_i^t \varphi_i$, we get

$$\begin{aligned}P^t(\omega, \omega') &= (P^t \delta_{\omega'})(\omega) \\ &= \Big(P^t \sum_{i=1}^{|\Omega|} \varphi_i(\omega') \pi(\omega') \varphi_i \Big)(\omega) \\ &= \Big(\sum_{i=1}^{|\Omega|} \varphi_i(\omega') \pi(\omega') P^t \varphi_i \Big)(\omega) \\ &= \Big(\sum_{i=1}^{|\Omega|} \varphi_i(\omega') \pi(\omega') \lambda_i^t \varphi_i \Big)(\omega) \\ &= \sum_{i=1}^{|\Omega|} \varphi_i(\omega) \varphi_i(\omega') \lambda_i^t \pi(\omega') \,.\end{aligned}$$

Dividing by $\pi(\omega') \neq 0$, we obtain

$$\frac{P^t(\omega, \omega')}{\pi(\omega')} = \sum_{i=1}^{|\Omega|} \varphi_i(\omega) \varphi_i(\omega') \lambda_i^t \,,$$

and choosing $\varphi_1 = (1, \dots, 1)^T$ with corresponding eigenvalue $\lambda_1 = 1$, we finally get

$$\frac{P^t(\omega, \omega')}{\pi(\omega')} = 1 + \sum_{i=2}^{|\Omega|} \varphi_i(\omega) \varphi_i(\omega') \lambda_i^t \,.$$

□

2.3.2 Bounding Mixing Times via Spectral Gaps

The so-called spectral gap of a Markov chain has a direct impact on its convergence behavior and therefore on its mixing time. We are interested in bounding the ε-mixing time using this spectral gap. Firstly, we clarify what is meant by this term.

Definition 2.38. *Let $(X_t)_{t\geq 0}$ be a reversible Markov chain with transition matrix P. Define $\hat{\lambda} := \max\{|\lambda| \neq 1 \colon \lambda \text{ is an eigenvalue of } P\}$, then the* absolute spectral gap *is given by*

$$\hat{\gamma} := 1 - \hat{\lambda}.$$

We will often use another quantity that is directly related to the absolute spectral gap. This quantity is the so-called *relaxation time*.

Definition 2.39. *Let $(X_t)_{t\geq 0}$ be a reversible Markov chain with transition matrix P and absolute spectral gap $\hat{\gamma}$. Then the* relaxation time t_{rel} *of this chain is defined by*

$$t_{\text{rel}} := \frac{1}{\hat{\gamma}}.$$

Using the following inequalities, we can bound the mixing time of a Markov chain if we know the spectrum (the eigenvalues) of its transition matrix.

Theorem 2.40. *Let $(X_t)_{t\geq 0}$ be an irreducible and aperiodic Markov chain with transition matrix P and stationary distribution $\pi \in \mathscr{M}_1(\Omega)$. Fix $\varepsilon \in (0,1)$ and define $\pi_{\min} := \min_{x\in\Omega} \pi(x)$, then the following holds:*

$$\log\left(\frac{1}{2\varepsilon}\right)(t_{\text{rel}} - 1) \leq t_{\text{mix}}(\varepsilon) \leq \log\left(\frac{1}{2\varepsilon\pi_{\min}}\right)t_{\text{rel}}\,. \tag{2.16}$$

Proof. Firstly, we want to derive the lower bound of the mixing time. Therefore, let φ be an eigenfunction of P with corresponding eigenvalue $\lambda \neq 1$, i.e. $P\varphi = \lambda\varphi$. Recall that different eigenfunctions are orthogonal with respect to $\langle\cdot,\cdot\rangle_\pi$ and that $(1,\dots,1)^T$ is an eigenfunction to the corresponding eigenvalue $\lambda = 1$. Hence

$$\langle (1,\dots,1)^T, \varphi\rangle_\pi = \sum_{\omega'\in\Omega} \pi(\omega')\varphi(\omega') = 0$$

and therefore for all $\omega \in \Omega$, we can write

$$\begin{aligned}
|\lambda^t \varphi(\omega)| &= |(P^t\varphi)(\omega)| \\
&= \Big| \sum_{\omega' \in \Omega} P^t(\omega, \omega')\varphi(\omega') - \sum_{\omega' \in \Omega} \pi(\omega')\varphi(\omega') \Big| \\
&= \Big| \sum_{\omega' \in \Omega} \Big(P^t(\omega, \omega') - \pi(\omega')\Big)\varphi(\omega') \Big| \\
&\leq \sum_{\omega' \in \Omega} |P^t(\omega, \omega') - \pi(\omega')|\, |\varphi(\omega')| \\
&\leq 2 \max_{\omega \in \Omega} \Big\| P^t(\omega, \cdot) - \pi \Big\|_{\mathrm{TV}} \max_{\omega' \in \Omega} |\varphi(\omega')| \\
&= 2\, d(t)\, \|\varphi\|_\infty \,.
\end{aligned}$$

Choosing $\omega \in \operatorname*{argmax}_{\omega' \in \Omega} |\varphi(\omega')|$, we obtain $|\varphi(\omega)| = \|\varphi\|_\infty$ and therefore we have $|\lambda|^t \leq 2d(t)$. If we take $t = t_{\mathrm{mix}}(\varepsilon)$, we will get $|\lambda|^{t_{\mathrm{mix}}(\varepsilon)} \leq 2d(t_{\mathrm{mix}}(\varepsilon)) \leq 2\varepsilon$. Setting $|\lambda| = \hat{\lambda}$, we can write

$$\frac{1}{2\varepsilon} \leq \frac{1}{\hat{\lambda}^{t_{\mathrm{mix}}(\varepsilon)}} \quad \Leftrightarrow \quad \log\left(\frac{1}{2\varepsilon}\right) \leq \log\left(\frac{1}{\hat{\lambda}^{t_{\mathrm{mix}}(\varepsilon)}}\right) = t_{\mathrm{mix}}(\varepsilon) \log\left(\frac{1}{\hat{\lambda}}\right),$$

since the natural logarithm is monotonically increasing. Using the fact that $\log(x) \leq x - 1$ for all $x > 1$, we get

$$\log\left(\frac{1}{2\varepsilon}\right) \leq t_{\mathrm{mix}}(\varepsilon)\left(\frac{1}{\hat{\lambda}} - 1\right) = t_{\mathrm{mix}}(\varepsilon)\frac{1}{1/\hat{\gamma} - 1} = t_{\mathrm{mix}}(\varepsilon)\frac{1}{t_{\mathrm{rel}} - 1}\,,$$

and hence

$$\log\left(\frac{1}{2\varepsilon}\right)(t_{\mathrm{rel}} - 1) \leq t_{\mathrm{mix}}(\varepsilon)\,.$$

In order to derive the upper bound of the mixing time, we rewrite (2.14) using the Cauchy-Schwarz inequality, i.e.

$$\begin{aligned}
\left| \frac{P^t(\omega, \omega')}{\pi(\omega')} - 1 \right| &= \left| \sum_{i=2}^{|\Omega|} \varphi_i(\omega)\varphi(\omega')_i \lambda_i^t \right| \\
&\leq \hat{\lambda}^t \sum_{i=2}^{|\Omega|} |\varphi_i(\omega)|\, |\varphi_i(\omega')| \qquad (2.17) \\
&\leq \hat{\lambda}^t \Big(\sum_{i=2}^{|\Omega|} \varphi_i(\omega)^2 \Big)^{\frac{1}{2}} \Big(\sum_{j=2}^{|\Omega|} \varphi_j(\omega')^2 \Big)^{\frac{1}{2}}\,.
\end{aligned}$$

Using the decomposition (2.15) of δ_ω, we obtain

$$\begin{aligned}\pi(\omega) = \langle \delta_\omega, \delta_\omega \rangle_\pi &= \Big\langle \sum_{i=1}^{|\Omega|} \varphi_i(\omega)\pi(\omega)\varphi_i, \sum_{j=1}^{|\Omega|} \varphi_j(\omega)\pi(\omega)\varphi_j \Big\rangle_\pi \\ &= \pi(\omega)^2 \sum_{i=1}^{|\Omega|}\sum_{j=1}^{|\Omega|} \varphi_i(\omega)\varphi_j(\omega)\langle \varphi_i, \varphi_j \rangle_\pi \,.\end{aligned}$$

Since $\langle \varphi_i, \varphi_j \rangle = \delta_i(j)$ we have

$$\pi(\omega) = \pi(\omega)^2 \sum_{i=1}^{|\Omega|} \varphi_i(\omega)^2 \geq \pi(\omega)^2 \sum_{i=2}^{|\Omega|} \varphi_i(\omega)^2$$

and therefore

$$\sum_{i=2}^{|\Omega|} \varphi_i(\omega)^2 \leq \frac{1}{\pi(\omega)} \,. \tag{2.18}$$

Looking at the total variation distance and using (2.5), we see that

$$\begin{aligned}\Big\| P^t(\omega, \cdot) - \pi \Big\|_{\mathrm{TV}} &= \frac{1}{2} \sum_{\omega' \in \Omega} |P^t(\omega, \omega') - \pi(\omega')| \\ &= \frac{1}{2} \sum_{\omega' \in \Omega} \pi(\omega') \left| \frac{P^t(\omega, \omega')}{\pi(\omega')} - 1 \right| \\ &\leq \frac{1}{2} \max_{\omega' \in \Omega} \left| \frac{P^t(\omega, \omega')}{\pi(\omega')} - 1 \right|\end{aligned}$$

and hence, using (2.17) and (2.18), we obtain

$$d(t) \leq \frac{1}{2} \max_{\omega, \omega' \in \Omega} \left| \frac{P^t(\omega, \omega')}{\pi(\omega')} - 1 \right| \leq \frac{1}{2} \max_{\omega, \omega' \in \Omega} \frac{\hat{\lambda}^t}{\sqrt{\pi(\omega)\pi(\omega')}} \leq \frac{\hat{\lambda}^t}{2\pi_{\min}} = \frac{(1-\hat{\gamma})^t}{2\pi_{\min}} \,.$$

Since $(1-\hat{\gamma})^t \leq \exp(-\hat{\gamma}t)$ for all $t \geq 0$ and $\hat{\gamma} \in (0,1)$, we obtain

$$d(t) \leq \frac{\exp(-\hat{\gamma}t)}{2\pi_{\min}} \,.$$

Setting the upper bound equal to $\varepsilon \in (0,1)$, we get $d(t) \leq \varepsilon$, and hence

$$t_{\mathrm{mix}}(\varepsilon) \leq t \leq \log\Big(\frac{1}{2\varepsilon\pi_{\min}}\Big)\frac{1}{\hat{\gamma}} = \log\Big(\frac{1}{2\varepsilon\pi_{\min}}\Big) t_{\mathrm{rel}} \,.$$

□

2.3.3 Rate of Convergence

In Section 2.2.2, we proved the convergence theorem but we did not get a useful expression to quantify the speed of convergence. In this section, we aim to obtain an upper bound for the total variation distance using eigenvalues and eigenfunctions of the transition matrix. As a result, we will get another proof of the Convergence Theorem for Markov Chains including a quantitative statement on the rate of convergence.

We will use *Jensen's inequlity* which, in the context of probability theory, using the notion of the expectation of a random variable, is given in the following way:

Proposition 2.41. *Let $I \subset \mathbb{R}$ and let $X : \Omega \to I$ be a random variable with finite expectation, i.e. $\mathbb{E}[X] < \infty$. If $g : I \to \mathbb{R}$ is a convex function, then*

$$g\Big(\mathbb{E}[X]\Big) \leq \mathbb{E}\Big[g(X)\Big]\,. \tag{2.19}$$

Proof. See for instance [Kle13, p. 152]. □

Remark 2.42. If g is concave instead, then $-g$ is convex and hence the opposite inequality $g(\mathbb{E}[X]) \geq \mathbb{E}[g(X)]$ holds. In both cases, equality holds if and only if X constant.

Definition 2.43. *Let $f : \Omega \to \mathbb{R}$ be a random variable. For $\pi \in \mathscr{M}_1(\Omega)$ and $p \in \mathbb{N}$, the $\ell^p(\pi)$-norm on $\mathbb{R}^\Omega$ is given by*

$$\|f\|_p := \left(\sum_{\omega\in\Omega} |f(\omega)|^p \pi(\omega)\right)^{\frac{1}{p}}.$$

Remark 2.44. Using the expectation $\mathbb{E}_\pi[\,\cdot\,]$, we can rewrite the $\ell^p(\pi)$-norm as

$$\|f\|_p = \left(\mathbb{E}_\pi\Big[\,|f|^p\Big]\right)^{\frac{1}{p}}.$$

Lemma 2.45. *For any random variable $f : \Omega \to \mathbb{R}$, the function $p \mapsto \|f\|_p$ is non-decreasing for all $p \in \mathbb{N}$.*

Proof. For $p \in \mathbb{N}$, we have

$$\|f\|_p^{p+1} = \Big(\mathbb{E}_\pi\Big[\,|f|^p\Big]\Big)^{\frac{p+1}{p}}.$$

Let $z := \mathbb{E}_\pi\Big[\,|f|^p\Big] \geq 0$, and define $g(z) := z^{(p+1)/p}$. Calculating the second derivative, we obtain

$$\frac{\mathrm{d}^2}{\mathrm{d}z^2}\, g(z) = \frac{1}{p}\Big(1 + \frac{1}{p}\Big) z^{(1/p)-1} \geq 0\,,$$

because $z \geq 0$ and $p \geq 1$. Therefore g is convex and we can apply Jensen's inequality (2.19). Thus, we obtain

$$\Big(\mathbb{E}_\pi\Big[\,|f|^p\Big]\Big)^{\frac{p+1}{p}} \leq \mathbb{E}_\pi\Big[\,|f|^{p+1}\Big]$$

and after taking the $(p+1)$-th root, we altogether have

$$\|f\|_p = \Big(\mathbb{E}_\pi\Big[\,|f|^p\Big]\Big)^{\frac{1}{p}} \leq \Big(\mathbb{E}_\pi\Big[\,|f|^{p+1}\Big]\Big)^{\frac{1}{p+1}} = \|f\|_{p+1}$$

which finishes the proof. □

Theorem 2.46. *Let $(X_t)_{t\geq 0}$ be an irreducible Markov chain with transition matrix P and stationary distribution $\pi \in \mathscr{M}_1(\Omega)$. Let the eigenvalues of P be given by $1 = \lambda_1 > \lambda_2 \geq \ldots \geq \lambda_{|\Omega|} \geq -1$ with associated eigenfunctions $\{\varphi_i\}_{i=1}^{|\Omega|}$, orthonormal with respect to $\langle\cdot,\cdot\rangle_\pi$. Then the following holds:*

$$\Big\|P^t(\omega,\cdot) - \pi\Big\|_{\mathrm{TV}}^2 \leq \frac{1}{4}\sum_{i=2}^{|\Omega|} \varphi_i(\omega)^2 \lambda_i^{2t}\,.$$

Proof. According to Proposition 2.24, we can write

$$\begin{aligned}\left\|P^t(\omega,\cdot)-\pi\right\|_{\mathrm{TV}}^2 &= \frac{1}{4}\left(\sum_{\omega'\in\Omega}\left|\frac{P^t(\omega,\omega')}{\pi(\omega')}-1\right|\pi(\omega')\right)\\ &= \frac{1}{4}\left\|\frac{P^t(\omega,\cdot)}{\pi(\cdot)}-1\right\|_1^2\\ &\leq \frac{1}{4}\left\|\frac{P^t(\omega,\cdot)}{\pi(\cdot)}-1\right\|_2^2\end{aligned}$$

in which the inequality holds because of Lemma 2.45. Using (2.14), we obtain

$$\begin{aligned}\left\|P^t(\omega,\cdot)-\pi\right\|_{\mathrm{TV}}^2 &\leq \frac{1}{4}\left\|\sum_{i=2}^{|\Omega|}\lambda_i^t\varphi_i(\omega)\varphi_i\right\|_2^2\\ &= \frac{1}{4}\sum_{i=2}^{|\Omega|}\sum_{j=2}^{|\Omega|}\varphi_i(\omega)\varphi_j(\omega)\lambda_i^t\lambda_j^t\delta_i(j)\\ &= \frac{1}{4}\sum_{i=2}^{|\Omega|}\varphi_i(\omega)^2\lambda_j^{2t}\,.\end{aligned}$$

□

Corollary 2.47. *The distance to stationarity of a Markov chain $(X_t)_{t\geq 0}$ with transition matrix P is bounded by*

$$d(t)\leq C\hat{\lambda}^t\,,$$

with $C\in\mathbb{R}^+$ being a constant and $\hat{\lambda}:=\max\{|\lambda|\neq 1\colon \lambda \text{ is an eigenvalue of } P\}$.

Proof. Using (2.46), we have

$$\begin{aligned}d(t)=\max_{\omega\in\Omega}\left\|P^t(\omega,\cdot)-\pi\right\|_{\mathrm{TV}} &\leq \max_{\omega\in\Omega}\frac{1}{2}\left(\sum_{i=2}^{|\Omega|}\varphi_i(\omega)^2\lambda_i^{2t}\right)^{\frac{1}{2}}\\ &\leq \frac{1}{2}\max_{\omega\in\Omega}\left(\sum_{i=2}^{|\Omega|}\varphi_i(\omega)^2\right)^{\frac{1}{2}}\hat{\lambda}^t\\ &= C\hat{\lambda}^t\,,\end{aligned}$$

where we defined $C:=\frac{1}{2}\max_{\omega\in\Omega}\left(\sum_{i=2}^{|\Omega|}\varphi_i(\omega)^2\right)^{\frac{1}{2}}\in\mathbb{R}^+$. □

Remark 2.48. Since $\hat{\lambda} < 1$ and $d(t) \geq 0$ for all $t \geq 0$, we see that the distance to stationarity $d(t)$ converges to zero as the time t goes to infinity, i.e. $d(t) \to 0$ as $t \to \infty$.

We can also use Theorem 2.46 to derive a better upper bound for $t_{\text{mix}}(\varepsilon)$ than in Theorem 2.40. This bound is stated in the following Corollary:

Corollary 2.49. *Let $(X_t)_{t\geq 0}$ be an irreducible and aperiodic Markov chain with transition matrix P and stationary distribution $\pi \in \mathscr{M}_1(\Omega)$. Then the ε-mixing time is bounded by*

$$t_{\text{mix}}(\varepsilon) \leq \log\left(\frac{1}{2\varepsilon\sqrt{\pi_{\min}}}\right) t_{\text{rel}}\,,$$

with $\pi_{\min} := \min_{\omega\in\Omega} \pi(\omega)$.

Proof. According to Theorem 2.46, we obtain

$$\left\| P^t(\omega,\cdot) - \pi \right\|_{\text{TV}}^2 \leq \frac{1}{4}\sum_{i=2}^{|\Omega|} \varphi_i(\omega)^2 \lambda_i^{2t} \leq \frac{1}{4}\hat{\lambda}^{2t} \sum_{i=2}^{|\Omega|} \varphi_i(\omega) \leq \frac{1}{4}\frac{\hat{\lambda}^{2t}}{\pi(\omega)} \leq \frac{1}{4}\frac{\hat{\lambda}^{2t}}{\pi_{\min}}\,,$$

where we used the definition of $\hat{\lambda}$ and $\pi_{\min}$ as well as (2.18). Taking the square root and rewriting $\hat{\lambda} = 1 - \hat{\gamma}$ gives us

$$d(t) \leq \frac{\hat{\lambda}^t}{2\sqrt{\pi_{\min}}} = \frac{(1-\hat{\gamma})^t}{2\sqrt{\pi_{\min}}}. \tag{2.20}$$

If we now use the same arguments as in the last step of the proof of Theorem 2.40, we finally obtain

$$t_{\text{mix}}(\varepsilon) \leq \log\left(\frac{1}{2\varepsilon\sqrt{\pi_{\min}}}\right) t_{\text{rel}}\,.$$

□

2.3.4 Cutoff Phenomenon

In the following, we consider a sequence of irreducible Markov chains $(X_t)_{t\geq 0}^{(n)}$ with corresponding state spaces Ω_n labelled by $n \geq 1$. Each such chain is characterized by its transition matrix P_n and since the chains are always irreducible, there also exists a stationary distribution π_n for each chain. In the following, we denote such a sequence of chains by $(\Omega_n, P_n, \pi_n)_{n\geq 1}$.

Recalling Definitions 2.26 and 2.32, the distance to stationarity and the ε-mixing time of the n-th chain are given by

$$d_n(t) = \max_{\omega\in\Omega_n} \left\| P_n^t(\omega, \cdot) - \pi_n \right\|_{\mathrm{TV}}$$

and

$$t_{\mathrm{mix}}^{(n)}(\varepsilon) = \min\{t \in \mathbb{N} \mid d_n(t) \leq \varepsilon\}\,.$$

Moreover, we defined

$$t_{\mathrm{mix}}^{(n)} = t_{\mathrm{mix}}^{(n)}\left(\tfrac{1}{4}\right).$$

In 1986, D. Aldous and P. Diaconis investigated the question of how many times a deck of n cards must be shuffled until it is close to random. Therefore, they considered the top-in-at-random shuffle, i.e. removing the top card and inserting it back into the deck at a random position. Using the distance to stationarity in order to answer the given question, they found out that there exists a critical number of shuffles $k_n = n\log(n)$ with the following property: shortly before k_n, the distance to stationarity is close to 1 and shortly after k_n, it is close to 0. Hence they concluded that $n\log(n)$ shuffles are enough to mix up a deck consisting of n cards. The two authors denoted this sharp drop in the distance to stationarity as *cutoff phenomenon*. [AD86].

In the previous chapters about Markov chains, we were mostly interested in the limiting behavior of a chain. We proved that the distance to stationarity $d_n(t)$ for an irreducible and aperiodic Markov chain tends to 0 for $t \to \infty$, according to the Convergence Theorem 2.28. However, this description completely misses the cutoff phenomenon. A helpful tool for characterizing this phenomenon are instead mixing times, as we can see in the following definition:

Definition 2.50. *A sequence of irreducible Markov chains* $(\Omega_n, P_n, \pi_n)_{n\geq 1}$ *is said to exhibit the* cutoff phenomenon *if, for any* $\varepsilon \in (0, \frac{1}{2})$*, we have*

$$\lim_{n\to\infty} \frac{t_{\text{mix}}^{(n)}(\varepsilon)}{t_{\text{mix}}^{(n)}(1-\varepsilon)} = 1\,. \tag{2.21}$$

Remark 2.51. The above definition implies that $t_{\text{mix}}^{(n)}(\varepsilon)$ and $t_{\text{mix}}^{(n)}(1-\varepsilon)$ are asymptotically equivalent, i.e. we can write $t_{\text{mix}}^{(n)}(\varepsilon) \sim t_{\text{mix}}^{(n)}(1-\varepsilon)$. The expression (2.21) is also equivalent to

$$\lim_{n\to\infty} \frac{t_{\text{mix}}^{(n)}(\varepsilon) - t_{\text{mix}}^{(n)}(1-\varepsilon)}{t_{\text{mix}}^{(n)}(\varepsilon)} = 0\,.$$

This means that the difference of the mixing times $t_{\text{mix}}^{(n)}(\varepsilon)$ and $t_{\text{mix}}^{(n)}(1-\varepsilon)$ becomes arbitrary small compared to the mixing time $t_{\text{mix}}(\varepsilon)$ itself.

There is another equivalent description of the cutoff phenomenon which includes explicitly the distance to stationarity and only the (standard) mixing time $t_{\text{mix}}^{(n)}$:

Proposition 2.52. *A sequence of irreducible Markov chains* $(\Omega_n, P_n, \pi_n)_{n\geq 1}$ *exhibits the* cutoff phenomenon *if, for any* $\varepsilon \in (0, \frac{1}{2})$*, we have*

$$\lim_{n\to\infty} d_n\Big(ct_{\text{mix}}^{(n)}\Big) = \begin{cases} 1 & \text{if } c < 1\,, \\ 0 & \text{if } c > 1\,. \end{cases}$$

Proof. See for instance [LPW09, p. 347]. □

According to this proposition, it is clear that the cutoff phenomenon describes a sharp drop in the distance to stationarity from close to 1 to close to 0 (see Figure 2). This sharp drop occurs around the mixing time $t_{\text{mix}}^{(n)}$ in an interval of time that is of smaller order than $t_{\text{mix}}^{(n)}$ itself. We call this interval of time the *cutoff window* and make the following definition, following [BHP17]:

Definition 2.53. *A sequence* $(w_n)_{n\geq 1}$ *is called a* cutoff window *for the sequence of irreducible Markov chains* $(\Omega_n, P_n, \pi_n)_{n\geq 1}$ *if* $w_n \in o(t_{\text{mix}}^{(n)})$ *and for all* $\varepsilon \in (0, \frac{1}{2})$*, there exists a constant* $c_\varepsilon > 0$ *such that for all* $n \geq 1$*, we have*

$$t_{\text{mix}}^{(n)}(\varepsilon) - t_{\text{mix}}^{(n)}(1-\varepsilon) \leq c_\varepsilon w_n\,.$$

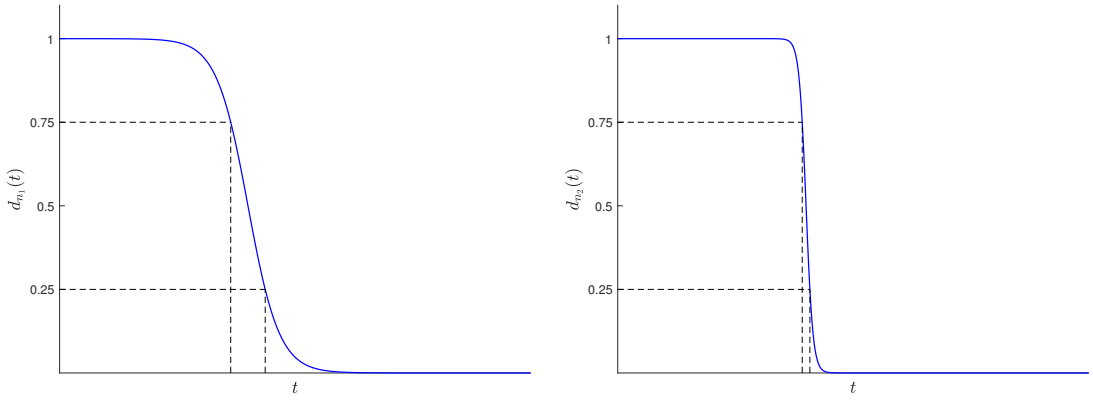

Fig. 2: For a sequence of Markov chains $(\Omega_n, P_n, \pi_n)_{n\geq 1}$ that exhibit the cutoff phenomenon, the distance to stationarity $d_n(t)$ plotted against the time t approaches a step function on a time-scale of $t_{\text{mix}}(\varepsilon)$ as $n \to \infty$. In the graphic, the distance $d_n(t)$ is shown for two Markov chains $(\Omega_{n_1}, P_{n_1}, \pi_{n_1})$ and $(\Omega_{n_2}, P_{n_2}, \pi_{n_2})$ with $n_1 < n_2$. The dotted lines represent the mixing times $t^{(n)}_{\text{mix}}(\varepsilon)$ and $t^{(n)}_{\text{mix}}(1-\varepsilon)$ for $\varepsilon = \frac{1}{4}$, $n \in \{n_1, n_2\}$.

Thus, the cutoff window describes the interval of time in which the distance to stationary drops from a value close to 1 to one near 0. Additionally, this interval of time is negligible compared to the mixing time of the chain.

The appearance of the cutoff phenomenon can be connected with some results from Spectral Theory in Chapter 2.3, in particular by considering the relaxation time of the n-th chain given by $t^{(n)}_{\text{rel}} = (1-\hat{\lambda}_n)^{-1}$ with $\hat{\lambda}_n$ being the eigenvalue with second largest absolute value, i.e. $\hat{\lambda}_n := \max\{|\lambda_n| \neq 1 \colon \lambda_n \text{ is an eigenvalue of } P_n\}$.

Proposition 2.54. *Consider a sequence of irreducible and aperiodic Markov chains $(\Omega_n, P_n, \pi_n)_{n\geq 1}$ with mixing times $t^{(n)}_{\text{mix}}$ and relaxation times $t^{(n)}_{\text{rel}}$. If*

$$\lim_{n\to\infty} \frac{t^{(n)}_{\text{mix}}}{t^{(n)}_{\text{rel}}} < \infty\,, \tag{2.22}$$

then the Markov chain does not exhibit the cutoff phenomenon.

Proof. Let $\varepsilon \in (0, \frac{1}{2})$. We recall the first bound from Theorem 2.40 and, for a fixed $n \in \mathbb{N}$, we have

$$\left(t^{(n)}_{\text{rel}} - 1\right) \log\left(\frac{1}{2\varepsilon}\right) \leq t^{(n)}_{\text{mix}}(\varepsilon)\,. \tag{2.23}$$

Using the fact that $\varepsilon \in (0, \frac{1}{2})$ and (2.23), we can write

$$\frac{t_{\text{mix}}^{(n)}(\varepsilon)}{t_{\text{mix}}^{(n)}(1-\varepsilon)} \geq \frac{t_{\text{mix}}^{(n)}(\varepsilon)}{t_{\text{mix}}^{(n)}} \geq \frac{t_{\text{rel}}^{(n)} - 1}{t_{\text{mix}}^{(n)}} \log\left(\frac{1}{2\varepsilon}\right).$$

According to the limit (2.22), there exists a constant $C > 0$ and an $N \in \mathbb{N}$ such that for all $n \geq N$, we have

$$\frac{t_{\text{rel}}^{(n)} - 1}{t_{\text{mix}}^{(n)}} \geq C\,.$$

Hence we obtain

$$\lim_{n\to\infty} \frac{t_{\text{mix}}^{(n)}(\varepsilon)}{t_{\text{mix}}^{(n)}(1-\varepsilon)} \geq C \log\left(\frac{1}{2\varepsilon}\right)$$

and letting $\varepsilon \to 0$, we have

$$\lim_{n\to\infty} \frac{t_{\text{mix}}^{(n)}(\varepsilon)}{t_{\text{mix}}^{(n)}(1-\varepsilon)} = \infty$$

which means that, by observing (2.22), there cannot be a cutoff. □

Remark 2.55. According to this proposition, the expression

$$\lim_{n\to\infty} \frac{t_{\text{mix}}^{(n)}}{t_{\text{rel}}^{(n)}} = \infty\,,$$

or equivalently $t_{\text{rel}}^{(n)} \in o(t_{\text{mix}}^{(n)})$, represents a necessary condition for the cutoff phenomenon.

Many families of Markov chains are known to exhibit the cutoff phenomenon but proving it is often an extremely challenging task [BHP17]. But why are we so interested in this phenomenon? Suppose we want to simulate a probability distribution using an MCMC-algorithm (see Section 4.1). Then the largest part of the running time of the simulation is given by the mixing time of the underlying Markov chain [Sin93]. Hence knowing that a family of Markov chains exhibits the cutoff phenomenon is quite useful: It means that in order to get a reasonably accurate result for the chain $(X_t)_{t\geq 0}^{(n)}$, we have to wait at least $t_{\text{mix}}^{(n)}$ time steps. Moreover, due to the cutoff phenomenon, we know that it is not efficient to run the chain any longer after $t_{\text{mix}}^{(n)}$ and thus we can stop the chain.

We might also ask what causes the cutoff phenomenon. One explanation makes use of Theorem 2.46, i.e. that for an irreducible Markov chain $(X_t)_{t\geq 0}^{(n)}$ on Ω_n with transition matrix P_n and stationary distribution π_n, we have

$$\left\| P_n^t(\omega, \cdot) - \pi_n \right\|_{\mathrm{TV}}^2 \leq \frac{1}{4} \sum_{i=2}^{|\Omega_n|} \varphi_{n,i}(\omega)^2 \lambda_{n,i}^{2t}\,, \tag{2.24}$$

where $\lambda_{n,i}$ are the eigenvalues of P_n with associated eigenfunctions $\varphi_{n,i}$ orthonormal with respect to $\langle \cdot, \cdot \rangle_{\pi_n}$. This upper bound is quite accurate and serves as a good approximation for the left side of (2.24). Now consider the eigenvalue with second largest absolute value, i.e. $\hat{\lambda}_n$ with its associated eigenfunction $\hat{\varphi}_n$. Then it appears that in many chains the term $\hat{\varphi}_n(\omega)^2 \hat{\lambda}_n^{2t}$ is the most important: Indeed, it dominates the other terms in the sum and it also determines the final behavior of the chain, i.e. the exponential decay for $t \to \infty$. A possible cause for the cutoff phenomenon is said to be a high algebraic multiplicity of the eigenvalue $\hat{\lambda}_n$ caused by a high symmetry of the underlying chain. But there are also examples where cutoff occurs eventhough the chain is less symmetric. So in order to understand the cutoff phenomenon of a sequence of chains and to prove it, one needs to have detailed knowledge about this sequence, that is knowing all its eigenvalues and eigenfunctions. As mentioned before, this is not an easy task and it is the reason why other methods (e.g. coupling) are also developed and used to prove this phenomenon. [Dia96]

3 Curie-Weiss Potts Model

This chapter aims to give a detailed overview of the most important aspects and results of the so-called Curie-Weiss Potts model. Topics discussed in this chapter are, for example, the general Potts model, Gibbs distributions, the free energy function and phase transitions.

3.1 Introduction to Spin Systems

Firstly, we define the classical Potts model and introduce the Hamiltonian which plays a fundamental role in the upcoming theory. Moving forward, we discuss the so-called mean-field approximation and use it to derive heuristically the Curie-Weiss Potts model later.

3.1.1 Planar and standard Potts Model

The original model was proposed by C. Domb to his research student R. B. Potts as the topic of his Ph. D. thesis. It was meant as a generalization of the Ising model for more than two possible spin values. Potts actually studied two such models in his thesis: the *planar Potts model*, as it was suggested by Domb, and the so-called *standard Potts model*. [Wu82]

Before describing these two models, we need to summarize the most important notions and concepts of spin systems. We denote the set of possible spin values (sometimes called *colors*) by $Q = \{1, \dots, q\}$ and hence speak of a *q-state Potts model*. First of all, this model of interacting spins is defined on a finite lattice where a spin is assigned to each site. For convenience, we identify each such lattice with a finite graph $G = (\Lambda, \mathscr{E})$, where Λ denotes the set of vertices (sites) and $\mathscr{E}$ represents the set of all edges $\{i, j\}$, where $i, j \in \Lambda$ are adjacent vertices. We define a configuration ω on Λ as an element of the state space $\Omega = Q^{\Lambda}$, so that a configuration $\omega \in \Omega$ is of the form $\omega = (\omega_i)_{i \in \Lambda}$. Now, the essential quantity concerning a configuration is its total energy which is given by the *Hamiltonian* $H : \Omega \to \mathbb{R}$. We will see that, for all $\omega \in \Omega$, the total energy $H(\omega)$ depends only on the interaction of adjacent spins and the temperature of the system. Therefore, we define the *inverse temperature* $\beta \in (0, \infty)$ which is, as its name suggests, inversely proportional to the absolute temperature.

The *planar Potts model* can be regarded as a true generalization of the Ising model. In the Ising case, in fact, we have two possible parallel spin values pointing in opposite directions, namely $+1$ and -1. We generalize this by taking q two-dimensional unit vectors that point in equally spaced directions. These spin vectors are clearly determined by their angle ϑ from a well-selected axis. For simplification, we set $Q = \{1, \dots, q\}$ and associate with each spin $\omega_i \in Q$ its angle $\vartheta(\omega_i) = \frac{2\pi}{q}\omega_i$. The interaction energy of adjacent spins is then proportional to their scalar product, and hence the Hamiltonian for the planar Potts model can be written as

$$H(\omega) := -J\beta \sum_{\{i,j\}\in\mathscr{E}} \cos\left(\frac{2\pi}{q}(\omega_i - \omega_j)\right),$$

where $J \in \mathbb{R} \setminus \{0\}$ is an interaction constant.

Additionally, Potts suggested a different model which is nowadays known as the *(standard) Potts model*. In this model only two different energies of interaction exist: Two adjacent spins contribute to the total energy only if they are equal. Hence the Hamiltonian of the (standard) Potts model is given by

$$H(\omega) := -J\beta \sum_{\{i,j\}\in\mathscr{E}} \delta(\omega_i, \omega_j), \tag{3.1}$$

where $\delta(\cdot\,,\cdot)$ is the Kronecker delta defined in (2.8) and J is as above. We call the standard Potts model *ferromagnetic* if $J > 0$ and *antiferromagnetic* if $J < 0$. In the ferromagnetic case, the spins tend to align locally with one another in order to minimize their total energy, i.e. to minimize the Hamiltonian (3.1). We will soon see that configurations with lower energy are more likely to be found than configurations with higher energy. Therefore, the spins form clusters (magnetic domains) when considering the model on a lattice (see Figure 3, left). Regarding the antiferromagnetic model, the Hamiltonian (3.1) is minimized for configurations where neighboring spins are different so that such configurations have a higher probability to be observed. To avoid a misunderstanding regarding this terminology, note that the term "ferromagnetic" does not necessarily imply that the model always behaves like a ferromagnet (the same goes for the term "antiferromagnetic"). [Wu82]

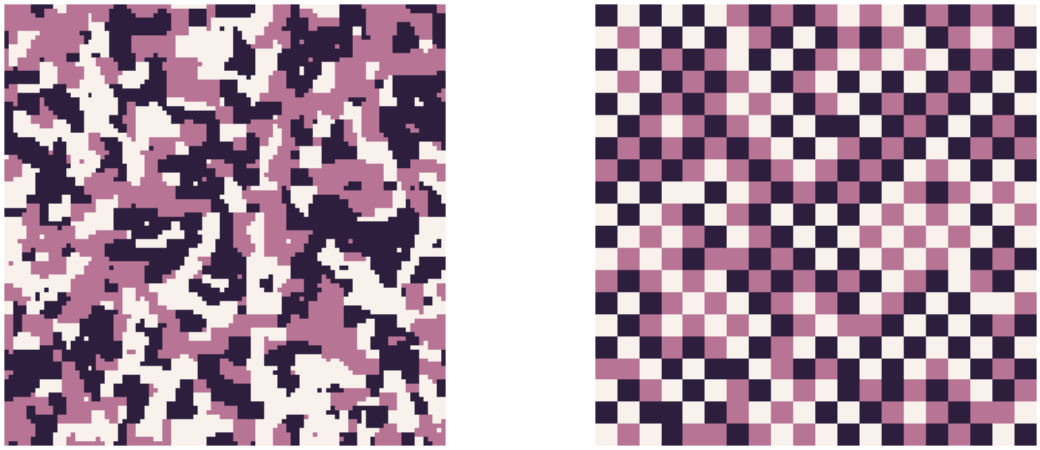

Fig. 3: Simulations of typical configurations for the 3-state standard Potts model on a square lattice using the Metropolis algorithm. Each spin state is represented in a different color. *Left*: ferromagnetic model ($J = 1$, $n = 100 \times 100$, $\beta = 100$). *Right*: antiferromagnetic model ($J = -1$, $n = 20 \times 20$, $\beta = 10$). From [Tsc18, p. 41, 43].

Additionally, we can include an external magnet field to this model. In this case, the Hamiltonian contains an extra term resulting from the interaction of the spins as magnetic moments with the magnetic field. In the case of the planar Potts model, one might define the magnetic field as a vector $h \in \mathbb{R}^2$ and the resulting interaction energy between a spin and the field as the scalar product between these two. Considering the standard Potts model, there exist different possibilities to define the interaction energy. Most of them are defined in such a way that exactly one spin variable is favored over the others as in [CS09].

In the following sections, we will consider the ferromagnetic ($J = 1$) standard Potts model without external magnetic field which we will only refer to as Potts model from now on.

3.1.2 Mean-field Models

Mean-field theory is used in various areas of physics. In statistical mechanics, it is often used to approximate a lattice model by a simpler one in order to make explicit computations possible. [BH19]

Deduced results from mean-field model may be used as an indicator for properties that one can expect from the original model [FV17]. In the case of the mean-field Potts model, an explicit computation of the *free energy* (a thermodynamic potential) is possible, allowing for an in-depth description of phase transitions. This simplified analysis is obtained by replacing the interactions between the spins by an average magnetic field that acts on every single spin [Cra07]. Nevertheless, this approximation will be unreliable if one wants to obtain accurate results, such as the exact value of the critical temperature or the order of the existing phase transition [BBL83]. For example, we will see that the Curie-Weiss Potts model, as the mean-field approximation of the Potts model, exhibits a first-order phase transition for all $q > 2$. However, for the two-dimensional Potts model, Baxter proved the existence of a first-order phase transition only for $q > 4$ and derived a transition of higher order for $q \leq 4$ [Bax73]. Nevertheless, the description of the phase transition of the mean-field model is useful because one can prove that lattice spin systems in sufficiently high dimensions or with long-range interactions show the same kind of phase transition as their mean-field version [GRW10].

The most commonly known mean-field spin model is the Curie-Weiss model, as the mean-field counterpart of the Ising model. In the following, we will give an insight in the analysis of the Curie-Weiss Potts model as the mean-field version of the Potts model. Hence this model can also be seen as a generalization of the Curie-Weiss model to more than two possible spin values.

3.2 Basic Definitions

We introduce the Hamiltonian and the Gibbs distribution of the Curie-Weiss Potts model in the following. Additionally, we examine the infinite-temperature limit as well as the zero-temperature limit of this distribution.

3.2.1 Gibbs Distribution

Let us consider the Hamiltonian of the Potts model on the graph $G = (\Lambda, \mathscr{E})$ as in (3.1) with $J = 1$ and $Q = \{1, \dots, q\}$. We label the elements of Λ by $\{1, \dots, n\}$ and denote the state space by $\Omega_n := Q^\Lambda$. Additionally, for every vertex $i \in \Lambda$, we define the set of its nearest-neighbors by $\mathcal{N}_i := \{j \in \Lambda \mid \{i, j\} \in \mathscr{E}\}$. Using this, we can rewrite the Hamiltonian as

$$H(\omega) = \sum_{i \in \Lambda} -\beta |\mathcal{N}_i| \Big(\frac{1}{|\mathcal{N}_i|} \sum_{j \in \mathcal{N}_i} \delta(\omega_i, \omega_j) \Big)$$

for any configuration $\omega \in \Omega_n$. Now, for each $i \in \Lambda$, the term in the brackets describes the average contribution of the neighbors of $i \in \Lambda$ to the total energy up to a multiplicative constant. This contribution to the Hamiltonian depends on $i \in \Lambda$, therefore it varies locally. We make the mean-field assumption that each local averaged contribution can be replaced with the global averaged contribution. Instead of only averaging over all neighbors of $i \in \Lambda$, we average over all sites, i.e. over Λ. Therefore, by replacing $\mathcal{N}_i$ by Λ and defining the modified inverse temperature $\beta' := \beta|\Lambda|$, we obtain

$$H(\omega) = \sum_{i \in \Lambda} -\beta' \Big(\frac{1}{|\Lambda|} \sum_{j \in \Lambda} \delta(\omega_i, \omega_j) \Big) .$$

For convenience, we only write β instead of β' and since $|\Lambda| = n$, we can make the following definition:

Definition 3.1. *The Curie-Weiss Potts Hamiltonian for a configuration $\omega \in \Omega_n$ at inverse temperature $\beta > 0$ is defined by*

$$H_{n,\beta}(\omega) := -\frac{\beta}{n} \sum_{i,j=1}^{n} \delta(\omega_i, \omega_j) . \tag{3.2}$$

It is also possible to derive a Hamiltonian in the form (3.2) by considering (a slightly different) version of the standard Potts model on the complete graph $\mathcal{C}_n$. The graph $\mathcal{C}_n$ consists of n vertices that are all connected with each other, hence it consists of $\binom{n}{2} = \frac{n(n-1)}{2}$ edges (see Figure 4). Since in (3.2) each spin also interacts with itself, the Hamiltonian on $\mathcal{C}_n$ would also differ by an additive constant, i.e. a shift in energy. Nevertheless, this would not change the behavior of our model under the special probability distribution on Ω_n that we consider (see Remark 3.3 below).

We are interested in computing the probability of observing a given configuration $\omega \in \Omega_n$. To describe the phenomenology of large systems, such as our spin systems, we are going to use the *Gibbs distribution*. This distribution is well suited to describe systems at thermodynamic equilibrium at fixed temperature T (at fixed inverse temperature β). As mentioned earlier, the probability of observing a system in a microstate $\omega \in \Omega_n$ depends on the energy $H_{n,\beta}(\omega)$ of this microstate as can be seen in the following definition [FV17]:

Definition 3.2. *The Gibbs distribution $\mu_{n,\beta}$ on Ω_n at inverse temperature $\beta > 0$ is given by*

$$\mu_{n,\beta}(\omega) = \frac{\exp(-H_{n,\beta}(\omega))}{Z_{n,\beta}}, \tag{3.3}$$

with Hamiltonian $H_{n,\beta}$ and normalization constant $Z_{n,\beta}$.

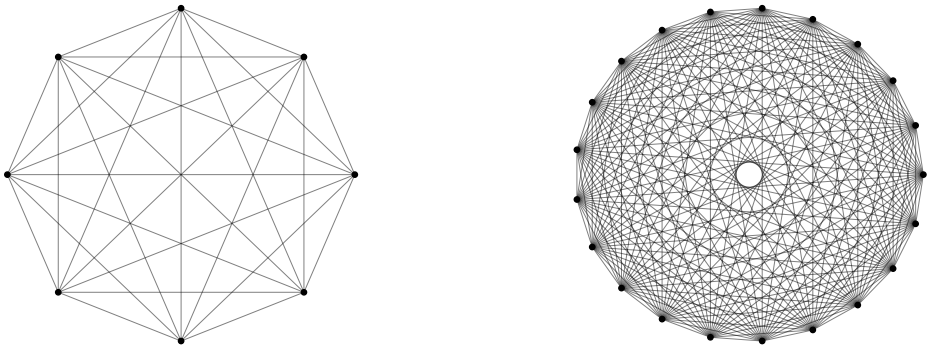

Fig. 4: The complete graphs $\mathcal{C}_8$ (*left*) and $\mathcal{C}_{21}$ (*right*): every pair of distinct vertices is connected by a unique edge.

In the context of statistical mechanics, we denote the normalization constant $Z_{n,\beta}$ as *partition function*. By examining (3.3) for a constant inverse temperature β, we see that configurations with higher energy are less observed (small probability) than configurations with lower energy (high probability).

Remark 3.3. For all configurations $\omega \in \Omega_n$, the Hamiltonians $H_{n,\beta}(\omega)$ and $\hat{H}_{n,\beta}(\omega) = H_{n,\beta}(\omega) + C$ for $C \in \mathbb{R}$ will lead to the same Gibbs distribution, i.e. $\mu_{n,\beta}(\omega) = \hat{\mu}_{n,\beta}(\omega)$. This is a direct consequence of the exponential function in the numerator of (3.3) and the normalization.

Applying Definition 3.2 to the Curie-Weiss Potts Hamiltonian gives us the following distribution as in [CDL12]:

Definition 3.4. *The (finite-volume) Gibbs distribution of the q-state Curie-Weiss Potts model on Ω_n at inverse temperature $\beta > 0$ is given by*

$$\mu_{n,\beta}(\omega) = \frac{1}{Z_{n,\beta}} \exp\left(\frac{\beta}{n} \sum_{i,j=1}^{n} \delta(\omega_i, \omega_j)\right), \tag{3.4}$$

where the partition function is given by

$$Z_{n,\beta} = \sum_{\omega \in \Omega_n} \exp\left(\frac{\beta}{n} \sum_{i,j=1}^{n} \delta(\omega_i, \omega_j)\right).$$

Remark 3.5. In the course of this chapter, we will also focus on *infinite-volume* Gibbs states, i.e. we are going to consider the limit $n \to \infty$. In our context, we refer to this limit as the *thermodynamic limit*.

Recalling the Hamiltonian of the Curie-Weiss Potts model, we ask for those configurations $\omega \in \Omega_n$ that minimize the total energy. By looking at (3.2), we see that the Hamiltonian is obviously minimized by those configurations where all spins have the same color.

Definition 3.6. *A configuration $\omega^{(k)} \in \Omega_n$ with all spins having the same color $k \in Q$, i.e.*

$$\omega_i^{(k)} := k \quad \textit{for all} \quad i \in \{1, \dots, n\}$$

is called ground state of the Curie-Weiss Potts model.

One goal of the next sections is to understand how the Gibbs distribution of the Curie-Weiss Potts model depends on the (inverse) temperature. To approach this question, we consider two limiting situations of the model, i.e. the case of *zero temperature* and the case of *infinite temperature*. The following theorem states amongst other things that the ground states play an important role in our model, especially when we consider the zero-temperature limit.

Theorem 3.7. *Let $\mu_{n,\beta}$ be the Gibbs distribution of the Curie-Weiss Potts model on $\Omega_n = Q^n$ at inverse temperature $\beta > 0$. Then the following statements hold:*

(i) In the infinite-temperature limit, the Gibbs distribution converges to the uniform distribution on Ω_n, i.e. for all $\omega \in \Omega_n$, we have

$$\lim_{\beta \to 0} \mu_{n,\beta}(\omega) = \frac{1}{|\Omega_n|}\,.$$

(ii) In the zero-temperature limit, the distribution of $\mu_{n,\beta}$ is concentrated on the ground states, i.e.

$$\lim_{\beta \to \infty} \mu_{n,\beta}(\omega) = \begin{cases} \frac{1}{|Q|} & \text{if } \omega \in \{\omega^{(k)}\}_{k \in Q}, \\ 0 & \text{otherwise}\,. \end{cases}$$

Proof. Firstly, we consider the infinite-temperature limit ($\beta \to 0$). By setting $\beta = 0$ in (3.4), we get

$$\lim_{\beta \to 0} \mu_{n,\beta}(\omega) = \mu_{n,0}(\omega) = \Big(\sum_{\omega \in \Omega_n} \exp(0) \Big)^{-1} \exp(0) = \frac{1}{|\Omega_n|}\,.$$

The zero-temperature limit ($\beta \to \infty$) requires more effort. Let $\omega \notin \{\omega^{(k)}\}_{k \in Q}$ be any configuration of Ω_n that is not a ground state. Then there exists at least one pair of vertices $\{p, q\} \subset \{1, \dots, n\}$ with $\omega_p \neq \omega_q$. Hence, for such a configuration

ω and any ground state $\omega^{(k)}$, we have

$$\begin{aligned} H_{n,\beta}(\omega) - H_{n,\beta}(\omega^{(k)}) &= -\frac{\beta}{n} \sum_{i,j=1}^{n} \Big(\delta(\omega_i, \omega_j) - \delta(\omega_i^{(k)}, \omega_j^{(k)}) \Big) \\ &= \frac{\beta}{n} \sum_{i,j=1}^{n} \Big(1 - \delta(\omega_i, \omega_j) \Big) \\ &\geq \frac{2\beta}{n} \,. \end{aligned}$$

Since the probability $\mu_{n,\beta}(\omega^{(k)})$ of the system being in a ground state $\omega^{(k)}$ at finite inverse temperature $\beta > 0$ is always positive, we obtain

$$\frac{\mu_{n,\beta}(\omega)}{\mu_{n,\beta}(\omega^{(k)})} = \exp\Big(- \Big(H_{n,\beta}(\omega) - H_{n,\beta}(\omega^{(k)}) \Big) \Big) \leq \exp\Big(- \frac{2\beta}{n} \Big) \overset{\beta\to\infty}{\longrightarrow} 0 \,.$$

Hence $\lim_{\beta\to\infty} \mu_{n,\beta}(\omega) = 0$ for all $\omega \notin \{\omega^k\}_{k\in Q}$. Additionally, all the probabilities of the ground states are equal, i.e. $\mu_{n,\beta}(\omega^{(k)}) = \mu_{n,\beta}(\omega^{(k')})$ for all $k, k' \in Q$. Since there are $|Q|$ such ground states and the distribution is completely concentrated on these ground states, we have $\mu_{n,\beta}(\omega^{(k)}) = 1/|Q|$ for all $k \in Q$ which finishes the proof. □

Remark 3.8. One can show that the family of spin variables $\{\omega_i\}_{i\in\{1,\dots,n\}}$ is independent and identically distributed in the infinite-temperature case. On the other hand, in the low-temperature regime, the spins become more and more dependent. In the limit of zero temperature, the Gibbs distribution freezes the system in one of its ground states. [FV17]

Theorem 3.7 provides some suggestions what we might expect for intermediate values of the temperature. For high temperatures, we anticipate that in a typical configuration the spins are nearly equally distributed. As the temperature decreases, there might arise a *critical temperature* at which the system starts to favor a certain spin color. In the next sections, we introduce the necessary tools to answer the question whether such a critical temperature exists and to possibly determine it.

3.2.2 Proportions Vector and Entropy

We introduce the proportions vector which will be a useful tool in the analysis of our model at hand. After that, we will take a deeper look at a quantity called entropy. This quantity plays a major role in many different areas like information theory or thermodynamics. A similar quantity that we define at the end of this chapter will also help us later on in the analysis of phase transitions in the Curie-Weiss Potts model.

Another way of describing a configuration is to refer to the fractions of spins that have the same color. This idea leads naturally to the following definition according to [CDL12]:

Definition 3.9. *For each $\omega \in \Omega_n$, the vector $x(\omega) = \Big(x_1(\omega), \ldots, x_q(\omega)\Big)$ with components*

$$x_k(\omega) := \frac{1}{n} \sum_{i=1}^{n} \delta(\omega_i, k)$$

is called proportions vector *of the configuration $\omega \in \Omega_n$.*

This vector includes the fractions of spins equal to k for all $k \in Q$. Therefore, this vector is also called *fractions vector*. We see that, up to a permutation of the vertices, each configuration $\omega \in \Omega_n$ is clearly described by its proportions vector $x(\omega)$.

Remark 3.10. The proportions vector $x(\omega)$ takes values in the set of probability vectors

$$\mathcal{S} := \left\{ x \in \mathbb{R}_+^q \;\middle|\; \sum_{i=1}^{q} x_i = 1 \right\}.$$

Therefore, the function $x : \Omega \to \mathcal{S}$ is an $\mathcal{S}$-valued random variable.

Before introducing the concept of entropy, we define the distribution of the fractions vector. We will later study this distribution in the thermodynamic limit which will lead to the phenomenon of phase transition.

Definition 3.11. *The distribution of the proportions vector x under the (finite-volume) Gibbs measure $\mu_{n,\beta}$ is given by $\sigma_{n,\beta} := \mu_{n,\beta} \circ x^{-1} : \mathcal{S} \to [0,1]$, i.e. for any $s \in \mathcal{S}$ we have*

$$\sigma_{n,\beta}(s) = \mu_{n,\beta}(x = s)\,.$$

In the following, we introduce the entropy as defined by C. E. Shannon [Sha48]. Even though he defined it in the field of information theory, we can adapt it to our statistical mechanics setting.

Definition 3.12. *Let $\mu \in \mathscr{M}_1(\Omega)$ be a probability distribution on Ω. Then the* Shannon entropy $S : \mathscr{M}_1(\Omega) \to \mathbb{R}$ *is defined by*

$$S(\mu) := -\sum_{x\in\Omega} \mu(x) \log \mu(x)\,.$$

Remark 3.13. For $\mu(x) = 0$, the term $\log \mu(x)$ diverges; by convention we set $0 \cdot \log(0) := 0$. This can be justified by observing the following limit and applying L'Hôpital's rule: in fact

$$\lim_{x\to 0^+} x \log(x) = \lim_{x\to 0^+} \frac{\log(x)}{1/x} = 0\,,$$

since

$$\lim_{x\to 0^+} \frac{(\log(x))'}{(1/x)'} = \lim_{x\to 0^+} \frac{1/x}{-1/x^2} = \lim_{x\to 0^+} -x = 0\,.$$

In the following, we establish some properties of the entropy, and see that this quantity may be used to characterize probability distributions.

Remark 3.14. An easy application of Jensen's inequality (2.19) shows that $S(\mu) \geq 0$ for all $\mu \in \mathscr{M}_1(\Omega)$. Using the fact that $f(x) := -\log(x)$ is convex, since $f''(x) = 1/x^2 > 0$ for $x \in (0, 1]$, and Remark 3.13, we can write

$$S(\mu) = \mathbb{E}_\mu[-\log \mu] \geq -\log \mathbb{E}_\mu[\mu] = -\log\Big(\sum_{\omega\in\Omega} \mu(\omega)^2\Big) \geq -\log\Big(\sum_{\omega\in\Omega} \mu(\omega)\Big) = 0.$$

Lemma 3.15. *The Shannon entropy $S : \mathscr{M}_1(\Omega) \to \mathbb{R}$ is concave.*

Proof. Setting $g(x) := -x \log(x)$, we rewrite the entropy as $S(\mu) = \sum_{\omega\in\Omega} g(\mu(\omega))$. Since $\mu(\omega) \in [0, 1]$, we also have $x \in [0, 1]$. Now the second derivative of g with respect to x is given by $g''(x) = -1/x$. Hence the function g is concave, because $g''(x) < 0$ for all $x \in (0, 1]$ and $\lim_{x\to 0^+} -1/x = -\infty < 0$. Since the sum of concave functions is also concave, we obtain that S is concave. □

Proposition 3.16. *The uniform distribution on Ω maximizes the Shannon entropy S, and the Dirac mass at $\omega \in \Omega$ minimizes it, i.e.*

$$\operatorname*{argmax}_{\mu \in \mathscr{M}_1(\Omega)} S(\mu) = \{\mathcal{U}_\Omega\} \qquad \textit{and} \qquad \operatorname*{argmin}_{\mu \in \mathscr{M}_1(\Omega)} S(\mu) = \{\delta_\omega\}_{\omega \in \Omega}\,.$$

Moreover, the Shannon entropy is bounded: for all $\mu \in \mathscr{M}_1(\Omega)$, we have $S(\mu) \in [0, \log|\Omega|\,]$.

Proof. Let $\mu \in \mathscr{M}_1(\Omega)$ and define again $g(x) := -x\log(x)$. Using the notation of the expectation, we can write

$$S(\mu) = |\Omega| \sum_{\omega \in \Omega} \frac{1}{|\Omega|} g\Big(\mu(x)\Big) = |\Omega|\, \mathbb{E}_{\mathcal{U}_\Omega}\Big[g(\mu)\Big]\,.$$

We already know that g is concave. Therefore, we can apply Jensen's inequality (Remark 2.42) and obtain

$$S(\mu) \leq |\Omega|\, g\Big(\mathbb{E}_{\mathcal{U}_\Omega}[\mu]\Big) = |\Omega|\, g\Big(\sum_{\omega \in \Omega} \frac{1}{|\Omega|}\mu(\omega)\Big) = -\log\left(\frac{1}{|\Omega|}\right) = S(\mathcal{U}_\Omega)\,.$$

Equality holds if and only if $\mu(\cdot)$ is constant, hence if $\mu = \mathcal{U}_\Omega$. Considering the second part of Proposition 3.16, Remark 3.14 tells us that $S(\mu) \geq 0$ for all $\mu \in \mathscr{M}_1(\Omega)$. Additionally one does easily see that $S(\delta_\omega) = 0$ for all $\omega \in \Omega$ which completes the proof. □

Proposition 3.16 also tells us that the entropy can be used to measure how far from being uniform a probability distribution is. The closer the entropy is to zero, the more the distribution is concentrated on a few outcomes. If the entropy is close to its maximum value $\log|\Omega|$, then all outcomes are nearly identically distributed. [FV17]

At this point, let us frame the proportions vector in the context of the Curie-Weiss Potts model. This vector $x = x(\omega) \in \mathcal{S}$ tells us the relative frequency by which a color $q \in Q$ appears in a fixed configuration $\omega \in \Omega_n$. This frequency can be interpreted as a probability distribution on the possible spin states. Hence, we can assign an entropy value to each proportions vector $x = (x_1, \ldots, x_q)$. Therefore, we define the following quantity analogous to the Shannon entropy:

Definition 3.17. *The* entropy density *of the q-state Curie-Weiss Potts model is the function* $\tilde{S} : \mathcal{S} \to [0, \log(q)]$ *defined by*

$$\tilde{S}(x) = -\sum_{i=1}^{q} x_i \log(x_i) .$$

3.2.3 Mean-field Free Energy Function

In statistical mechanics, many phenomena are described by an interplay between two quantities, one favoring disorder, the other favoring order. In our model, these quantities are the entropy and the energy, both depending on the temperature. We will see that this interplay is well described by the *free energy function* which will be derived in the course of this chapter.

Using the concept of the proportions vector, we derive an alternative representation of the Curie-Weiss Potts Hamiltonian describing the energy of a configuration.

Lemma 3.18. *Let* $\omega \in \Omega_n$ *be a configuration and let* $x(\omega) \in \mathcal{S}$ *be its proportions vector. Then the Hamiltonian of the q-state Curie-Weiss Potts model can be rewritten as*

$$H\Big(x(\omega)\Big) = -n\beta \sum_{r=1}^{q} x_r(\omega)^2 .$$

Proof. Using Definition 3.9, we can write

$$\begin{aligned} H(\omega) &= -\frac{\beta}{n} \sum_{i,j=1}^{n} \delta(\omega_i, \omega_j) \\ &= -\frac{\beta}{n} \sum_{r=1}^{q} \left(\sum_{i=1}^{n} \delta(\omega_i, r) \sum_{j=1}^{n} \delta(\omega_j, r) \right) \\ &= -n\beta \sum_{r=1}^{q} \left(\frac{1}{n} \sum_{i=1}^{n} \delta(\omega_i, r) \right)^2 \\ &= -n\beta \sum_{r=1}^{q} x_r^2 . \end{aligned}$$

□

Since Lemma 3.18 tells us that the energy of a configuration $\omega \in \Omega_n$ only depends on the different proportions of possible spin values, we consider the Hamiltonian as a function of the proportions vector $x = x(\omega) \in \mathcal{S}$ for now. We will see that it is also convenient to introduce the energy density $\tilde{H}(x) = H(x)/n$. In analogy to the entropy density $\tilde{S}$, we make the following definition using Lemma 3.18:

Definition 3.19. *The* energy density *of the q-state Curie-Weiss Potts model is the function* $\tilde{H} : \mathcal{S} \to \mathbb{R}$ *given by*

$$\tilde{H}(x) := -\beta \sum_{r=1}^{q} x_r^2 \,.$$

In order to describe the interplay between the energy (density) and the entropy (density), we introduce the *free energy function* f_β in a similar way as in [FV17] . We will see that this is an auxiliary function that allows for a different approach to the phenomenon of phase transition. This free energy function is defined by $f_\beta : \mathcal{S} \to \mathbb{R},\ f_\beta(x) := \tilde{H}(x) - \tilde{S}(x)$. Regarding the Curie-Weiss Potts model, this leads to the following definition:

Definition 3.20. *The* free energy function $f_\beta : \mathcal{S} \to \mathbb{R}$ *of the q-state Curie-Weiss Potts model on* Ω_n *at inverse temperature* $\beta > 0$ *is given by*

$$f_\beta(x) := \sum_{r=1}^{q} \Big(-\beta x_r^2 + x_r \log(x_r) \Big) \,. \tag{3.5}$$

Using results from Large Deviation theory, one can show that typical values of the proportions vector $x \in \mathcal{S}$ are those that minimize the free energy function f_β [FV17]. The free energy function f_β is shown for $q = 3$ in Figure 5 on the next page. We see that the occurrence of local or even global minima is directly connected with the inverse temperature $\beta > 0$. Before we take a closer look at the different regimes depending on the inverse temperature, we want to clarify some terminology following [ENR80]:

Definition 3.21. *Let* $\omega \in \Omega_n$ *be a configuration,* $x(\omega) \in \mathcal{S}$ *its proportions vector and* $f_\beta : \mathcal{S} \to \mathbb{R}$ *the free energy function. If* $x(\omega)$ *corresponds to a global (local) minimum of* f_β*, then the configuration* $\omega \in \Omega_n$ *is called a stable (metastable) state.*

Remark 3.22. If there is only a unique global minimum of the free energy function f_β, then we say we consider a *pure phase*. If there are multiple global minima, then the system is in a *mixed phase*.

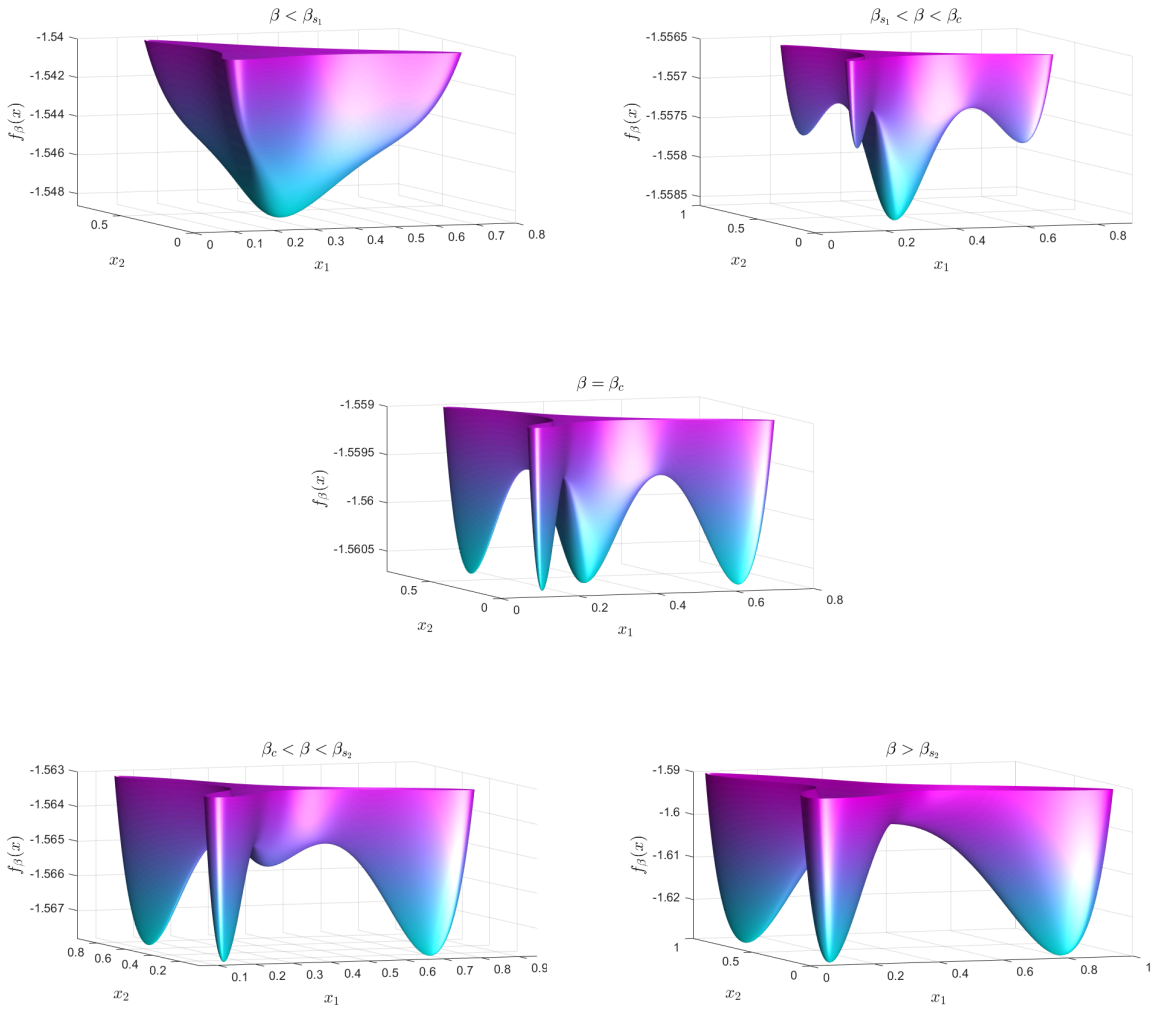

Fig. 5: Free energy function $f_\beta : \mathcal{S} \to \mathbb{R}$ for the Curie-Weiss Potts model with $q = 3$ colors as a function of the proportions vector x. The domain $\mathcal{S}$ is mapped into the XY-plane by $(x_1, x_2, x_3) \mapsto (x_1, x_2, 1 - x_1 - x_2)$. The form of the surface graph strongly depends on the inverse temperature $\beta > 0$. The lower the free energy $f_\beta(x)$ of a proportions vector $x \in \mathcal{S}$, the higher is the probability $\sigma_{n,\beta}(x)$ to observe this proportions vector [CDL12].

At this point, we want to examine the graph of the free energy function in more detail. We refer to Figure 5 showing the case $q = 3$ but keeping in mind that the situation is qualitatively the same for all $q \geq 3$ [LPW09]. The advantage of considering $q = 3$ lies in the fact that the free energy function can be represented as a three dimensional plot.

We start with the high-temperature regime, i.e. the plot in the upper-left corner titled $\beta < \beta_{s_1}$. We see that there is only one global minimum at the center, i.e. for a proportions vector with equal proportions of each color. This minimum corresponds to a pure phase. Additionally, the Curie-Weiss Potts Gibbs distribution is supported almost completely on configurations $\omega \in \Omega_n$ with approximately equal proportions for each color $q \in Q$.

Increasing the inverse temperature, we arrive β_{s_1}, the *first spinodal inverse temperature*. At this inverse temperature, q other local minima begin to appear. This is shown in the upper right plot. So in the regime $\beta_{s_1} < \beta < \beta_c$, we have q metastable states, each with one color dominating, and still one stable state at the center.

By increasing the inverse temperature β even more, we come about a point, where the q local minima become global minima – this happens at the *critical inverse temperature* β_c, as can be seen in the center plot – so that we have $(q+1)$ global minima, corresponding to a mixed phase. At criticality, the ordered and the disordered phase coexist. Moreover, the behavior of the system changes at β_c: We have seen that for $\beta < \beta_c$, the typical configurations $\omega \in \Omega_n$ are those whose proportions vectors $x(\omega)$ have roughly equally distributed colors.

For inverse temperatures $\beta_c < \beta < \beta_{s_2}$, the Gibbs distribution is supported almost completely on the configurations $\omega \in \Omega_n$ where one of the q colors is dominating – as depicted in the plot in the bottom left corner. So we have q stable states corresponding to global minima and one metastable state which corresponds to the local minima in the center.

If we increase the inverse temperature even more, the local minimum in the center disappears. The threshold value for the inverse temperature at which this happens is called the *second spinodal inverse temperature* β_{s_2}. So the graph of the free energy function f_β has q global minima, each corresponding to a stable state where one color $q \in Q$ dominates. This situation is shown in the plot in the bottom right corner.

Now we introduce a thermodynamic potential, the so-called *free energy*. As one might expect, we will see that this quantity is connected with the free energy function f_β. We make the following definitions according to [FV17]:

Definition 3.23. *The* finite-volume free energy $\Psi_n : (0,\infty) \to \mathbb{R}$ *of the q-state Curie-Weiss Potts model is given by*

$$\Psi_n(\beta) := -\frac{1}{\beta n} \log Z_{n,\beta} \,,$$

where $Z_{n,\beta}$ denotes the partition function of the model.

To make this quantity independent of the size of the system n, we consider the thermodynamic limit. We will soon see that this has another advantage regarding possible non-analyticities.

Definition 3.24. *The* infinite-volume free energy $\Psi : (0,\infty) \to \mathbb{R}$ *of the q-state Curie-Weiss Potts model is given by*

$$\Psi(\beta) := \lim_{n\to\infty} \Psi_n = -\lim_{n\to\infty} \frac{1}{\beta n} \log Z_{n,\beta} \,,$$

where $Z_{n,\beta}$ denotes the partition function of the model.

We say that our model exhibits a *phase transition* at some inverse temperature $\beta > 0$ if the free energy in the thermodynamic limit Ψ is not analytic in β. It is necessary to consider the thermodynamic limit because it is the only way that a non-analyticity can arise. Indeed, let us for a moment consider the free energy of the finite system, i.e.

$$\Psi_n = -\frac{1}{\beta n} \log Z_{n,\beta} = -\frac{1}{\beta n} \log \left(\sum_{\omega\in\Omega_n} \exp\left(\frac{\beta}{n} \sum_{i,j=1}^{n} \delta(\omega_i, \omega_j) \right) \right).$$

Since the partition function $Z_{n,\beta}$ is a polynomial in the variable $\exp(\beta/n)$ with non-negative integer coefficients, the free energy Ψ_n must be real analytic in β and hence cannot exhibit a phase transition. The only way for non-analyticity to occur is in the thermodynamic limit $n \to \infty$, i.e. in an infinitely large system. One may ask how this corresponds to our everyday experience of phase transitions. Of course, real systems are always finite and hence the thermodynamic properties are always analytic. However, if we consider very large systems, then

their behavior is well approximated by the behavior of an infinitely large system. In fact, experimentally, one cannot distinguish between the behavior of a large finite and that of an infinitely large system. [FV17]

The following theorem provides the connection between our auxiliary free energy function f_β and the (infinite-volume) free energy Ψ (see [EW90, p. 62]) by way of a variational principle.

Theorem 3.25. *The infinite-volume free energy $\Psi(\beta)$ of the q-state Curie-Weiss Potts model corresponds to a global minimum of the free energy function $f_\beta(x)$, i.e.*

$$\beta\Psi(\beta) = \min_{x\in\mathcal{S}} f_\beta(x) + \log(q)\,. \tag{3.6}$$

Proof. A proof using results from the theory of Large Deviations can be found in [OO18]. □

Since the infinite-volume free energy might not be analytic in some $\beta > 0$, there must be a way that a non-analyticity can occur on the right-hand-side of (3.6). The only way for this to happen is due to the minimum function. So instead of examining the thermodynamic limit of the free energy, we will study minima as well as the minimizers of the free energy function f_β.

3.3 Results

Firstly, we introduce the order parameter which will help us in the following analysis of the Curie-Weiss Potts model. Having done this, we examine the critical inverse temperature of the model that is directly connected with the phenomenon of phase transition. In addition, we study two other interesting temperatures, namely the first and the second spinodal inverse temperature. Finally, we consider the distribution of the proportions vector in the thermodynamic limit.

3.3.1 Order Parameter and Self-Consistency Equations

The first step in our analysis is to determine the states that minimize the free energy function f_β. More precisely, we want to find the proportions vectors $x \in \mathcal{S}$ that minimize f_β. Therefore, we consider

$$f_\beta(x) := \sum_{r=1}^{q} \Big(-\beta x_r^2 + x_r \log(x_r) \Big) .$$

Since we intend to find local minima of f_β under the equality constraint

$$g(x) := \sum_{r=1}^{q} x_r - 1 = 0 \,, \tag{3.7}$$

we use the method of Lagrange multipliers according to [KMS54]. The Lagrangian function $\mathscr{L}$ with Lagrange multiplier λ is then given by

$$\begin{aligned} \mathscr{L}(x,\lambda) &= f_\beta(x) - \lambda g(x) \\ &= \sum_{r=1}^{q} \Big(-\beta x_r^2 + x_r \log(x_r) \Big) - \lambda \Big(\sum_{r=1}^{q} x_r - 1 \Big) . \end{aligned}$$

The condition $\nabla_{x,\lambda} \mathscr{L}(x,\lambda) = 0$ yields

$$-2\beta x_r + 1 + \log(x_r) - \lambda = 0 \tag{3.8}$$

for all $r \in \{1, \ldots, q\}$ and of course the constraint $g(x) = 0$. By rewriting (3.8) as $x_r = \exp(2\beta x_r - 1 + \lambda)$ and substituting this into (3.7), we see that the Lagrange

multiplier λ is given by

$$\lambda = 1 - \log\Big(\sum_{r=1}^{q} \exp(2\beta x_r)\Big)\,.$$

By substituting this back into (3.8) and rearranging terms, we obtain

$$x_r = \exp(2\beta x_r)\Big(\sum_{r=1}^{q} \exp(2\beta x_r)\Big)^{-1} \tag{3.9}$$

for all $r \in \{1, \ldots, q\}$. These equations represent conditions that a proportions vector $x \in \mathcal{S}$ must satisfy in order to be a local minimum of f_β.

Lemma 3.26. *Equation* (3.8) *has at most two roots* $\alpha_1, \alpha_2 \in [0, 1]$.

Proof. Let us consider $h(x_r) := -2\beta x_r + 1 + \log(x_r) - \lambda = 0$. Suppose that $h(x_r) = 0$ has three or more roots. Then Rolle's theorem claims that $h'(x_r)$ has at at least two roots. But we have $h'(x_r) = -2\beta + 1/x_r = 0$ if and only if $x_r = 1/(2\beta)$. Therefore our assumption is false and $h(x_r)$ must have at most two roots. □

We assume w.l.o.g. that $\alpha_1 \geq \alpha_2$. Then we have

$$x_1 = \ldots = x_j = \alpha_1 \quad \text{and} \quad x_{j+1} = \ldots = x_q = \alpha_2\,.$$

Due to [KMS54], only the state corresponding to $j = 1$ leads to a global minimum of the free energy function f_β. Hence for the rest of this thesis, we will only consider this case. We define the *order parameter* $\xi = \alpha_1 - \alpha_2 \in [0, 1]$. In this case, we only have (at most) two different conditions in the form of (3.9). Subtracting those conditions from each other and using the definition of the order parameter, after some straightforward computation, we obtain the following *self-consistency equation* for the Curie-Weiss Potts model:

$$\xi = \Big(\exp(2\beta\xi) - 1\Big)\Big(\exp(2\beta\xi) + q - 1\Big)^{-1}\,. \tag{3.10}$$

This equation describes implicitly how the order parameter $\xi \in [0, 1]$ depends on the inverse temperature β. Obviously, $\xi = 0$ is always a solution, but for higher inverse temperatures β, there is another solution $\xi > 0$. Unfortunately, we cannot solve this equation analytically for ξ in general. However, we will later investigate

a special case, where we are able to obtain exact solutions.

Let us consider a different approach to finding minimal solutions of f_β using the order parameter. We have

$$x_1 - \xi = x_2 = \ldots = x_q$$

and by using (3.7), after some calculations, we obtain

$$\begin{aligned} x_1 &= \frac{1}{q}\Big(1 + (q-1)\xi\Big), \\ x_k &= \frac{1}{q}(1-\xi) \quad \text{for} \quad k \in \{2, \ldots, q\}\,. \end{aligned} \tag{3.11}$$

Due to the simple structure of the possible solutions $x = (x_1, \ldots, x_q)$, we see that the issue of finding them reduces to an one-dimensional optimization problem [GRW10].

By inserting (3.11) in the expression of the free energy function (3.5), we can express f_β as a function of the order parameter, i.e. we have $f_\beta : [0,1] \to \mathbb{R}$ with $\xi \mapsto f_\beta(\xi)$. For simplicity, we then define $\tilde{f}_\beta(\xi) := f_\beta(\xi) - f_\beta(0)$ and, after some straightforward computations, obtain

$$\tilde{f}_\beta(\xi) = \frac{1 + (q-1)\xi}{q} \log\Big(1 + (q-1)\xi\Big) + \frac{q-1}{q}(1-\xi)\log(1-\xi) - \frac{q-1}{q}\beta\xi^2\,,$$

with $f_\beta(0) = -\beta/q - \log(q)$. This equation describes the dependence of the free energy function f_β of the order parameter ξ. It will play a central role in the upcoming analysis of the Curie-Weiss Potts model, in particular for determining the critical point of its phase transition.

Considering the representation of the proportions vector x in (3.11), we are now interested in finding the order parameter ξ that minimizes the free energy function f_β. Therefore, we consider the first derivative of f_β with respect to ξ, i.e.

$$\frac{\mathrm{d}}{\mathrm{d}\xi} f_\beta(\xi) = \frac{q-1}{q}\Big(\log\Big(1 + (q-1)\xi\Big) - \log(1-\xi) - 2\beta\xi\Big)\,. \tag{3.12}$$

A necessary condition to have a local minimum in ξ is for (3.12) to be equal to

zero. Imposing this equality and rearranging the terms, we end up again with the self-consistency equation of our model as we could have expected.

Remark 3.27. In our model, the order parameter ξ depends on the inverse temperature β. In general, it is defined to be zero in the unordered phase and finite in the ordered one. We will later see that this is consistent with our definition of the order parameter. [BH19]

3.3.2 Critical and Spinodal Inverse Temperatures

We have already mentioned three important values of the inverse temperature $\beta > 0$ in Section 3.2.3 about the free energy function. In particular, we saw that the value of β has a direct impact on the shape of the graph of the free energy function f_β. In the following, we examine these special inverse temperatures even more and try to derive their exact values depending on the number of colors q.

When we spoke about phase transitions near the end of Section 3.2.3, we mentioned that there is often a critical inverse temperature β_c that separates the ordered ($\beta > \beta_c$) from the disordered phase ($\beta < \beta_c$). Especially at criticality ($\beta = \beta_c$), we will see that both phases coexist which implies that the free energy function f_β has global minima corresponding to each phases. We can define the critical inverse temperature β_c according to [KMS54] as follows:

Definition 3.28. *Let $f_\beta : [0,1] \to \mathbb{R}$, $\xi \mapsto f_\beta(\xi)$ be the free energy function of the q-state Curie-Weiss Potts model. The unique inverse temperature $\beta_c(q)$ at which f_{β_c} has two global minima is called* critical inverse temperature.

The next theorem states the exact value of this critical inverse temperature (as given in [CDL12]). Both for this Theorem and for Proposition 3.33 below, we provide only a sketch of the proofs which highlights the central ideas and tries to give a dynamical understanding how the graph of f_β transforms for varying inverse temperatures $\beta > 0$.

Theorem 3.29. *The critical inverse temperature of the q-state Curie-Weiss Potts model for $q \geq 3$ is given by*

$$\beta_c(q) = \frac{(q-1)\log(q-1)}{q-2}\,.$$

Proof. We want to determine the order parameter ξ that minimizes the free energy function f_β. So we are interested in the global minima of the free energy function for different inverse temperatures β (see Figure 6). These order parameters ξ minimizing the free energy function will depend on β and we can expect some kind of discontinuity. By looking at the solutions of $\frac{\mathrm{d}}{\mathrm{d}\xi} f_\beta(\xi) = 0$, i.e.

$$\frac{q-1}{q}\Big(\log\big(1+(q-1)\xi\big) - \log(1-\xi) - 2\beta\xi\Big) = 0\,,$$

we see that $\xi = 0$ is always a solution. However for certain values of β, there are other solutions which yield an even lower value of the free energy function than $\xi = 0$ (see Figure 6 on the next page). We want to determine this critical inverse temperature β_c at which this shift in the order parameter occurs. As a byproduct, we will obtain the order parameter ξ_c at criticality. So β_c and ξ_c must solve the system of equations

$$\begin{cases} \frac{\mathrm{d}}{\mathrm{d}\xi} f_\beta(\xi) = 0\,, \\ f_\beta(\xi) = f_\beta(0)\,. \end{cases}$$

The first equality assures the existence of a local extremum for β_c in ξ_c, while the second equality provides the condition that this local extremum is a global minimum as well as the one at $\xi = 0$. It is not possible to solve this system of equations by elementary tools but it is an easy task to verify that

$$\xi_c = \frac{q-2}{q-1} \quad \text{and} \quad \beta_c = \frac{(q-1)\log(q-1)}{q-2}$$

is a solution for this system of equations. □

We mentioned earlier that at criticality, we have coexistence of phases. So it is natural to ask what these coexisting phases look like.

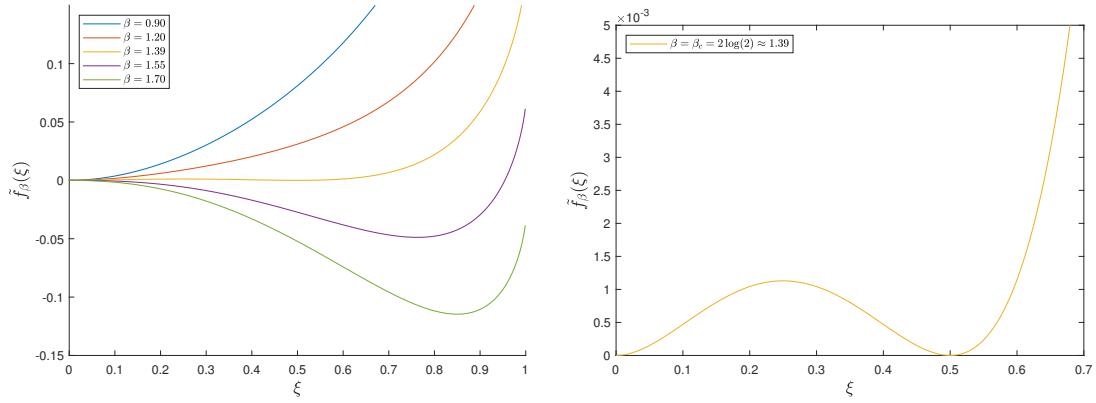

Fig. 6: For $q = 3$, the function $\tilde{f}_\beta(\xi) = f_\beta(\xi) - f_\beta(0)$ is plotted for different values of β. Since the term $f_\beta(0)$ only shifts each graph more downward depending on β, the global minima of $\tilde{f}_\beta$ correspond to those of the free energy function f_β. *Left*: Hence for small β, the free energy function f_β is always minimized for $\xi = 0$. But if β exceeds a critical value β_c, a new global minimum emerges at $\xi(\beta) > 0$. *Right*: The function $\tilde{f}_\beta$ is plotted at criticality ($\beta = \beta_c$). We see two global minima: the one at $\xi = 0$ corresponding to the ordered phase and the one at $\xi = 0.5$ corresponding to the disordered phase.

Remark 3.30. At inverse temperature $\beta_c(q)$, the free energy function f_{β_c} has two global minima. The minimum in $\xi = 0$ corresponds to the unordered phase, while the minimum in $\xi = \xi_c$ corresponds to the ordered phase. By substituting the two order parameters that minimize the free energy function at criticality, i.e. $\xi = 0$ and $\xi = \xi_c$, back into (3.11), we obtain

$$x(0) = \left(\frac{1}{q}, \dots, \frac{1}{q}\right) =: \hat{q}$$

and

$$x(\xi_c) = \left(1 - \frac{1}{q}, \frac{1}{q(q-1)}, \dots, \frac{1}{q(q-1)}\right) =: \hat{x}_{\beta_c(q),q}\,.$$

So in the unordered phase, we have evenly distributed proportions, while in the ordered phase, the fraction of spins of a certain color is clearly dominating. In this case, we say that the *symmetry is broken* following [FV17]. Since no color is special, we can exchange the first and the k-th component of $x(\xi_c)$ for $k \in \{2, \dots, q\}$ in order to obtain the other configurations that minimize the free energy function f_β. Hence at criticality, we have $q+1$ global minima, one corresponding to the disordered phase and q representing ordered states.

Next, we want to derive some information about the concrete location of the first and second spinodal inverse temperatures. For small inverse temperatures β, the free energy function f_β has only one local minimum. Above a certain inverse temperature β_{s_1}, there are q new local minima that begin to appear [CDL12] (see Figure 5 for the case $q = 3$). Using the order parameter ξ in the same way as above, we can define this first spinodal inverse temperature as follows:

Definition 3.31. *Let $f_\beta : [0,1] \to \mathbb{R}, \xi \mapsto f_\beta(\xi)$ be the free energy function of the q-state Curie-Weiss Potts model. The threshold value $\beta_{s_1}(q)$ such that for $\beta > \beta_{s_1}(q)$ a local minimum of f_β begins to appear in $\xi \neq 0$ is called* first spinodal inverse temperature.

There is a similar behavior at high values of β at which the local minimum corresponding to the unordered phase ceases to exist [CDL12] (see the two lowermost graphs in Figure 5). This gives rise to the following definition:

Definition 3.32. *Let $f_\beta : [0,1] \to \mathbb{R}, \xi \mapsto f_\beta(\xi)$ be the free energy function of the q-state Curie-Weiss Potts model. The threshold value $\beta_{s_2}(q)$ such that for $\beta > \beta_{s_2}(q)$ the local minimum of f_β in $\xi = 0$ disappears is called* second spinodal inverse temperature.

Proposition 3.33. *The first and the second spinodal inverse temperatures of the q-state Curie-Weiss Potts model for $q \geq 3$ are given by*

$$\beta_{s_1}(q) = \min_{\xi \in (0,1)} \left\{ \beta(\xi) > 0 \mid \beta(\xi) = \tfrac{1}{2\xi} \log\left(\tfrac{1+(q-1)\xi}{1-\xi}\right) \right\} \quad \textit{and} \quad \beta_{s_2}(q) = \frac{q}{2}\,.$$

Proof. Firstly, we want to determine the threshold value of β at which the second local minima (next to $\xi = 0$) of $f_\beta(\xi)$ begins to appear. Therefore, we consider

$$\frac{\mathrm{d}}{\mathrm{d}\xi} f_\beta(\xi) = \frac{q-1}{q}\Big(\log\big(1 + (q-1)\xi\big) - \log(1-\xi) - 2\beta\xi \Big) \stackrel{!}{=} 0\,. \tag{3.13}$$

We have seen that $\xi_1 = 0$ is always a solution, hence a local extremum. If we examine Figure 6, then we expect that, for β big enough, for at least one other solution $\xi_2(\beta) > 0$ that corresponds to a local minimum to appear. We denote by β_{s_1} the smallest $\beta > 0$ for which such a $\xi_2(\beta)$ exists. For $\xi \neq 0$, we can solve

(3.13) for β and obtain

$$\beta(\xi) = \frac{1}{2\xi} \log\left(\frac{1+(q-1)\xi}{1-\xi}\right) \tag{3.14}$$

in which ξ must correspond to the position of the other local extremum since $\xi \neq 0$. In Figure 7, we can see the graph of (3.14) for some values of q. For a better understanding, it might be helpful to change the axes as in Figure 8 on the next page. We see that there is an inverse temperature gap on the left side of the graph. Then, for $\beta > \beta_{s_1}$ with

$$\beta_{s_1}(q) = \min_{\xi\in(0,1)} \left\{\beta(\xi) > 0 \mid \beta(\xi) = \tfrac{1}{2\xi} \log\left(\tfrac{1+(q-1)\xi}{1-\xi}\right)\right\}, \tag{3.15}$$

the free energy function f_β has another local minimum next to the one in $\xi = 0$ and of course a local maximum in between. Hence (3.15) is our desired first spinodal inverse temperature. By looking at the blue branch in Figure 8, we see that the position of the minimum converges to $\xi = 1$ for $\beta \to \infty$. In contrast to this behavior, we see that the red branch, i.e. the position of the local maximum, intersects $\xi = 0$ in β_{s_2}. We conclude that the original local minimum of f_β in $\xi = 0$ "fuses" with the local maximum and becomes a saddle point for inverse

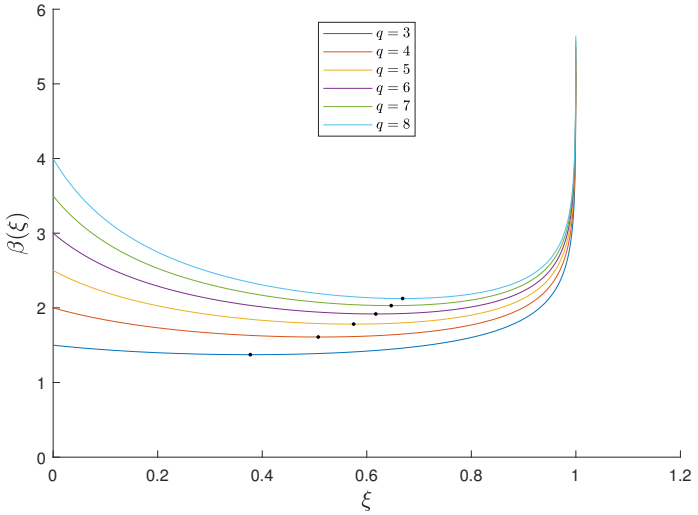

Fig. 7: Graphical representation of equation (3.14) for different numbers of colors q. Then minimum value of each curve $\beta(\xi)$ (marked by a black dot) corresponds to the threshold value of the inverse temperature at which local extrema of f_β next to the one at $\xi = 0$ begin to appear.

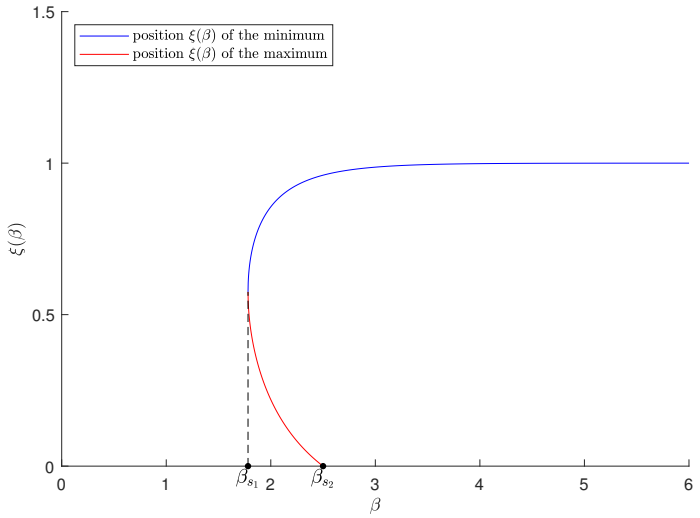

Fig. 8: Graphical representation of (3.14) for $q = 5$. For $\beta \in (\beta_{s_1}, \beta_{s_2})$, the free energy function has two local extrema (a minimum and a maximum) next to the minimum in $\xi = 0$. The blue branch corresponds to the position of the minimum and the red branch represents the maximum's position. For $\beta > \beta_{s_2}$ the local minimum in $\xi = 0$ becomes a saddle point.

temperatures $\beta \geq \beta_{s_2}$. In this case, we have

$$\beta_{s_2}(q) = \lim_{\xi \to 0^+} \beta(\xi) = \lim_{\xi \to 0^+} \frac{1}{2\xi} \log\Big(\frac{1 + (q-1)\xi}{1 - \xi}\Big) .$$

Since this is the limit of an indeterminate form, we can apply L'Hôpital's rule which yields

$$\lim_{\xi \to 0^+} \frac{\Big(\log\Big(\frac{1+(q-1)\xi}{1-\xi}\Big)\Big)'}{(2\xi)'} = \lim_{\xi \to 0^+} \frac{q}{2(1 + (q-1)\xi)(1-\xi)} = \frac{q}{2} .$$

Therefore, we obtain the second spinodal inverse temperature given by

$$\beta_{s_2}(q) = \lim_{\xi \to 0^+} \beta(\xi) = \frac{q}{2} .$$

□

Proposition 3.34. *Let $\beta_c(q)$, $\beta_{s_1}(q)$ and $\beta_{s_2}(q)$ be the critical inverse temperature as well as the first and the second spinodal inverse temperatures. For $q \geq 3$ we have that*

$$0 < \beta_{s_1}(q) < \beta_c(q) < \beta_{s_2}(q)\,.$$

Proof. See for instance [CDL12, p. 448]. □

Some (numerically) computed values of these important inverse temperatures can be found in Table 1. We see that the interval (β_{s_1}, β_c) is very small for $q = 3$ and it is only slowly increasing for bigger values of q. In contrast to that behavior, the length of the interval (β_c, β_{s_2}) is growing much faster.

q	3	4	5	6	7	8	9	10
β_{s_1}	1.373	1.609	1.782	1.918	2.030	2.125	2.207	2.280
β_c	1.386	1.648	1.848	2.012	2.150	2.270	2.377	2.472
β_{s_2}	1.5	2.0	2.5	3.0	3.5	4.0	4.5	5.0

Table 1: Critical inverse temperature β_c and both spinodal inverse temperatures β_{s_1} and β_{s_2} for different values of q for the Curie-Weiss Potts model.

3.3.3 Phase Transition

After our analysis, we are able to conclude that the Curie-Weiss Potts model for $q \geq 3$ undergoes a first-order (or discontinuous) phase transition at critical inverse temperature

$$\beta_c(q) = \frac{(q-1)\log(q-1)}{q-2} \tag{3.16}$$

since the order parameter $\xi(\beta)$ that minimizes the free energy function f_β has a jump discontinuity at β_c (see Figure 9).

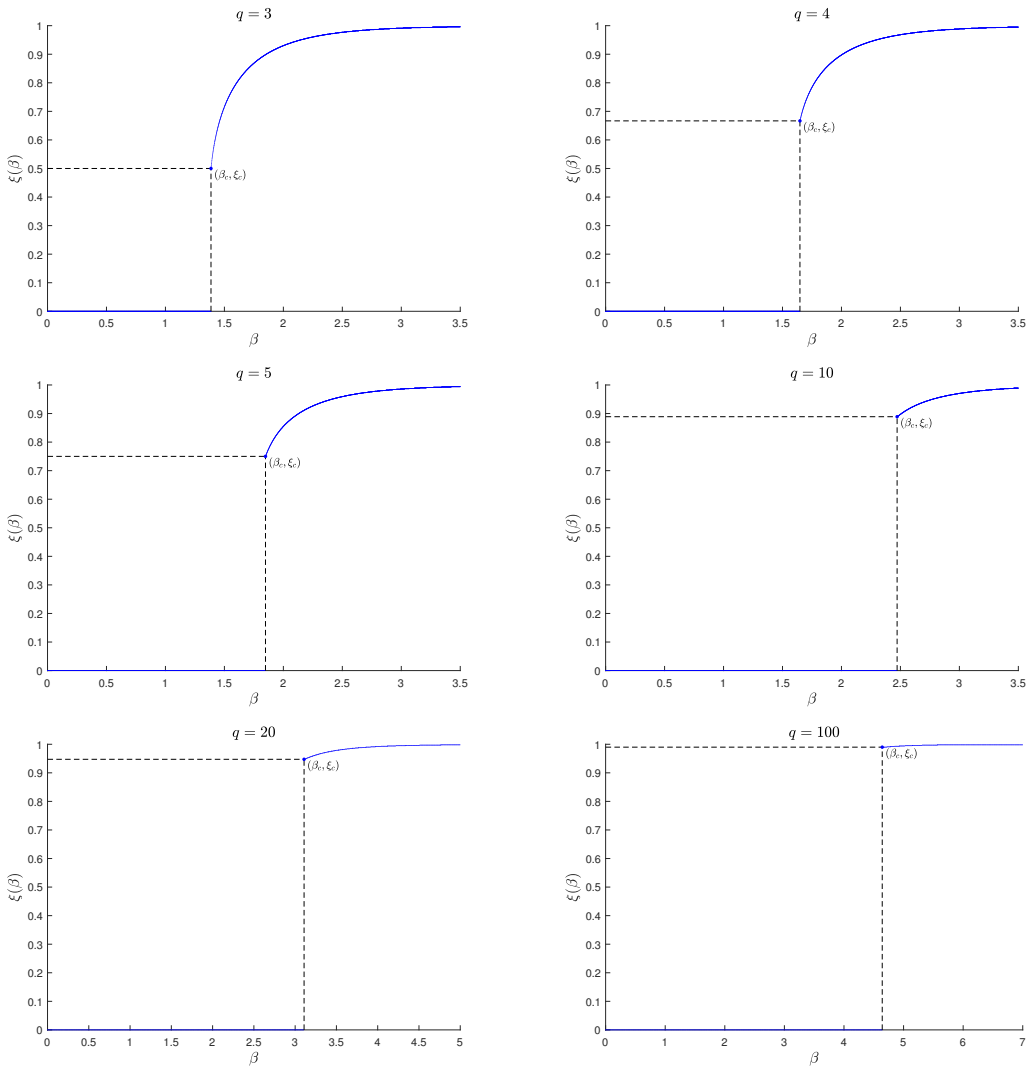

Fig. 9: Jump discontinuity of the minimizing order parameter $\xi(\beta)$ for different values of q. Since the order parameter jumps from zero to $\xi_c = (q-2)/(q-1)$, the corresponding width of the gap is given by ξ_c. Therefore, the graph approaches a step function for increasing values of q because $\xi_c(q) \to 1$ for $q \to \infty$.

This jump discontinuity in the order parameter is directly connected with a jump discontinuity in the entropy density $\tilde{S}$ at the critical inverse temperature β_c (see Figure 10 on the next page). At this transition point, we can calculate the so-called *latent heat* L. Following [KMS54], the latent heat of the q-state Curie-Weiss Potts model is defined by

$$L := \frac{1}{\beta_c}\Big(\tilde{S}(\hat{q}) - \tilde{S}(\hat{x}_{\beta_c(q),q})\Big)\,,$$

where $\beta_c(q)$ denotes the critical inverse temperature and $\tilde{S}$ is the entropy density of this model. The proportions vectors at the beginning ($x = \hat{x}_{\beta_c(q),q}$) and at the end ($x = \hat{q}$) of the transition are given in Remark 3.30. Hence the latent heat can be explicitly computed and we obtain the following result according to [KMS54]:

Proposition 3.35. *The q-state Curie-Weiss Potts model undergoes a first-order phase transition for $q \geq 3$ because the latent heat L of the transition is non-vanishing.*

Proof. We calculate the latent heat L and show that it is not zero for all $q \geq 3$. Since $\hat{q}$ is the uniform distribution on $Q = \{1, \ldots, q\}$, Proposition 3.16 tells us that it maximizes the entropy density, i.e. $\tilde{S}(\hat{q}) = \log(q)$. Additionally, we have

$$\begin{aligned}
\tilde{S}(\hat{x}_{\beta_c(q),q}) &= -\Big(1 - \frac{1}{q}\Big)\log\Big(1 - \frac{1}{q}\Big) - (q-1)\frac{1}{q(q-1)}\log\Big(\frac{1}{q(q-1)}\Big) \\
&= -\frac{1}{q}\Big((q-1)\Big(\log(q-1) - \log(q)\Big) - \log(q) - \log(q-1)\Big) \\
&= -\frac{1}{q}\Big((q-2)\log(q-1) - q\log(q)\Big) \\
&= -\frac{q-2}{q}\log(q-1) + \log(q)\,.
\end{aligned}$$

Using (3.16), we obtain

$$L = \frac{1}{\beta_c}\Big(\tilde{S}(\hat{q}) - \tilde{S}(\hat{x}_{\beta_c(q),q})\Big) = \frac{(q-2)^2}{q(q-1)}\,.$$

We see that $L \neq 0$ for all $q \geq 3$. In that case, the latent heat is non-vanishing which is directly connected with a jump in the entropy density and in the order parameter. Therefore, we have a first order phase transition.

□

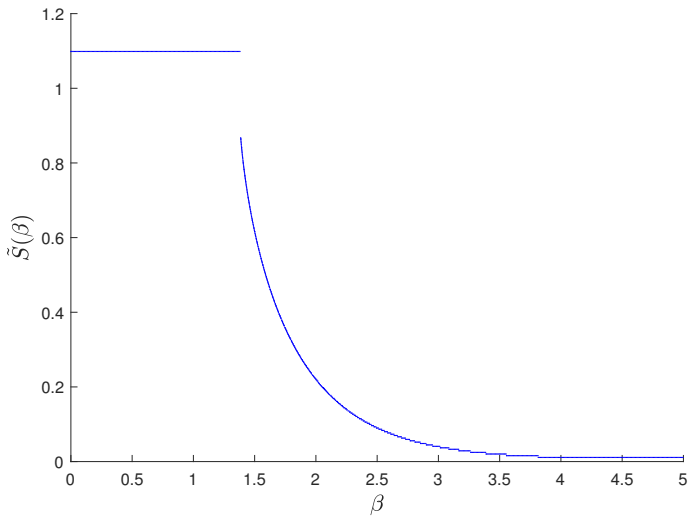

Fig. 10: Entropy density $\tilde{S}(\beta)$ of the Curie-Weiss Potts model for $q = 3$ states as a function of the inverse temperature $\beta > 0$. The entropy density in the unordered phase is maximal. Between the ordered and the disordered phase, there is a discontinuity (a jump in entropy).

At this point, we want to discuss this first-order phase transition from a Physics perspective. Imagine we start in the ordered phase; we continuously pump energy into the system which causes the temperature to rise (i.e. β decreases). But the temperature only increases until we reach the critical temperature (which is indirectly proportional to β_c). At this point, all the energy we put into the system is used to transform the ordered phase into the disordered one. During this transition between phases, the temperature stays constant. The temperature of the system will increase again as soon as the system is completely in the unordered phase. The amount of energy that is needed to transfer the phases into each other is called *latent heat*. We calculated it in the proof of Proposition 3.35. We have to put this amount of energy into the system when going from the ordered phase to the disordered one. When going the opposite way, the system releases this energy when crossing the phase boundary.

3.3.4 Limiting Distribution of the Proportions Vector

At the end of this chapter, we take a closer look at the thermodynamic limit. More precisely, we describe the behavior of the proportions vector $x \in \mathcal{S}$ and its distribution $\sigma_{n,\beta}(\cdot) = \mu_{n,\beta}(x \in \cdot)$ when the underlying graph becomes infinitely large, i.e. for $n \to \infty$.

We will soon see that the free energy function $f_\beta : \mathcal{S} \to \mathbb{R}$ again plays a central role. Therefore, we look at the structure of its global minima. We already calculated the global minimum points for the case $\beta = \beta_c$ when we tried to understand the phase transition of the model. Obviously, the position of these global minima depends on the inverse temperature β and the number of colors q. We denote the set of global minimizers of f_β by $\Gamma_{\beta,q}$ and state its structure following [CDL12]:

Proposition 3.36. *Let $\beta_c(q)$ be the critical inverse temperature of the q-state Curie-Weiss Potts model. Then the set of global minimizers $\Gamma_{\beta,q}$ of the free energy function $f_\beta : \mathcal{S} \to \mathbb{R}$ is given by*

$$\Gamma_{\beta,q} = \begin{cases} \{\hat{q}\} & \text{if } \beta < \beta_c(q)\,, \\ \{\hat{q},\, T^1\hat{x}_{\beta_c(q),q}, \ldots,\, T^q\hat{x}_{\beta_c(q),q}\} & \text{if } \beta = \beta_c(q)\,, \\ \{\, T^1\hat{x}_{\beta,q}, \ldots,\, T^q\hat{x}_{\beta,q}\} & \text{if } \beta > \beta_c(q)\,, \end{cases}$$

with $T^k : \mathcal{S} \to \mathcal{S}$ interchanging the first and the k-th component, and

$$\hat{x}_{\beta,q} = \Big(\frac{1+(q-1)\xi}{q}, \frac{1-\xi}{q}, \ldots, \frac{1-\xi}{q}\Big)\,.$$

Proof. The general form $\hat{x}_{\beta,q}$ of the global minimizers was derived in Section 3.3.1 and is given in (3.11). The set of global minimizers at criticality is stated in Remark 3.30. The missing parts of the proof can be found in [EW90]. □

Remark 3.37. Let $x = (x_1, \ldots, x_q) \in \mathcal{S}$ be a global minimizer of f_β and let $Q = \{1, \ldots, q\}$. Then the following statements are true:

(i) The inequality $\min_{i \in Q}(x_i) > 0$ holds.

(ii) The proportions vector x has at least $(q-1)$ times the same component $\min_{i \in Q}(x_i)$.

(iii) The value of ξ needed to obtain $\hat{x}_{\beta,q}$ is known in implicit form given by the self-consistency equation (3.10).

(iv) In particular for $\beta = \beta_c$, we have, next to the trivial solution $\xi = 0$, another exact solution $\xi_c = (q-2)/(q-1)$ of (3.10). Hence we have

$$\hat{x}_{\beta_c(q),q} = \left(1 - \frac{1}{q}, \frac{1}{q(q-1)}, \ldots, \frac{1}{q(q-1)}\right).$$

Proof. A proof of (i) and (ii) can be found in [GRW10]. □

If we know the location of the global minima of f_β, it is easy to compute the free energy $\Psi(\beta)$ of the system in the thermodynamic limit according to (3.6) (see Figure 11).

The following theorem following [EW90] states that the limiting distribution of the sequence $(\sigma_{n,\beta})_{n\geq 1}$ depends completely on the location of the global minima of the free energy function, i.e. on the set of global minimizers $\Gamma_{\beta,q}$. We consider the weak convergence of measures and write $\sigma_{n,\beta} \Rightarrow \sigma_\beta$ for $n \to \infty$.

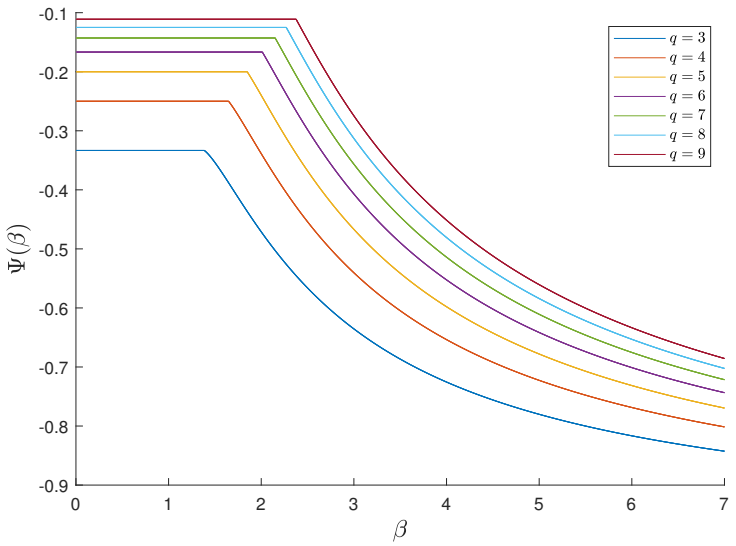

Fig. 11: Free energy $\Psi(\beta) = \beta^{-1}\Big(\min_{x\in\mathcal{S}} f_\beta(x) + \log(q)\Big)$ in the thermodynamic limit ($n \to \infty$) of the q-state Curie-Weiss Potts model for different values of q. The function has a kink at the critical inverse temperature $\beta_c(q)$ which corresponds to a non-analyticity and hence a phase transition.

Theorem 3.38. *Let $\sigma_{n,\beta}$ be the distribution of the proportions vector for the q-state Curie-Weiss Potts model. Then we have*

(i) for $0 < \beta < \beta_c$ that

$$\sigma_{n,\beta} \Rightarrow \delta_{\hat{q}} \quad as\ n \to \infty\,,$$

(ii) for $\beta > \beta_c$ that

$$\sigma_{n,\beta} \Rightarrow \frac{1}{q}\sum_{k=1}^{q} \delta_{T^k \hat{x}_{\beta,q}} \quad as\ n \to \infty$$

(iii) and for $\beta = \beta_c$ that

$$\sigma_{n,\beta} \Rightarrow a\delta_{\hat{q}} + \frac{1-a}{q}\sum_{k=1}^{q} \delta_{T^k \hat{x}_{\beta_c(q),q}} \quad as\ n \to \infty$$

with $a \in (0,1)$.

Proof. A proof can be found in [EW90]. □

Theorem 3.38 summarizes some findings that we made in the course of this thesis. For high temperatures, i.e. for small β, the system always chooses configurations which proportions vector is close to uniformly distributed. For small temperatures, i.e. for high β, the system is always in an ordered state with one color dominating over the others. We also see that each ordered state has the same probability $1/q$ to appear. The special case appears at criticality. Here the system chooses either the one unordered state with probability a or one of the q ordered phases with probability $(1-a)/q$. Hence the distribution of the proportions vector of the Curie-Weiss Potts model is completely described by the set of global minimizers $\Gamma_{\beta,q}$ of the free energy function f_β. This and the statement of the theorem is summarized in the following corollary.

Corollary 3.39. *Let $\sigma_{n,\beta}$ be the distribution of the proportions vector and let f_β be the free energy function of the q-state Curie-Weiss Potts model. Then the set of global minimizers of f_β is the support of the limiting distribution σ_β, i.e.*

$$\mathrm{supp}(\sigma_\beta) = \Gamma_{\beta,q}\,.$$

Proof. This is a direct consequence of Theorem 3.38. □

4 Glauber Dynamics

We start by giving a short introduction to Markov Chain Monte Carlo (MCMC) methods as a way to sample from a given probability distribution. We then focus on the Glauber dynamics as a special MCMC-method and apply it to the Curie-Weiss model as well as to the Curie-Weiss Potts model. Additionally, two simulations regarding the Curie-Weiss Potts model are presented and discussed.

4.1 Introduction to Markov Chain Monte Carlo

In Section 2.2.2, we saw that a given Markov chain $(X_t)_{t\geq 0}$ with irreducible and aperiodic transitions matrix P converges to its unique stationary distribution π. At this point we want to consider the inverse problem. Given any probability distribution $\tilde{\pi} \in \mathscr{M}_1(\Omega)$, can we construct a Markov chain that has $\tilde{\pi}$ as its stationary distribution?

When being concerned with this question, one might also ask why we are interested in constructing such a chain. Therefore, let us consider an example from the context of statistical mechanics, e.g. the standard nearest-neighbor q-state Potts model on a graph $G = (\Lambda, \mathscr{E})$. If we want to sample from the Gibbs distribution μ of this model, we have to calculate the partition function, that is of the form

$$Z = \sum_{\omega \in \Omega} \exp\Big(- H(\omega)\Big),$$

where H denotes the Hamiltonian of the model. This is a sum over $|\Omega| = q^{|\Lambda|}$ exponential terms and one has to consider that there is also a sum over $|\mathscr{E}|$ terms included in the Hamiltonian. In order to measure the computational efficiency of an algorithm (here a computation), we want to know the number of elementary operations (e.g. arithmetic operations) that are performed as a function of the input [AB07]. So suppose our underlying graph G is the complete graph $\mathcal{C}_n$ with n vertices and $n(n-1)/2$ edges. Then our input is given by the number of vertices n. So in order to compute the partition function, there are at least

$$q^n \cdot \frac{n(n-1)}{2} \in \mathcal{O}(q^n)$$

elementary operations required. Hence the computational efficiency of computing

the partition function is of exponential order. In concrete terms: for $n = 100$ and $q = 3$ we have approximately $2.55 \cdot 10^{51}$ required arithmetic operations which is of unthinkable magnitude. If we even consider some realistic system of macroscopic size ($n \approx 10^{23}$), then the evaluation of the partition function Z seems impossible even for any computer with an extremely high level of performance in reasonable times [Bax07].

So for large values of n, the state space Ω is even larger and the distribution μ cannot be easily generated because of the form of its normalization constant. The idea is then to construct a Markov chain $(X_t)_{t\geq 0}$ that has the desired distribution μ as stationary distribution. If the constructed chain is also irreducible and aperiodic, then Theorem 2.28 tells us that the chain will converge towards its stationary distribution. Hence, if we wait long enough, i.e. for large enough $t \geq 0$, then the distribution of X_t will be close to μ. [Kle13]

This described strategy of sampling from a given probability distribution using Markov chains is called *Markov Chain Monte Carlo* (MCMC). These methods also play a significant role not only in statistical mechanics but also in Bayesian inference and optimization theory. Let us suppose we want to generate samples from the distribution $\pi \in \mathscr{M}_1(\Omega)$, because these samples cannot be drawn directly. If we can evaluate $\pi(x)$ for all $x \in \Omega$ up to a normalization constant, then MCMC is the method of our choice. The irreducible and aperiodic Markov chain with stationary distribution π we construct is called *MCMC - sampler*. The problem is normally not to construct such a sampler but to design it in a way that it converges quickly to the desired distribution. [AdF03]

The *Metropolis-Hastings algorithm* represents one popular realization of the MCMC - method. We intend to generate samples from the distribution $\pi \in \mathscr{M}_1(\Omega)$. Let us suppose we have an irreducible Markov chain with transition matrix Q, state space Ω and an arbitrary stationary distribution different from π. Now this algorithm is based on modifying this chain in a way that it converges to the desired target distribution π. According to [LPW09], the transition

matrix P of the Metropolis chain is given by

$$P(x,y) := \begin{cases} Q(x,y)\min\left(\frac{\pi(y)Q(y,x)}{\pi(x)Q(x,y)},1\right) & \text{if } y \neq x\,, \\ 1 - \sum\limits_{z\in\Omega\setminus\{x\}} Q(x,z)\min\left(\frac{\pi(z)Q(z,x)}{\pi(x)Q(x,z)},1\right) & \text{if } y = x\,, \end{cases}$$

with $x, y \in \Omega$. It can be shown that this transition matrix defines a reversible Markov chain with stationary distribution $\pi \in \mathscr{M}_1(\Omega)$ (see e.g. [BZ20, p. 73]).

4.2 Single-Site Glauber Dynamics

Given a probability distribution $\pi \in \mathscr{M}_1(\Omega)$, we consider another method instead of the aforementioned Metropolis-Hastings algorithm to construct a Markov chain with given stationary distribution π. This MCMC - method is called *Glauber dynamics* and is used if the state space Ω is of the form Q^Λ where Q is a finite set and Λ denotes the vertex set of a graph.

4.2.1 Definition

The Glauber dynamics is based on the idea to adjust the current state of the Markov chain locally (at a single site) to the desired stationary distribution $\pi \in \mathscr{M}_1(\Omega)$ [Kle13]. We are then especially interested in those configurations that only differ from a given configuration in at most one vertex. Therefore, we make the following definition according to [LPW09]:

Definition 4.1. *Let $\omega \in \Omega$ be a configuration and $i \in \Lambda$ be a vertex. Then*

$$\Omega_i(\omega) := \{\omega' \in \Omega \mid \omega_i = \omega'_j \text{ for all } j \neq i\}$$

is defined as the set of all configurations in Ω that are identical to $\omega \in \Omega$ except in $i \in \Lambda$.

Lemma 4.2. *Let $\omega, \omega' \in \Omega$ and $i \in \Lambda$. If we have $\omega \in \Omega_i(\omega')$, then we also have $\omega' \in \Omega_i(\omega)$ and consequently $\Omega_i(\omega) = \Omega_i(\omega')$ for a fixed $i \in \Lambda$.*

Proof. Since $\omega \in \Omega_i(\omega')$ we have have that the configurations ω and ω' only differ in the i-th component. This is obviously the same statement as $\omega' \in \Omega_i(\omega)$. So in total we have $\omega_i = \omega'_i$ for all $i \neq j$ and due to Definition 4.1 we obtain $\Omega_i(\omega) = \Omega_i(\omega')$. □

Now we describe the *(single-site) Glauber dynamics* for the target distribution $\pi \in \mathscr{M}_1(\Omega)$ whose support is Ω following [LPW09]. This Markov chain updates a configuration $\omega \in \Omega$ in the following way:

(1) Choose a vertex $i \in \Lambda$ according to a probability distribution $\nu \in \mathscr{M}_1(\Lambda)$ with $\nu(i) > 0$ for all $i \in \Lambda$.

(2) Choose a new configuration $\omega' \in \Omega$ according to the the distribution π conditioned on the set $\Omega_i(\omega)$ of all configurations that are equal to ω except in i.

According to this rule for updating a configuration, we can of course construct a corresponding transition matrix $P \in \mathbb{R}^{|\Omega|\times|\Omega|}$. This (stochastic) matrix is given in the next theorem.

Theorem 4.3. *Let $\nu \in \mathscr{M}_1(\Lambda)$ and $\pi \in \mathscr{M}_1(\Omega)$ be two probability distributions with $\operatorname{supp}(\nu) = \Lambda$ and $\operatorname{supp}(\pi) = \Omega$. Then the (single-site) Glauber dynamics for π is the irreducible, aperiodic and reversible Markov chain $(X_t)_{t\geq 0}$ with transition matrix*

$$P(\omega, \omega') = \sum_{i\in\Lambda} \nu(i)\pi(\omega' \mid \Omega_i(\omega)) \tag{4.1}$$

and stationary distribution π.

Proof. Firstly, we realize that we can rewrite the conditional probability in (4.1) using the indicator function:

$$P(\omega, \omega') = \sum_{i\in\Lambda} \nu(i) \frac{\pi\Big(\{\omega'\} \cap \Omega_i(\omega)\Big)}{\pi\Big(\Omega_i(\omega)\Big)} = \sum_{i\in\Lambda} \nu(i) \frac{\pi(\omega')}{\pi\Big(\Omega_i(\omega)\Big)} \mathbb{1}_{\Omega_i(\omega)}(\omega')\,. \tag{4.2}$$

Before we prove the important properties of this chain, we show that the matrix P defined by (4.1) really is stochastic. This is indeed the case since

$$\begin{aligned}
\sum_{\omega'\in\Omega} P(\omega, \omega') &= \sum_{\omega'\in\Omega} \sum_{i\in\Lambda} \nu(i) \frac{\pi(\omega')}{\pi\Big(\Omega_i(\omega)\Big)} \mathbb{1}_{\Omega_i(\omega)}(\omega') \\
&= \sum_{i\in\Lambda} \nu(i) \sum_{\omega'\in\Omega_i(\omega)} \frac{\pi(\omega')}{\pi\Big(\Omega_i(\omega)\Big)} \\
&= 1\,.
\end{aligned}$$

We now are ready to prove (i) irreducibility, (ii) aperiodicity and (iii) reversibility with respect to π. We do this in the given order starting with irreducibility.

(i) According to Definition 2.8, we have to show that for all $\omega, \omega' \in \Omega$ there exists some $k \in \mathbb{N}$ such that $P^k(\omega, \omega') > 0$. Let $\omega, \omega' \in \Omega$ and let $1 \leq k \leq |\Lambda|$ be the number of vertices $i \in \Lambda$ with $\omega_i \neq \omega'_i$; we will show that $P^k(\omega, \omega') > 0$.

Without loss of generality, we assume that the components of ω and ω' are labelled by $1, \dots, |\Lambda|$ in a way such that the first k components of ω and ω' are different. Then, we can construct a sequence of states $(\omega^{(i)})_{i=0}^{k}$ in Ω starting in ω and ending in ω' where at each step one component is changed, i.e.

$$\begin{aligned}
\omega^{(0)} &= (\omega_1, \dots, \omega_{|\Lambda|}) = \omega \\
\omega^{(1)} &= (\omega'_1, \omega_2, \dots, \omega_{|\Lambda|}) \\
\omega^{(2)} &= (\omega'_1, \omega'_2, \omega_3, \dots, \omega_{|\Lambda|}) \\
&\vdots \\
\omega^{(k)} &= (\omega'_1, \dots, \omega'_k, \omega_{k+1}, \dots, \omega_{|\Lambda|}) = \omega' \,.
\end{aligned}$$

Then for all $j \in \{0, \dots, k-1\}$, we have

$$P(\omega^{(j)}, \omega^{(j+1)}) = \sum_{i=1}^{|\Lambda|} \nu(i) \frac{\pi(\omega^{(j+1)})}{\pi\Big(\Omega_i(\omega^{(j)})\Big)} \mathbb{1}_{\Omega_i(\omega^{(j)})}(\omega^{(j+1)}) \,.$$

By construction of the sequence $(\omega^{(i)})_{i=0}^{k}$, we see that

$$\mathbb{1}_{\Omega_i(\omega^{(j)})}(\omega^{(j+1)}) = \begin{cases} 1 & \text{if } i = j+1 \,, \\ 0 & \text{if } i \neq j+1 \,, \end{cases}$$

and hence we obtain

$$P(\omega^{(j)}, \omega^{(j+1)}) = \nu(j+1) \frac{\pi(\omega^{(j+1)})}{\pi\Big(\Omega_{j+1}(\omega^{(j)})\Big)} > 0$$

where we used that $\Omega_i(\omega) \subset \Omega = \mathrm{supp}(\pi)$ and $\mathrm{supp}(\nu) = \Lambda$. Using this result, we finally obtain

$$P^k(\omega, \omega') \geq \prod_{j=0}^{k-1} P(\omega^{(j)}, \omega^{(j+1)}) > 0 \,, \tag{4.3}$$

and hence P is irreducible.

(ii) According to Lemma 2.12, we only have to show that the matrix P has at least one diagonal entry $P(\omega, \omega) > 0$ for $\omega \in \Omega$ since we already know that P

is irreducible. We have

$$P(\omega,\omega) = \sum_{i\in\Lambda} \nu(i) \frac{\pi(\omega)}{\pi\Big(\Omega_i(\omega)\Big)} \mathbb{1}_{\Omega_i(\omega)}(\omega) = \sum_{i\in\Lambda} \nu(i) \frac{\pi(\omega)}{\pi\Big(\Omega_i(\omega)\Big)} > 0\,,$$

where we used the same arguments as in (4.3). Thus, in our case, all diagonal elements are positive. Hence P is aperiodic.

(iii) Lastly, we have to show that P is reversible with respect to π. Therefore, we show that π satisfies the detailed balance equations

$$\pi(\omega)P(\omega,\omega') = \pi(\omega')P(\omega',\omega)$$

for all $\omega,\omega' \in \Omega$. As a direct consequence, we obtain that π is also stationary for P. Let $\omega,\omega' \in \Omega$. We consider three different cases. The first case $\omega = \omega'$ is trivial. In the second case, we assume that $\omega_i \neq \omega'_j$ for more than one $i \in \Lambda$. Hence the indicator function in (4.2) is always zero, consequently we have $P(\omega,\omega') = P(\omega',\omega) = 0$ and the detailed balance equations are satisfied. For the third and final case, we assume that $\omega_i \neq \omega'_i$ for exactly one $i \in \Lambda$. Hence $\omega \in \Omega_i(\omega')$ and according to Lemma 4.2 we have that $\Omega_i(\omega') = \Omega_i(\omega')$. Then we have

$$\pi(\omega)P(\omega,\omega') = \pi(\omega)\nu(i)\frac{\pi(\omega')}{\pi\Big(\Omega_i(\omega)\Big)} = \pi(\omega')\nu(i)\frac{\pi(\omega)}{\pi\Big(\Omega_i(\omega')\Big)} = \pi(\omega')P(\omega',\omega)\,,$$

so the detailed balance equations are also satisfied. □

Since the constructed chain is irreversible and aperiodic, it will converge to its stationary distribution according to Remark 2.29.

Remark 4.4. When we construct a chain using the Glauber dynamics, we normally pick a vertex i uniformly at random from Λ at each step. So in the following, we set $\nu = \mathcal{U}_\Lambda$ and have $\nu(i) = 1/|\Lambda|$ for all $i \in \Lambda$. Hence, the transition matrix for the Glauber dynamics is in general given by

$$P(\omega,\omega') = \frac{1}{|\Lambda|}\sum_{i\in\Lambda} \frac{\pi(\omega')}{\pi\Big(\Omega_i(\omega)\Big)} \mathbb{1}_{\Omega_i(\omega)}(\omega')\,.$$

4.2.2 Example: Curie-Weiss Model

Before we examine the Glauber dynamics for the Curie-Weiss Potts model, we consider the simpler *Curie-Weiss model*. This is the mean-field approximation of the classical Ising model and it corresponds to the Curie-Weiss Potts model with $q = 2$ colors.

We denote the two colors with $+1$ and -1. Then, for $|\Lambda| = n$ vertices, the state space of the Curie-Weiss model is given by $\Omega_n := \{\pm 1\}^n$. Since the Curie-Weiss model is a special case of the Curie-Weiss Potts model, their Hamiltonians are the same. Nevertheless, we denote the Curie-Weiss Hamiltonian by $H^{\mathrm{CW}}_{n,\beta}$ in order to remind the reader that only two different kind of spins exist, i.e. that $\omega_i \in \{\pm 1\}$ for any $i \in \Lambda$.

Definition 4.5. *The Curie-Weiss Hamiltonian for a configuration $\omega \in \Omega_n$ at inverse temperature $\beta > 0$ is given by*

$$H^{\mathrm{CW}}_{n,\beta}(\omega) := -\frac{\beta}{n} \sum_{i,j=1}^{n} \delta(\omega_i, \omega_j)\,. \tag{4.4}$$

In order to describe configurations of the Curie-Weiss model, we introduce two additional quantities following [FV17]:

Definition 4.6. *The* magnetization density $m \in [-1, 1]$ *of a configuration $\omega \in \Omega_n$ of the Curie-Weiss model is given by*

$$m(\omega) := \frac{M(\omega)}{n}\,,$$

where $M(\omega) := \sum_{i=1}^{n} \omega_i$ denotes the total magnetization *of $\omega \in \Omega_n$.*

Let us recall the proportions vector $x \in \mathcal{S}$ as given in Definition 3.9. For the Curie-Weiss model, i.e. for $q = 2$, this vector takes the form

$$x(\omega) = \Big(x_{+1}(\omega), x_{-1}(\omega)\Big) = \left(\frac{1}{n}\sum_{i=1}^{n} \delta(\omega_i, +1), \frac{1}{n}\sum_{i=1}^{n} \delta(\omega_i, -1)\right).$$

We observe that, for $\omega_i \in \{\pm 1\}$, the identity $\omega_i = \delta(\omega_i, +1) - \delta(\omega_i, -1)$ holds.

Using this, we can write

$$x_{+1}(\omega) - x_{-1}(\omega) = \frac{1}{n}\sum_{i=1}^{n}\Big(\delta(\omega_i,+1) - \delta(\omega_i,-1)\Big) = \frac{1}{n}\sum_{i=1}^{n}\omega_i = m(\omega)\,,$$

i.e. there is a relation between the proportions vector and the magnetization density defined above. So instead of using the magnetization density, we could also use the proportions vector.

Let us go one step further. Therefore, we consider the Gibbs distribution $\mu_{n,\beta} : \Omega_n \to [0,1]$ for the Curie-Weiss model on Ω_n given by

$$\mu_{n,\beta}(\omega) = \frac{\exp(-H^{\mathrm{CW}}_{n,\beta}(\omega))}{Z_{n,\beta}}$$

with $\mathrm{supp}(\mu_{n,\beta}) = \Omega_n$ for every finite $\beta > 0$. Our aim is to sample from this distribution using the Glauber dynamics.

Proposition 4.7. *Let $\mu_{n,\beta}$ be the Gibbs distribution for the Curie-Weiss model on Ω_n. Then the entries of the transition matrix $P \in \mathbb{R}^{n^2\times n^2}$ of the Glauber dynamics for $\mu_{n,\beta}$ are given by*

$$P(\omega,\omega') = \frac{1}{n}\sum_{i=1}^{n}\frac{1}{1+\exp\left(2\frac{\beta}{n}(1 - M(\omega')\,\omega_i')\right)}\,\mathbb{1}_{\Omega_i(\omega)}(\omega') \tag{4.5}$$

with $\omega, \omega' \in \Omega_n$.

Proof. For $\omega_i, \omega_j \in \{\pm 1\}$, we easily verify that

$$\delta(\omega_i,\omega_j) = \frac{1+\omega_i\omega_j}{2}$$

holds. Hence, we can rewrite the Hamiltonian (4.4) using the total magnetization which yields

$$H^{\mathrm{CW}}_{n,\beta}(\omega) = -\frac{\beta}{n}\sum_{i,j=1}^{n}\left(\frac{1+\omega_i\omega_j}{2}\right) = -\frac{n\beta}{2} - \frac{\beta}{2n}\sum_{i=1}^{n}\omega_i\sum_{j=1}^{n}\omega_j = -\frac{n\beta}{2} - \frac{\beta}{2n}M(\omega)^2\,.$$

According to Theorem 4.3, we have to calculate $\mu_{n,\beta}(\omega' \mid \Omega_i(\omega))$. We have

$$\begin{aligned}\mu_{n,\beta}\Big(\omega' \mid \Omega_i(\omega)\Big) &= \frac{\mu_{n,\beta}(\omega')}{\sum\limits_{\tilde{\omega}\in\Omega_i(\omega)} \mu(\tilde{\omega})}\, \mathbb{1}_{\Omega_i(\omega)}(\omega') \\ &= \frac{Z_{n,\beta}^{-1}\, \exp\left(\frac{n\beta}{2} + \frac{\beta}{2n} M(\omega')^2\right)}{\sum\limits_{\tilde{\omega}\in\Omega_i(\omega)} Z_{n,\beta}^{-1}\, \exp\left(\frac{n\beta}{2} + \frac{\beta}{2n} M(\tilde{\omega})^2\right)}\, \mathbb{1}_{\Omega_i(\omega)}(\omega') \qquad (4.6) \\ &= \frac{\exp\left(\frac{\beta}{2n} M(\omega')^2\right)}{\sum\limits_{\tilde{\omega}\in\Omega_i(\omega)} \exp\left(\frac{\beta}{2n} M(\tilde{\omega})^2\right)}\, \mathbb{1}_{\Omega_i(\omega)}(\omega')\,,\end{aligned}$$

where we see that the partition function $Z_{n,\beta}$ and some other terms cancel out. In the next step, we examine what elements $\tilde{\omega}$ are contained in the set $\Omega_i(\omega)$ to rewrite the sum in the denominator of (4.6). Since this is only of interest if the indicator function in (4.6) is non-zero, we already know that $\omega' \in \Omega_i(\omega)$. So we are interested in all configurations $\tilde{\omega} \in \Omega_n$ that are identical to ω' except in i. Since there are only the two possibilities $+1$ and -1 for the spin in i, this implies that $\Omega_i(\omega)$ only consists of the two elements

$$\begin{aligned}\tilde{\omega}^{(1)} &= (\omega'_1, \ldots, \omega'_i, \ldots, \omega'_n) = \omega'\,, \\ \tilde{\omega}^{(2)} &= (\omega'_1, \ldots, -\omega'_i, \ldots, \omega'_n)\,.\end{aligned}$$

Therefore, the squared total magnetizations are given by $M\Big(\tilde{\omega}^{(1)}\Big)^2 = M(\omega')^2$ and

$$M\Big(\tilde{\omega}^{(2)}\Big)^2 = \Big(\sum_{j=1}^{n} \omega'_j - 2\omega'_i\Big)^2 = M(\omega')^2 - 4\,\omega'_i\, M(\omega') + 4 = M(\omega')^2 + 4\Big(1 - M(\omega')\omega'_i\Big)\,.$$

Hence the denominator in (4.6) reduces to

$$\begin{aligned}\sum_{\tilde{\omega}\in\Omega_i(\omega)} \exp\left(\frac{\beta}{2n} M(\tilde{\omega})^2\right) &= \exp\left(\frac{\beta}{2n} M(\omega')^2\right) + \exp\left(\frac{\beta}{2n}\Big(M(\omega')^2 + 4(1 - M(\omega')\omega'_i)\Big)\right) \\ &= \exp\left(\frac{\beta}{2n} M(\omega')^2\right)\left(1 + \exp\left(2\frac{\beta}{n}\Big(1 - M(\omega')\omega'_i\Big)\right)\right).\end{aligned}$$

Substituting this expression back into (4.6), we see that one exponential term

cancels out and we obtain

$$\mu_{n,\beta}(\omega' \mid \Omega_i(\omega)) = \frac{1}{1+\exp\left(2\frac{\beta}{n}(1-M(\omega')\,\omega_i')\right)}\,\mathbb{1}_{\Omega_i(\omega)}(\omega')\,.$$

We recall Remark 4.4 and acquire the expression

$$P(\omega,\omega') = \frac{1}{n}\sum_{i=1}^{n}\frac{1}{1+\exp\left(2\frac{\beta}{n}(1-M(\omega')\,\omega_i')\right)}\,\mathbb{1}_{\Omega_i(\omega)}(\omega')$$

for an entry of the transition matrix P of the Glauber dynamics for $\mu_{n,\beta}$. □

Next, we determine some information about the speed of convergence of the Glauber dynamics for $\mu_{n,\beta}$. Hence, we try to find bounds for the distance to stationarity $d(t)$ and for the ε-mixing time $t_{\text{mix}}(\varepsilon)$. In order to do so, we use some results from section 2.3 about spectral methods for Markov chains. Therefore, we are interested in the eigenvalues of the transition matrix P of the Glauber dynamics. Unfortunately, determining these eigenvalues is not an easy task. For demonstration, we consider the Glauber dynamics for the Curie-Weiss model with only $n = 2$ vertices. Then the spate state consists of only 4 elements, i.e.

$$\Omega_2 = \{(+1,+1),(+1,-1),(-1,+1),(-1,-1)\}\,.$$

This is the simplest non-trivial case but finding the eigenvalues of the transition matrix requires some exhausting calculations.

Proposition 4.8. *The eigenvalues λ of the transition matrix P with entries given in* (4.5) *for the Curie-Weiss model on Ω_2 are given by*

$$\lambda_1 = 0\,,\quad \lambda_2 = \frac{1}{\mathrm{e}^{\beta}+1}\,,\quad \lambda_3 = \frac{\mathrm{e}^{\beta}}{\mathrm{e}^{\beta}+1}\quad \textit{and}\quad \lambda_4 = 1\,.$$

Proof. Since we consider $n = 2$ vertices, the transition matrix is on the set $\mathbb{R}^{2\times 2}$. Using (4.5), we can directly write down the transition matrix P. We have

$$P = \begin{pmatrix} \frac{\mathrm{e}^{\beta}}{\mathrm{e}^{\beta}+1} & \frac{1}{2}\frac{1}{\mathrm{e}^{\beta}+1} & \frac{1}{2}\frac{1}{\mathrm{e}^{\beta}+1} & 0 \\ \frac{1}{2}\frac{\mathrm{e}^{\beta}}{\mathrm{e}^{\beta}+1} & \frac{1}{\mathrm{e}^{\beta}+1} & 0 & \frac{1}{2}\frac{\mathrm{e}^{\beta}}{\mathrm{e}^{\beta}+1} \\ \frac{1}{2}\frac{\mathrm{e}^{\beta}}{\mathrm{e}^{\beta}+1} & 0 & \frac{1}{\mathrm{e}^{\beta}+1} & \frac{1}{2}\frac{\mathrm{e}^{\beta}}{\mathrm{e}^{\beta}+1} \\ 0 & \frac{1}{2}\frac{1}{\mathrm{e}^{\beta}+1} & \frac{1}{2}\frac{1}{\mathrm{e}^{\beta}+1} & \frac{\mathrm{e}^{\beta}}{\mathrm{e}^{\beta}+1} \end{pmatrix} = \frac{1}{\mathrm{e}^{\beta}+1}\begin{pmatrix} \mathrm{e}^{\beta} & \frac{1}{2} & \frac{1}{2} & 0 \\ \frac{1}{2}\mathrm{e}^{\beta} & 1 & 0 & \frac{1}{2}\mathrm{e}^{\beta} \\ \frac{1}{2}\mathrm{e}^{\beta} & 0 & 1 & \frac{1}{2}\mathrm{e}^{\beta} \\ 0 & \frac{1}{2} & \frac{1}{2} & \mathrm{e}^{\beta} \end{pmatrix}$$

where we additionally wrote P in the form $P = a\tilde{P}$ with $a := (\mathrm{e}^{\beta}+1)^{-1}$ and P as above. To determine the eigenvalues, we calculate the zeroes of the characteristic polynomial χ_P. To simplify further calculations, we write

$$\chi_P(\lambda) = \det(P - \lambda I_4) = \det(a\tilde{P} - a\tilde{\lambda} I_4) = a^4 \det(\tilde{P} - \tilde{\lambda} I_4) = a^4\, \chi_{\tilde{P}}(\tilde{\lambda})$$

with $\lambda := a\tilde{\lambda}$ and characteristic polynomial $\chi_{\tilde{P}}$. We obviously have $\chi_P(\lambda) = 0$ if and only if $\chi_{\tilde{P}}(\tilde{\lambda}) = 0$. Hence we calculate the solutions $\tilde{\lambda}$ of $\chi_{\tilde{P}}(\tilde{\lambda}) = 0$, and consequently, we obtain indirectly our wanted eigenvalues λ. We have

$$\begin{aligned}
\chi_{\tilde{P}}(\tilde{\lambda}) &= \det(\tilde{P} - \tilde{\lambda} I_4) \\
&= \det \begin{pmatrix} \mathrm{e}^{\beta} - \tilde{\lambda} & \frac{1}{2} & \frac{1}{2} & 0 \\ \frac{1}{2}\mathrm{e}^{\beta} & 1-\tilde{\lambda} & 0 & \frac{1}{2}\mathrm{e}^{\beta} \\ \frac{1}{2}\mathrm{e}^{\beta} & 0 & 1-\tilde{\lambda} & \frac{1}{2}\mathrm{e}^{\beta} \\ 0 & \frac{1}{2} & \frac{1}{2} & \mathrm{e}^{\beta} - \tilde{\lambda} \end{pmatrix} \\
&= (\mathrm{e}^{\beta} - \tilde{\lambda}) \det \begin{pmatrix} 1-\tilde{\lambda} & 0 & \frac{1}{2}\mathrm{e}^{\beta} \\ 0 & 1-\tilde{\lambda} & \frac{1}{2}\mathrm{e}^{\beta} \\ \frac{1}{2} & \frac{1}{2} & \mathrm{e}^{\beta} - \tilde{\lambda} \end{pmatrix} - \frac{1}{2}\mathrm{e}^{\beta} \det \begin{pmatrix} \frac{1}{2} & \frac{1}{2} & 0 \\ 0 & 1-\tilde{\lambda} & \frac{1}{2}\mathrm{e}^{\beta} \\ \frac{1}{2} & \frac{1}{2} & \mathrm{e}^{\beta} - \tilde{\lambda} \end{pmatrix} \\
&\quad + \frac{1}{2}\mathrm{e}^{\beta} \det \begin{pmatrix} \frac{1}{2} & \frac{1}{2} & 0 \\ 1-\tilde{\lambda} & 0 & \frac{1}{2}\mathrm{e}^{\beta} \\ \frac{1}{2} & \frac{1}{2} & \mathrm{e}^{\beta} - \tilde{\lambda} \end{pmatrix} \\
&= (\mathrm{e}^{\beta} - \tilde{\lambda}) \det \begin{pmatrix} 1-\tilde{\lambda} & 0 & \frac{1}{2}\mathrm{e}^{\beta} \\ 0 & 1-\tilde{\lambda} & \frac{1}{2}\mathrm{e}^{\beta} \\ \frac{1}{2} & \frac{1}{2} & \mathrm{e}^{\beta} - \tilde{\lambda} \end{pmatrix} - \mathrm{e}^{\beta} \det \begin{pmatrix} \frac{1}{2} & \frac{1}{2} & 0 \\ 0 & 1-\tilde{\lambda} & \frac{1}{2}\mathrm{e}^{\beta} \\ \frac{1}{2} & \frac{1}{2} & \mathrm{e}^{\beta} - \tilde{\lambda} \end{pmatrix}
\end{aligned}$$

where we used Laplace expansion along the first column and the fact that the determinants of the second and third sub-matrix are the same. Now, we apply the Rule of Sarrus and obtain

$$\begin{aligned}
\chi_{\tilde{P}}(\tilde{\lambda}) &= (\mathrm{e}^{\beta} - \tilde{\lambda})\Big((1-\tilde{\lambda})^2(\mathrm{e}^{\beta} - \tilde{\lambda}) - \tfrac{1}{2}(1-\tilde{\lambda})\,\mathrm{e}^{\beta}\Big) - \mathrm{e}^{\beta}\left(\tfrac{1}{2}(1-\tilde{\lambda})(\mathrm{e}^{\beta} - \tilde{\lambda})\right) \\
&= (1-\tilde{\lambda})^2(\mathrm{e}^{\beta} - \tilde{\lambda})^2 - \mathrm{e}^{\beta}(1-\tilde{\lambda})(\mathrm{e}^{\beta} - \tilde{\lambda}) \\
&= -\tilde{\lambda}(1-\tilde{\lambda})(\mathrm{e}^{\beta} - \tilde{\lambda})(\mathrm{e}^{\beta} + 1 - \tilde{\lambda}) \\
&\overset{!}{=} 0\,,
\end{aligned}$$

hence the eigenvalues of $\tilde{P}$ are given by

$$\tilde{\lambda}_1 = 0\,, \quad \tilde{\lambda}_2 = 1\,, \quad \tilde{\lambda}_3 = \mathrm{e}^{\beta} \quad \text{and} \quad \tilde{\lambda}_4 = \mathrm{e}^{\beta} + 1\,.$$

Using the transformation $\lambda = a\tilde{\lambda}$, we obtain the wanted eigenvalues. □

Remark 4.9. If we consider the zero-temperature limit (i.e. $\beta \to \infty$), then the matrix P is not irreducible. In this case, for $n = 2$, we have

$$P_\infty := \lim_{\beta\to\infty} \begin{pmatrix} \frac{\mathrm{e}^{\beta}}{\mathrm{e}^{\beta}+1} & \frac{1}{2}\frac{1}{\mathrm{e}^{\beta}+1} & \frac{1}{2}\frac{1}{\mathrm{e}^{\beta}+1} & 0 \\ \frac{1}{2}\frac{\mathrm{e}^{\beta}}{\mathrm{e}^{\beta}+1} & \frac{1}{\mathrm{e}^{\beta}+1} & 0 & \frac{1}{2}\frac{\mathrm{e}^{\beta}}{\mathrm{e}^{\beta}+1} \\ \frac{1}{2}\frac{\mathrm{e}^{\beta}}{\mathrm{e}^{\beta}+1} & 0 & \frac{1}{\mathrm{e}^{\beta}+1} & \frac{1}{2}\frac{\mathrm{e}^{\beta}}{\mathrm{e}^{\beta}+1} \\ 0 & \frac{1}{2}\frac{1}{\mathrm{e}^{\beta}+1} & \frac{1}{2}\frac{1}{\mathrm{e}^{\beta}+1} & \frac{\mathrm{e}^{\beta}}{\mathrm{e}^{\beta}+1} \end{pmatrix} = \begin{pmatrix} 1 & 0 & 0 & 0 \\ 1/2 & 0 & 0 & 1/2 \\ 1/2 & 0 & 0 & 1/2 \\ 0 & 0 & 0 & 1 \end{pmatrix},$$

and we can see that the ground states $\omega^{(+1)} = (+1, +1)$ and $\omega^{(-1)} = (-1, -1)$ trap the chain which implies that the matrix P_∞ is reducible. Hence, it will not converge necessarily to its stationary distribution $(\frac{1}{2}, 0, 0, \frac{1}{2}) \in \mathscr{M}_1(\Omega_2)$ given in Theorem 3.7. In fact, for an arbitrary initial distribution $\nu = (\nu_1, \nu_2, \nu_3, \nu_4) \in \mathscr{M}_1(\Omega)$, we have

$$\nu P_\infty^t = \nu P_\infty = \left(\nu_1, \tfrac{1}{2}(\nu_1 + \nu_4), \tfrac{1}{2}(\nu_1 + \nu_4), \nu_4\right) \quad \text{for all} \quad t \geq 1\,,$$

since P_∞ is idempotent, i.e. $P_\infty^2 = P_\infty$. Thus, the chain will never converge to its stationary distribution for $\beta \to \infty$.

Now, we are interested in the speed of convergence of the Glauber dynamics for the Curie-Weiss Potts model with $n = 2$ vertices. Therefore, we consider the distance to stationarity $d(t)$ and the ε-mixing time $t_{\mathrm{mix}}(\varepsilon)$ of this Markov chain. Of special interest is the dependency of this quantities on the (inverse) temperature.

In Section 2.3.2, we found out that the distance to stationarity is in particular determined by the eigenvalues of the transition matrix P of the corresponding Markov chain. Especially we derived an upper bound for the distance to stationarity given in (2.20). Adapting this bound to our context, we obtain

$$d(t) \leq \frac{\lambda_3^t}{2\sqrt{\min\limits_{\omega\in\Omega_2} \mu_{2,\beta}(\omega)}}\,,$$

with stationary distribution $\mu_{2,\beta}$ and the second-largest eigenvalue λ_3 of the transition matrix P given in Proposition 4.8. In order to get the minimum in the denominator, we need to compute the partition function of our model. Since the state space Ω_2 consists of only 4 elements, this is easily done:

$$\begin{aligned} Z_{2,\beta} &= \sum_{\omega\in\Omega_2} \exp\left(\frac{\beta}{2}\sum_{i,j=1}^{2}\delta(\omega_i,\omega_j)\right) \\ &= \sum_{\omega\in\Omega_2} \exp\Big(\beta\Big(1+\delta(\omega_1,\omega_2)\Big)\Big) \\ &= 2\,\mathrm{e}^{2\beta}+2\,\mathrm{e}^{\beta}\ . \end{aligned}$$

Hence the entire distribution of $\mu_{2,\beta}$ is given by

$$\begin{aligned} \mu_{2,\beta}(+1,+1) = \mu_{2,\beta}(-1,-1) &= \frac{\mathrm{e}^{\beta}}{2(\mathrm{e}^{\beta}+1)}\,, \\ \mu_{2,\beta}(+1,-1) = \mu_{2,\beta}(-1,+1) &= \frac{1}{2(\mathrm{e}^{\beta}+1)} \end{aligned}$$

and therefore we have $\min_{\omega\in\Omega_2}\mu_{2,\beta}(\omega) = \mu_{2,\beta}(+1,-1)$. Using this and the exact value of λ_3 from Proposition 4.8, we obtain for the distance to stationarity

$$d(t) \le \sqrt{\frac{\mathrm{e}^{\beta}+1}{2}}\left(\frac{\mathrm{e}^{\beta}}{\mathrm{e}^{\beta}+1}\right)^{t}.$$

We see that this bound depends on the inverse temperature β. Therefore, we can suspect that the actual distance to stationarity also depends on β. This is actually true, as can be seen in Figure 12 (left). We see that, for high temperatures (i.e. small values of β), the distance to stationarity drops rapidly to zero. In contrast, for low temperatures (i.e. high values of β), the distance approaches zero much slower. In order to obtain a quantitative statement about the speed of convergence, we consider the mixing times of the chain for different values of $\beta > 0$. Firstly, we try to bound this mixing time using Theorem 2.40 and Corollary 2.49, i.e. we have

$$\log\left(\frac{1}{2\varepsilon}\right)(t_{\mathrm{rel}}-1) \le t_{\mathrm{mix}}(\varepsilon) \le \frac{1}{2}\log\left(\frac{\mathrm{e}^{\beta}+1}{2\varepsilon^2}\right)t_{\mathrm{rel}}$$

with relaxation time $t_{\mathrm{rel}} = \mathrm{e}^{\beta}+1$. In this case, we do not consider the standard

mixing time ($\varepsilon = 1/4$) and rather choose $\varepsilon = 1/10$, because our system is quite small (only $n = 2$ vertices) and therefore mixes quite fast. So we obtain the following bounds for the mixing time:

$$\log(5)\,\mathrm{e}^{\beta} \leq t_{\mathrm{mix}(1/10)} \leq \frac{\mathrm{e}^{\beta}+1}{2} \log\left(50(\mathrm{e}^{\beta}+1)\right). \tag{4.7}$$

These bounds are plotted for varying inverse temperatures β in Figure 12 (right). Additionally, the exact mixing times are plotted as well. We can see that the lower bound is quite accurate and might be a good approximation in contrast to the upper bound.

To summarize, it is quite a challenging task to obtain (good) bounds for the mixing times, let alone compute exact values. Even for a simple system of just two vertices and two possible spin states, we needed a computer to help us with the exhausting computations in order to obtain exact values for the mixing time. Nevertheless, we found out that the mixing time strongly depends on the (inverse) temperature. The system exhibits fast mixing for high temperatures and slow mixing for low temperatures. In the next sections, we will focus on this aspect more as well as how the mixing time depends on the system size n and on the number of colors q regarding the Curie-Weiss Potts model.

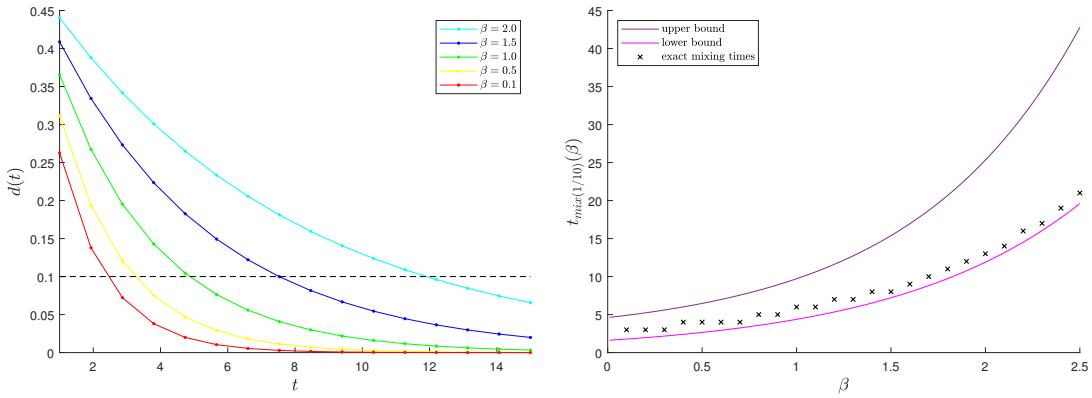

Fig. 12: Temperature dependence of Glauber dynamics for the Curie-Weiss model on Ω_2. *Left*: Distance to stationarity $d(t)$ for different values of $\beta > 0$. The actual distances are only the data points in the plot. The dashed line signals the (mixing) time for which $d(t)$ drops below 1/10. *Right*: Mixing times $t_{\mathrm{mix}(1/10)}$ for different values of $\beta > 0$ as well as the lower and upper bound given in (4.7). The distances and the mixing times were computed using a Python program which will be presented later on.

4.3 Glauber Dynamics for the Curie-Weiss Potts Model

Finally, we examine the Glauber dynamics for the q-state Curie-Weiss Potts model. We start with summarizing the most important results regarding mixing times. We then derive the transition matrix of this Markov chain and finally discuss two computer programs aiming to simulate the Glauber dynamics for the model at hand.

4.3.1 Mixing Time Analysis

In this section, we summarize some recent results regarding the mixing times of the Glauber dynamics for the Curie-Weiss Potts model. These results are primarily taken from the paper "Glauber Dynamics for the Mean-Field Potts Model" by Cuff et al. [CDL12].

Imagine we want to simulate the q-state Curie-Weiss Potts model on Ω_n for large values of n using the Glauber dynamics. We might ask ourselves whether the corresponding distance to stationarity $d_n(t)$ shows the cutoff phenomenon. The following theorem answers this question:

Theorem 4.10. *Let $\beta_{s_1}(q)$ be the first spinodal inverse temperature of the q-state Curie-Weiss Potts model for $q \geq 3$. If $\beta < \beta_{s_1}(q)$, then the Glauber dynamics for this model exhibits the cutoff phenomenon at mixing time*

$$t_{\text{mix}}^{(n)} \sim \frac{1}{2}\left(1 - 2\,\frac{\beta}{q}\right)^{-1} n \log(n)$$

with cutoff window $w_n \in \mathcal{O}(n)$.

Proof. The proof of this theorem is a major contribution of [CDL12]. □

Additionally, one might wonder whether the cutoff phenomenon also occurs for $q = 2$, i.e. in the Glauber dynamics for the Curie-Weiss model. There are some major differences between the models considering the critical inverse temperature $\beta_c(q)$ and the spinodal inverse temperatures $\beta_{s_1}(q)$ and $\beta_{s_2}(q)$. For the Curie-Weiss Potts model ($q \geq 3$), we mentioned that $\beta_{s_1}(q) < \beta_c(q) < \beta_{s_2}(q)$ (see Proposition 3.34), whereas in the Curie-Weiss model ($q = 2$), there exists a critical inverse temperature $\beta_c(2)$ but the spinodal points are absent [CDL12].

Additionally, the Curie-Weiss model exhibits a second-order (or continuous) phase transition [BH19], while on the contrary we proved a first-order phase transition for the Curie-Weiss Potts model.

Remark 4.11. The Glauber dynamics for the Curie-Weiss model ($q = 2$) also exhibits the cutoff phenomenon if $\beta < \beta_c(2) = 1$. In particular, the cutoff phenomenon occurs at mixing time

$$t_{\text{mix}}^{(n)} \sim \frac{1}{2(1-\beta)}\, n \log(n)$$

with cutoff window $w_n \in \mathcal{O}(n)$ [LLP08]. For $\beta \geq \beta_c(2)$, there is no cutoff phenomenon. Hence the situation is qualitatively the same as in the Curie-Weiss Potts case. The only difference is the exact threshold value which depends on the number of colors q.

The following theorem states what happens for $q \geq 3$ if we consider an inverse temperature $\beta \geq \beta_{s_1}(q)$:

Theorem 4.12. *Let $\beta_{s_1}(q)$ be the first spinodal inverse temperature of the q-state Curie-Weiss Potts model for $q \geq 3$. Then the following hold:*

(i) For any $\beta > \beta_{s_1}(q)$, there exist constants $C_1, C_2 > 0$ such that for all $n \geq 1$, the mixing time of the Glauber dynamics is bounded by

$$t_{\text{mix}}^{(n)} \geq C_1 \exp(C_2 n)\,.$$

(ii) If $\beta = \beta_{s_1}(q)$, then there exist constants $\tilde{C}_1, \tilde{C}_2 > 0$ and $N \in \mathbb{N}$ such that for all $n \geq N$, the mixing time of the Glauber dynamics satisfies

$$\tilde{C}_1\, n^{4/3} \leq t_{\text{mix}}^{(n)} \leq \tilde{C}_2\, n^{4/3}\,.$$

In particular, for $\beta \geq \beta_{s_1}(q)$, there is no cutoff phenomenon.

Proof. The proof of this theorem is also a major goal of [CDL12]. □

According to Theorem 4.10 and Theorem 4.12, the mixing time $t_{\text{mix}}^{(n)}$ is at most polynomial in n for $\beta \leq \beta_{s_1}(q)$ and at least exponential in n for $\beta > \beta_{s_1}(q)$. In the first case, we say the Markov chain mixes *rapidly* and in the second case, we say the Markov chain mixes *slowly*. The reason for this *slowdown* depending on the inverse temperature $\beta > 0$ are states that *trap* the Markov chain. These are the *metastable states*, i.e. local minimizers of the free energy function f_β which begin to appear for $\beta > \beta_{s_1}(q)$ (see Figure 5).

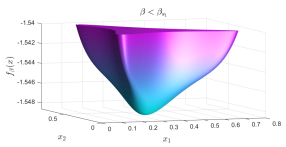

For $\beta < \beta_{s_1}(q)$, i.e. in the absence of metastable states, when only one global minimum of the free energy function f_β exists, the mixing is rapid. For $n \to \infty$, we know, according to Theorem 3.38, that the distribution of the proportions vector $\sigma_{n,\beta}$ converges weakly to the uniform distribution $\delta_{\hat{q}}$. Hence the proportions vector of the Glauber dynamics converges in a short amount of time towards the global minimizer of the free energy function f_β (see Figure 15, left).

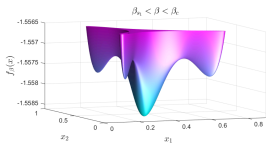

Next let $\beta_{s_1}(q) < \beta < \beta_c(q)$. Then there exists one global minimum and q additional local minima. Now consider an initial configuration $\omega \in \Omega_n$ which has a proportions vector $x(\omega)$ that is close to a local minimizer. Starting the Glauber dynamics from this configuration, it will spend a time that is exponential in n in the neighborhood of this minimizer before escaping to the global minimizer (see Figure 15, right). Since the definition of the mixing time (especially the distance to stationarity) involves the worst case initial distribution, the existence of metastable states will result in (exponentially) slow mixing.

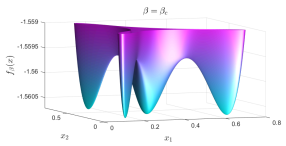

At criticality, i.e. for $\beta = \beta_c$, we observed that the ordered and the disordered phases coexist. In total, the free energy function f_β has $q+1$ global minima, one corresponding to the unordered phase, and the other q corresponding to the ordered phases. This coexistence implies slow mixing because in order to get from one phase to another, one must pass through many states which are exponentially unlikely.

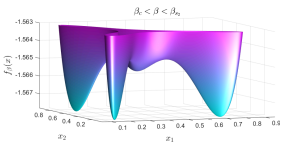

In the inverse temperature regime $\beta_c(q) < \beta < \beta_{s_2}(q)$, we also have slow mixing because of the aforementioned reasons: getting from one ordered phase to another requires passing through many exponentially unlikely states. In particular, the dynamics of the system might get trapped in the local minimum of the free energy function at the center.

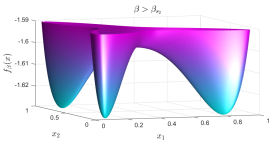

For $\beta > \beta_{s_2}(q)$, the situation is qualitatively the same as at criticality. Instead of $q+1$, we have exactly q global minima, each corresponding to an ordered phase. There are no metastable states that might trap the chain. Again, the reason for slow mixing is the fact that the chain must pass through states with exponential low probability to get from one phase to another.

We might also ask how the mixing behavior changes with temperature for the Glauber dynamics of the Curie-Weiss model, i.e. $q = 2$. To answer this question, we look at the graph of the free energy function f_β for this model given in Figure 13. For all $\beta > 0$, there are no local minimizers of the free energy function in which the Markov chain might get trapped. Hence there are no spinodal inverse temperatures. For $\beta \leq \beta_c(2)$, there exists only one global minimum, hence the mixing is fast. For $\beta > \beta_c(2)$, two phases coexist, i.e. there are two global minima of the free energy function which implies slow mixing. [LLP08]

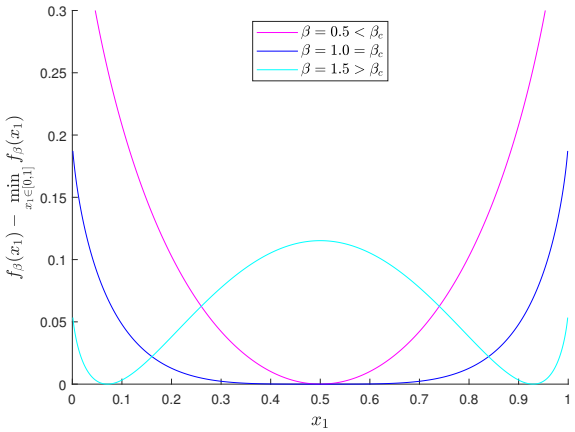

Fig. 13: Free energy function f_β for the Curie-Weiss model as a function of the proportions vector $x = (x_1, x_2)$. We used the map $(x_1, x_2) \mapsto (x_1, 1 - x_1)$ to plot f_β as a one dimensional function of $x_1 \in [0, 1]$ and shifted the graph by $\min_{x_1 \in [0,1]} f_\beta(x_1)$.

4.3.2 Derivation of the Transition Matrix

Since we intend to reproduce some of the results given in the theorems of Section 4.3.1 using simulations, we need to derive an explicit formula for the transition matrix of the Glauber dynamics for the q-state Curie-Weiss Potts model. We will see that the proportions vector introduced in Section 3.2.2 plays a similar role to that of the magnetization in the last section and can be used to simplify the expression of the transition probabilities.

Theorem 4.13. *Let $\mu_{n,\beta}$ be the Gibbs distribution for the q-state Curie-Weiss Potts model on Ω_n with $Q = \{1, \dots, q\}$ and $\beta > 0$. Then the transition matrix $P_n \in \mathbb{R}^{n^q \times n^q}$ of the Glauber dynamics for $\mu_{n,\beta}$ is given by*

$$P_n(\omega, \omega') = \frac{1}{n} \sum_{i=1}^{n} \frac{\exp\left(2\beta x_{\omega_i'}(\omega)\right)}{\sum_{k=1}^{q} \exp\left(2\beta x_k(\omega)\right)} \mathbb{1}_{\Omega_i(\omega)}(\omega') \,, \tag{4.8}$$

where x_k, $k \in Q$, denotes a component of the proportions vector x.

Proof. As in (4.2), we can write the transition probabilities as

$$P_n(\omega, \omega') = \frac{1}{n} \sum_{i=1}^{n} \frac{\mu_{n,\beta}(\omega')}{\mu_{n,\beta}(\Omega_i(\omega))} \mathbb{1}_{\Omega_i(\omega)}(\omega') \,, \tag{4.9}$$

where $\mu_{n,\beta}$ denotes the Gibbs distribution of the Curie-Weiss Potts model. For convenience, we denote $\Lambda := \{1, \dots, n\}$. For now, let us suppose that $\omega' \in \Omega_i(\omega)$ for some $i \in \Lambda$. We can then rewrite the numerator in (4.9): we have

$$\begin{aligned} \mu_{n,\beta}(\omega') &= \frac{1}{Z_{n,\beta}} \exp\left(\frac{\beta}{n} \sum_{u,v \in \Lambda} \delta(\omega_u', \omega_v')\right) \\ &= \frac{1}{Z_{n,\beta}} \exp\left(\frac{\beta}{n} \sum_{u,v \in \Lambda \setminus \{i\}} \delta(\omega_u', \omega_v') + \frac{2\beta}{n} \sum_{u \in \Lambda} \delta(\omega_i', \omega_u') - \frac{\beta}{n} \delta(\omega_i', \omega_i')\right). \end{aligned}$$

Using the fact that $\omega' \in \Omega_i(\omega)$ and the definition of the proportions vector, we

obtain

$$\begin{aligned}\mu_{n,\beta}(\omega') &= \frac{1}{Z_{n,\beta}} \exp\left(\frac{\beta}{n} \sum_{u,v\in\Lambda\setminus\{i\}} \delta(\omega_u,\omega_v) + 2\beta x_{\omega_i'}(\omega) - \frac{\beta}{n}\right) \\ &= \frac{1}{Z_{n,\beta}} \exp\left(\frac{\beta}{n} \sum_{u,v\in\Lambda\setminus\{i\}} \delta(\omega_u,\omega_v) - \frac{\beta}{n}\right) \exp\left(2\beta x_{\omega_i'}(\omega)\right) \\ &= \frac{1}{Z_{n,\beta}} \Theta(\omega) \exp\left(2\beta x_{\omega_i'}(\omega)\right),\end{aligned}$$

where

$$\Theta(\omega) := \exp\left(\frac{\beta}{n} \sum_{u,v\in\Lambda\setminus\{i\}} \delta(\omega_u,\omega_v) - \frac{\beta}{n}\right).$$

We can now use this expression to rewrite the fraction in (4.9) for the case $\omega' \in \Omega_i(\omega)$, yielding

$$P_n(\omega,\omega') = \frac{1}{n}\sum_{i=1}^{n} \frac{\Theta(\omega)\exp\left(2\beta x_{\omega_i'}(\omega)\right)}{\sum_{\zeta\in\Omega_i(\omega)} \Theta(\omega)\exp\left(2\beta x_{\zeta_i}(\omega)\right)} = \frac{1}{n}\sum_{i=1}^{n} \frac{\exp\left(2\beta x_{\omega_i'}(\omega)\right)}{\sum_{k=1}^{q} \exp\left(2\beta x_k(\omega)\right)}.$$

So in general, for all $\omega, \omega' \in \Omega_n$, we obtain

$$P_n(\omega,\omega') = \frac{1}{n}\sum_{i=1}^{n} \frac{\exp\left(2\beta x_{\omega_i'}(\omega)\right)}{\sum_{k=1}^{q} \exp\left(2\beta x_k(\omega)\right)} \mathbb{1}_{\Omega_i(\omega)}(\omega').$$

□

In the next section, we are interested in computing the distance to stationarity for the Glauber dynamics of the q-state Curie-Weiss Potts model on Ω_n for different values of n and q. Since this includes an enormous amount of computations, it will be done by a computer simulation. A central part of this simulation is the computation of the transition matrix P_n which is easily done by using (4.8).

4.3.3 Simulations and Results

Within the framework of this thesis, two simulations of the Curie-Weiss Potts model were programmed using the programming language Python. In this section, we describe the two computer programs, present their results and suggest possibilities for further improvement. The source code of the two computer programs can be found in the Appendix.

The first computer program (see Appendix A.1) aims to compute the distance to stationarity $d_n(t)$ for the Glauber dynamics for the q-state Curie-Weiss Potts model on Ω_n with Gibbs measure $\mu_{n,\beta}$ as stationary distribution. The program works in the following way:
The input parameters are the size of the system $n \geq 1$, the number of colors $q \geq 2$, the inverse temperature $\beta > 0$, a minimal distance to stationarity $d_{\min}$ and a maximal number of time steps $t_{\max}$ for the chain to move forward.
Firstly, the entire state space $\Omega_n = \{1, \dots, q\}^n$ is generated. This is needed to construct the transition matrix P_n in the next step. Therefore all q^{2n} transition probabilities $P_n(\omega, \omega')$ are computed using Theorem 4.13, i.e. for $\omega, \omega' \in \Omega_n$, we have

$$P_n(\omega, \omega') = \frac{1}{n} \sum_{i=1}^{n} \frac{\exp\left(2\beta x_{\omega_i'}(\omega)\right)}{\sum_{k=1}^{q} \exp\left(2\beta x_k(\omega)\right)} \mathbb{1}_{\Omega_i(\omega)}(\omega') \,, \tag{4.10}$$

with x denoting the proportions vector.
After the transition matrix P_n is completely constructed, the entire Gibbs distribution $\mu_{n,\beta}$ is also computed since we are interested in the distance to stationarity $d_n(t)$ for successive times t. This will be done using Proposition 2.24, i.e. we use

$$\begin{aligned} d_n(t) &= \max_{\omega \in \Omega_n} \left\| P_n^t(\omega, \cdot) - \mu_{n,\beta} \right\|_{\mathrm{TV}} \\ &= \frac{1}{2} \max_{\omega \in \Omega_n} \sum_{\omega' \in \Omega_n} \left| P_n^t(\omega, \omega') - \mu_{n,\beta}(\omega') \right| . \end{aligned} \tag{4.11}$$

This procedure is done for $t = 1$, then the resulting distance to stationarity $d_n(1)$ is written in a TXT file. After that, the program goes one time step further, i.e. we obtain the new transition matrix P_n^t by simple matrix multiplication:

$$P_n^t = P_n^{t-1} \cdot P_n \,,$$

where P_n^{t-1} denotes the transition matrix of the previous time step. The distance to stationarity of the current time step is then calculated again. All this is repeated until the current distance to stationarity $d_n(t)$ is smaller than the threshold $d_{\min}$ or the number of time steps t exceeds the input parameter $t_{\max}$. At the end, we have a TXT file consisting of a sequence of distances to stationarity for a certain system size n, number of colors q and inverse temperature β.

Theoretically, we should be able to see the cutoff phenomenon using this program. We chose $\beta = 1$ and considered $q \in \{2, \dots, 5\}$. Looking at Table 1, we see that $\beta < \beta_{s_1}(q)$ for $q \in \{3, 4, 5\}$. Hence Theorem 4.10 tells us that we can expect to see the cutoff phenomenon for large enough n. For $q = 2$ on the other hand, we have $\beta = \beta_c(2)$ and according to Remark 4.11, there will be no cutoff phenomenon.

The results of the simulation are presented in Figure 14 on the next page. The computed distances to stationarity were saved in a TXT file and afterwards plotted using MATLAB. By looking at the plots, we clearly see that no cutoff phenomenon appears for any value of q. In fact, due to the enormously large running time of this program, we were only able to produce graphs of the distance to stationarity $d_n(t)$ for relatively small values of n. Indeed, there are several large sums and the transition matrix also becomes quite large for increasing values of n and q. As an example, let us suppose, we have $n = 20$ vertices and consider $q = 3$ colors. Then the cardinality of the state space is given by

$$|\Omega_n| = q^n \approx 3.49 \cdot 10^9 \,.$$

So the first sum in (4.10) and the sum in (4.11) would contain approximately 3.49 billion summands. Additionally, the transition matrix P_{20} would have $|\Omega_n|^2 \approx 1.22 \cdot 10^{19}$ entries. Hence matrix multiplication is connected with a huge computational effort. All this results in the long running time of this program for bigger values of n. If we could run the program longer, i.e. for large values of n, then we should be able to see the cutoff phenomenon if the appropriate conditions are satisfied.

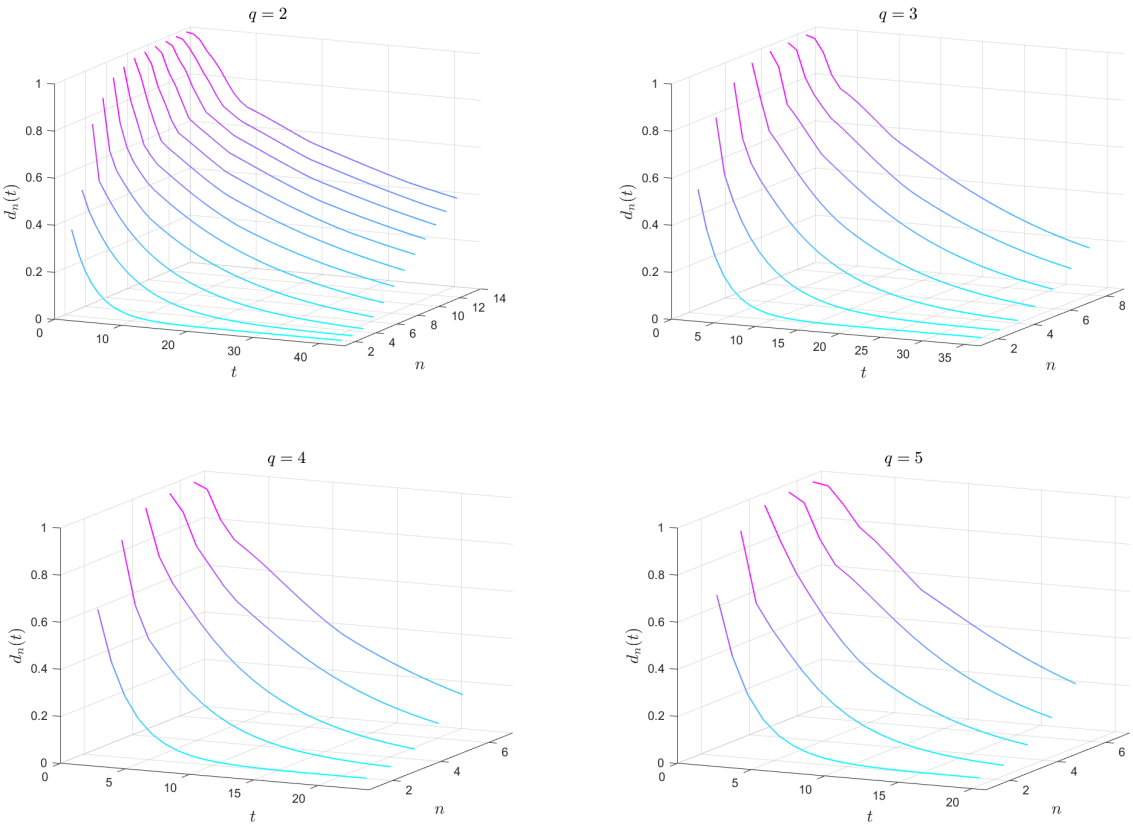

Fig. 14: Distance to stationarity $d_n(t)$ for a sequence of Glauber dynamics $(\Omega_n, P_n, \mu_{n,\beta})_{n\geq 2}$ of the q-state Curie-Weiss Potts model at inverse temperature $\beta = 1$ for selected values of q. Due to the enormous computational effort, only the distances $d_n(t)$ for small n could be determined. Keep in mind that $d_n(t)$ is only defined for integer values of t, i.e. the data points are only connected for a better visibility.

The second computer program (see Appendix A.2) aims to visualize the time-evolution of the proportions vector $x \in \mathcal{S}$ for the Glauber dynamics for the Curie-Weiss Potts model. In Section 4.3.1, we saw that the speed of convergence of the Glauber dynamics is connected to the free energy function f_β, in particular with the location of its local minima. Considering the case $q \geq 3$, we have rapid mixing if $\beta < \beta_{s_1}(q)$ and slow mixing for $\beta \geq \beta_{s_1}(q)$. We want to see whether the simulation of the Glauber dynamics yields this same result. This simulation works in the following way:

Firstly, the input parameters are specified, i.e. we choose the number of vertices n, the number of colors q, the inverse temperature $\beta > 0$ and a maximal number of time steps $t_{\max}$. Additionally we must specify an initial q-dimensional proportions

vector x_0. According to this proportions vector, the computer program constructs an initial configuration $\omega_0 \in \Omega_n$ with proportions vector $x(\omega_0)$ equal (or at least close) to x_0. Starting with $\omega = \omega_0$, our program (and in particular the Glauber dynamics) proceeds as follows:

(1) Choose a vertex $i \in \{1, \dots, n\}$ uniformly at random.

(2) Choose a new configuration $\omega' \in \Omega_n$ according to the probability distribution

$$\mu_{n,\beta}\Big(\omega' \mid \Omega_i(\omega)\Big) = \frac{\exp\Big(2\beta x_{\omega_i'}(\omega)\Big)}{\sum_{k=1}^{q} \exp\Big(2\beta x_k(\omega)\Big)} \mathbb{1}_{\Omega_i(\omega)}(\omega') \,.$$

(3) Compute the proportions vector $x(\omega')$ and the free energy function $f_\beta\Big(x(\omega')\Big)$. Save these results in a TXT file.

This sequence of commands is repeated $t_{\max}$ times after which the computer program terminates.

For our simulations, we chose $q = 3$ so that we are able to portray the proportions vector $x = (x_1, x_2, x_3)$ and the value of the free energy function $f_\beta(x)$ in the same plot. Additionally, only every tenth proportions vector and value of the free energy function is saved in order to reduce the total amount of data. As mentioned before, we ran two simulations: one for $\beta < \beta_{s_1}(3)$ (subcritical regime) and one for $\beta > \beta_{s_1}(3)$ (supercritical regime) in order to show rapid and slow mixing. The results are shown in Figure 15 on the next page using MATLAB.

We can see that, for $\beta = 1 < \beta_{s_1}(3)$, the dynamics converges quickly towards the global minimizer (Figure 15, left). In the other case, i.e. for an inverse temperature $\beta_{s_1} < \beta = 1.381 < \beta_c(3)$, the Markov chain starts close to a local minimizer according to the initial proportions vector $x_0 = (0.2, 0.2, 0.6)$. Hence the dynamics gets trapped near this metastable state and spends lots of time there before finally escaping to the global minimizer in the center (see Figure 15, right). So the simulations show exactly the behavior that we expected and talked about in the last sections.

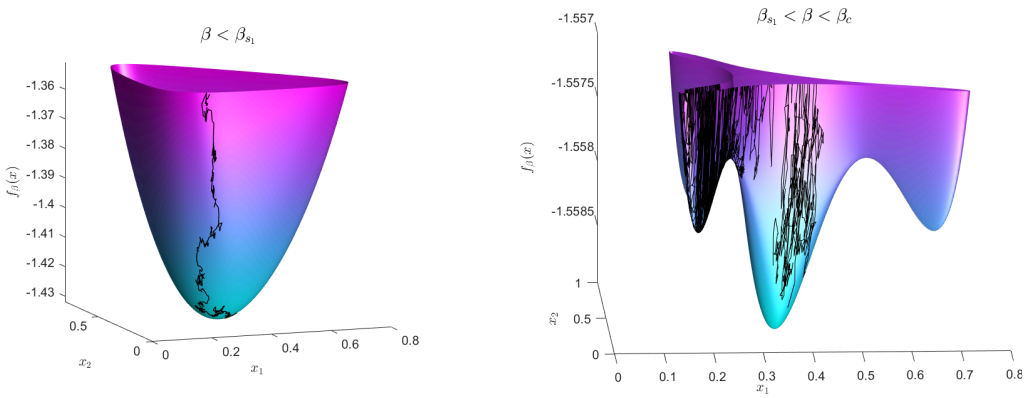

Fig. 15: The colored surface represents the free energy function f_β of the 3-state Curie-Weiss Potts model as function of the proportions vector $x \in \mathcal{S}$. The black curve marks the time-evolution of the proportions vector x of the Glauber dynamics for $\mu_{500,\beta}$. *Left:* In the subcritical regime (here $\beta = 1$), the proportions vector x reaches the global minimizer very fast, in fact $t \approx 5000$ time steps are needed starting from $x_0 = (0.2, 0.1, 0.7)$. *Right:* In the supercritical regime (here $\beta = 1.381$), the proportions vector x spends a great amount of time near a local minimizer before reaching the global minimizer. In the plot, $n \approx 55000$ time steps are shown with initial proportions vector $x_0 = (0.2, 0.2, 0.6)$.

A Python Programs

A.1 Program 1: Distance to Stationarity

```
# -*- coding: utf-8 -*-
"""
Distance to Stationarity
of the Glauber Dynamics
for the Curie-Weiss Potts Model
"""

import numpy as np
import random as rand
import copy
import itertools

global n,q,beta,d_min

def kronecker_delta(x,y):
    if x==y:
        return 1
    else:
        return 0

def in_possible_Omega(x,i,y):
    l=True
    for j in range(n):
        if j !=i:
            if x[j]!=y[j]:
                l=False
                break
    return l

def prop_vector (omega,i):
    count=0
    for j in range(n):
        count=count+kronecker_delta(omega[i],omega[j])
    return count/n

def probs_q(omega,i):
    prob_distr=[]
    omega_bar=copy.deepcopy(omega)
    for k in range(1,q+1):
        omega_bar[i]=k
        prob_distr.append(np.exp(beta*2*prop_vector(omega_bar,i)))
    N=sum(prob_distr)
    for p in range(len(prob_distr)):
        prob_distr[p]=prob_distr[p]/N
    return prob_distr

def transition_prob(x,i,y):
    if in_possible_Omega(x,i,y)==False:
```

```
49          return 0
50      else:
51          r=probs_q(x,i)
52          return r[int(y[i]-1)]
53
54  def state_space():
55      Q=np.arange(1,q+1)
56      l=[p for p in itertools.product(Q, repeat=n)]
57      l=np.array(l)
58      return l
59
60  def transition_matrix_entry(x,y):
61      p=0
62      for i in range(n):
63          p=p+transition_prob(x,i,y)
64      return p/n
65
66  def transition_matrix(Omega):
67      P=[]
68      for x in Omega:
69          P_0=[]
70          for y in Omega:
71              P_0.append(transition_matrix_entry(x,y))
72          P.append(P_0)
73      return P
74
75  def gibbs_measure(Omega):
76      l=[]
77      for omega in Omega:
78          count=0
79          for i in range(n):
80              for j in range(n):
81                  count=count+kronecker_delta(omega[i],omega[j])
82          l.append(np.exp(beta/n*count))
83      s=sum(l)
84      for k in range(len(l)):
85          l[k]=l[k]/s
86      return l
87
88  def tvd(Omega,omega_0,P,mu):
89      P=np.array(P)
90      a=0
91      for omega in Omega:
92          i=Omega.index(omega)
93          a=a+abs(P.item((Omega.index(omega_0),i))-mu[i])
94      return 0.5*a
95
96  def distance(Omega,P,mu):
97      l=[]
98      Omega=Omega.tolist()
99      for omega_0 in Omega:
100         l.append (tvd(Omega,omega_0,P,mu))
101     return max(l)
```

```
102
103 def distance_timeline(Omega,P,mu,t_max,file):
104     A=P
105     for t in range(1,t_max+1):
106         if t==1:
107             h=distance(Omega,A,mu)
108             file.write(str(h)+'\n')
109         else:
110             A=np.matmul(A,P)
111             h=distance(Omega,A,mu)
112             file.write(str(h)+'\n')
113             if h<=d_min:
114                 break
115
116 file=open("results.txt", "a+")
117 n=5
118 q=3
119 beta=1
120 d_min=0.1
121 t_max=50
122 file.write('\n'+'n='+str(n)+'\n')
123 file.write('q='+str(q)+'\n\n')
124 file.write('beta='+str(beta)+'\n\n')
125
126 Omega=state_space()
127 P=transition_matrix(Omega)
128 mu=gibbs_measure(Omega)
129 distance_timeline(Omega,P,mu,t_max,file)
130 file.close()
```

A.2 Program 2: Time-Evolution of the Proportions Vector

```
# -*- coding: utf-8 -*-
"""
Time Evolution of the Proportions Vector
for the Curie-Weiss Potts Model

"""

import numpy as np
import random as rand
import copy
import itertools

global n,q, beta,beta_n

def indicator_fct(x,y):
    if x==y:
        return 1
    else:
        return 0

def random_initial_configuration():
    omega=np.zeros(n)
    for i in range(n):
            omega[i]=rand.randint(1, q)
    return omega

def initial_configuration(proportions):
    omega=[]
    for k in range(1,q):
        for l in range(int(n*proportions[k-1])):
            omega.append(k)
    for m in range (n-len(omega)):
        omega.append(q)
    return omega

def counter (omega,v):
    count=0
    for i in range(n):
        count=count+indicator_fct(omega[i],omega[v])
    return count

def probs_q(omega,v):
    prob_distr=[]
    omega_bar=copy.deepcopy(omega)
    for q_i in range(1,q+1):
        omega_bar[v]=q_i
        prob_distr.append(np.exp(beta_n*(2*counter(omega_bar,v))))
    N=sum(prob_distr)
    for k in range(len(prob_distr)):
        prob_distr[k]=prob_distr[k]/N
    return prob_distr
```

```
52
53 def glauber_dyn(omega):
54     v=rand.choices(np.arange(n))
55     r=rand.choices(np.arange(1,q+1),probs_q(omega,v))
56     omega[v]=r[0]
57     return omega
58
59 def prop_vec(omega):
60     prop_vec=[]
61     for i in range(1,q):
62         count_i=0
63         for j in range(n):
64             if omega[j]==i:
65                 count_i=count_i+1
66         prop_vec.append(count_i)
67     prop_vec.append(n-sum(prop_vec))
68     return np.array(prop_vec)/n
69
70 def free_energy(prop_vec):
71     f=0
72     for s in prop_vec:
73         if s==0:
74             k=0
75         else:
76             k=s*np.log(s)
77         f=f+k-beta*s*s
78     prop_vec[-1]=f
79     return prop_vec
80
81 n=500
82 q=3
83 beta=1.381
84 beta_n=beta/n
85 t_max=100000
86 x_0=[0.2,0.2,0.6]
87
88 X=open("res_X.txt", "a+")
89 Y=open("res_Y.txt", "a+")
90 F=open("res_F.txt", "a+")
91 omega=np.array(initial_configuration(x_0))
92 for i in range(t_max):
93     if i%10==0:
94         p_v=free_energy(prop_vec(omega))
95         X.write(str(p_v[0])+'\n')
96         Y.write(str(p_v[1])+'\n')
97         F.write(str(p_v[2])+'\n')
98     omega=glauber_dyn(omega)
99 X.close()
100 Y.close()
101 F.close()
```

B Nomenclature

A^B	set of all functions from A to B
$\lvert A\rvert$	cardinality of A
$a \mid b$	a divides b
argmax, argmin	argument of the maximum, minimum
β	inverse temperature
β_c	critical inverse temperature
β_{s_1}, β_{s_2}	first spinodal and second spinodal inverse temperature
$\mathcal{C}_n$	complete graph with n vertices
χ_A	characteristic polynomial of the square matrix A
$\det A$	determinant of the square matrix A
$\gcd M$	greatest common divisor of all $m \in M \subset \mathbb{N}$
δ_ω	Dirac mass at ω
$\delta_\omega(\omega') = \delta(\omega, \omega')$	Kronecker delta
$d(t)$	distance to stationarity at time t
exp	natural exponential function
$\mathbb{E}[X]$, $\mathbb{E}_\pi[X]$	expectation of X (according to $\pi \in \mathscr{M}_1(\Omega)$)
f_β	free energy function
$G = (\Lambda, \mathscr{E})$	graph G with vertex set Λ and edge set $\mathscr{E}$
$\Gamma_{\beta,q}$	set of global minimizers of f_β
$\hat{\gamma}$	absolute spectral gap
$H_{n,\beta}$	Hamiltonian, total energy
$\tilde{H}$	energy density
log	natural logarithm
I_n	identity matrix of size n
J	interaction constant
λ	eigenvalue
$\hat{\lambda}$	$= \max\{\lvert\lambda\rvert \neq 1 \colon \lambda \text{ is an eigenvalue of } P\}$
M	total magnetization
m	magnetization density
max, min	maximum, minimum
$\mathscr{M}_1(\Omega)$	set of all probability measures on $(\Omega, \mathscr{P}(\Omega))$
$\mu_{n,\beta}$	Gibbs distribution
$\mathbb{N}$, $\mathbb{N}_0$	$\mathbb{N} = \{1, 2, 3, \ldots\}$, $\mathbb{N}_0 = \mathbb{N} \cup \{0\}$
$\mathcal{N}_i$	set of nearest neighbors of $i \in \Lambda$
$\binom{n}{k}$	binomial coefficient
$\nabla f(x)$	$= \left(\frac{\partial f}{\partial x_1}(x), \ldots, \frac{\partial f}{\partial x_n}(x)\right)$, nabla, gradient of f
$\mathcal{O}(f(n))$, $o(f(n))$	asymptotic Landau notation
Ω, Ω_n	state space (depending on n)
ω, ω', ζ	state (configuration), i.e. an element of the state space

$\mathbb{P}(A)$	probability of the event A
$\mathbb{P}(A\|B)$	probability of A conditioned B
$P(\omega, \omega')$	transition probability from state ω to state ω'
$\mathscr{P}(A)$	power set of A
φ	eigenvector (eigenfunction)
π	(in most contexts) stationary distribution
Ψ	free energy in the thermodynamic limit
Ψ_n	finite-volume free energy
Q	set of all colors, in general $Q = \{1, \dots, q\}$
$\mathbb{R}$	set of real numbers
$\mathbb{R}_+$	set of positive real numbers, i.e. $\{x \in \mathbb{R} \mid x \geq 0\}$
$\mathbb{R}^{n\times n}$	set of real square matrices of size n
L	latent heat
$\mathscr{L}$	Lagrangian function
S	$= S(\mu)$, entropy of the probability measure $\mu \in \mathscr{M}_1(\Omega)$
$\tilde{S}$	entropy density
$\mathcal{S}$	set of probability vectors
$\mathrm{supp}(\mu)$	support of the measure μ
$\sigma_{n,\beta}$	distribution of the fractions vector x under $\mu_{n,\beta}$
T	absolute temperature
$t_{\mathrm{mix}}(\varepsilon)$	ε-mixing time
t_{mix}	$= t_{\mathrm{mix}(1/4)}$
t_{rel}	relaxation time
$\mathscr{T}(\omega)$	$= \{t \in \mathbb{N} \mid P^t(\omega, \omega) > 0\}$
$\mathcal{U}_\Omega$	uniform distribution on Ω
w_n	cutoff window of the n-th Markov chain
$x = x(\omega)$	proportions vector
$(X_t)_{t\geq 0}$	discrete time Markov chain
ξ	order parameter
$Z_{n,\beta}$	partition function
$\mathbb{1}_A(\omega)$	indicator function
$\lvert\cdot\rvert$	absolute value
$\lceil\cdot\rceil$	rounded up
$\langle\cdot,\cdot\rangle$	standard inner product
$\langle\cdot,\cdot\rangle_\pi$	inner product with respect to $\pi \in \mathscr{M}_1(\Omega)$
$\mu_n \Rightarrow \mu$	weak convergence of measures
$X \sim \mu$	the law of X is μ
$f(n) \sim g(n)$	f and g are asymptotically equivalent
$\lVert\cdot\rVert_p$	$\ell^p(\pi)$-norm
$\lVert\cdot\rVert_\infty$	maximum norm
$\lVert\mu - \nu\rVert_{\mathrm{TV}}$	total variation distance of $\mu, \nu \in \mathscr{M}_1(\Omega)$

References

[AdF03] C. Andrieu, N. de Freitas, A. Doucet and M. I. Jordan. An Introduction to MCMC for Machine Learning. *Machine Learning*, 50: 5 – 43, 2003.

[AB07] S. Arora and B. Barak. *Computational Complexity: A Modern Approach*. Cambridge University Press, 2007.

[AD86] D. Aldous and P. Diaconis. Shuffling Cards and Stopping Times. *The American Mathematical Monthly*, 93(5): 333 – 348, 1986.

[Bax73] R. J. Baxter. Potts model at the critical temperature. *Journal of Physics C: Solid State Physics*, 6: 445 – 448, 1973.

[Bax07] R. J. Baxter. *Exactly Solved Models in Statistical Mechanics*. Dover Publications Inc., 2007.

[BBL83] A. Baracca, M. Bellesi, R. Livi, R. Rechtman and S. Ruffo. On the mean field solution of the Potts model. *Physics Letters A*, 99(4): 156 – 160, 1983.

[BD92] D. Bayer and P. Diaconis. Trailing the Dovetail Shuffle to its Lair. *The Annals of Applied Probability*, 2(2): 294 – 313, 1992.

[BH19] A. J. Berlinsky and A. B. Harris. *Statistical Mechanics: An Introductory Graduate Course*. Springer, 2019.

[BHP17] R. Basu, J. Hermon and Y. Peres. Characterization of cutoff for reversible Markov chains. *The Annals of Probability*, 45(3): 1448 – 1487, 2017.

[BZ20] A. Barbu and S.-C. Zhu. *Monte Carlo Methods*. Springer, 2020.

[CDL12] P. Cuff, J. Ding, O. Louidor, E. Lubetzky, Y. Peres, and A. Sly. Glauber Dynamics for the Mean-Field Potts Model. *Journal of Statistical Physics*, 149(3): 432 – 477, 2012.

[Cra07] N. J. Crawford. *Mean Field Theories and Models of Statistical Physics*. Dissertation, Los Angeles, 2007.

[CS09] S.-C. Chang and R. Shrock. Some exact results on the Potts model partition function in a magnetic field. *Journal of Physics A: Mathematical and Theoretical*, 42(38): 1 – 5, 2009.

[DGM04] S.N. Dorogovtsev, A.V. Goltsev and J.F.F. Mendes. Potts model on complex networks. *Physics of Condensed Matter*, 38(2), 177 – 182, 2004.

[Dia96] P. Diaconis. The cutoff phenomenon in finite Markov chains. *Proceedings of the National Academy of Sciences of the United States of America*, 93: 1659 – 1664, 1996.

[ENR80] R. S. Ellis, C. M. Newman and J. S. Rosen. Limit Theorems for Sums of Dependent Random Variables Occuring in Statistical Mechanics - II. Conditioning, Multiple Phases, and Metastability. *Zeitschrift für Wahrscheinlichkeitstheorie und verwandte Gebiete*, 51: 153 – 169, 1980.

[EW90] R. S. Ellis and K. Wang. Limit theorems for the empirical vector of the Curie-Weiss Potts model. *Stochastic Processes and their Applications*, 35: 59 – 79, 1990.

[FV17] S. Friedly and Y. Velenik. *Statistical Mechanics of Lattice Systems: A Concrete Mathematical Introduction*. Cambridge University Press, 2017.

[Geo15] H. - O. Georgii. Stochastik: *Einführung in die Wahrscheinlichkeitstheorie und Statistik*. Walter De Gruyter GmbH, 2015.

[GG92] F. Graner and J. Glazier. Simulation of Biological Cell Sorting Using a Two-Dimensional Extended Potts Model. *Physical Review Letters*, 69(13): 2013 – 2016, 1992.

[GRW10] D. Gandolfoa, J. Ruiza, and M. Woutsb. Limit theorems and coexistence probabilities for the Curie–Weiss Potts model with an external field. *Stochastic Processes and their Applications*, 120: 84 – 104, 2010.

[Kle13] A. Klenke. *Wahrscheinlichkeitstheorie*. Springer Spektrum, 2013.

[KMS54] T. Kihiara, Y. Midzuno and T. Shizume. Statistics of Two-Dimensional Lattices with Many Components. *Journal of the Physical Society of Japan*, 9(5): 681 – 687, 1954.

[LLP08] D. A. Levin, M. J. Luczak and Y. Peres. Glauber dynamics for the Mean-field Ising Model: cut-off, critical power law, and metastability. *Probability Theory and Related Fields*, 148: 1 – 40, 2008.

[LPW09] D. A. Levin, Y. Peres, and E. L. Wilmer. *Markov Chains and Mixing Times*. American Mathmatical Society, 2008.

[OO18] A. A. Opoku and G. Osabutey. Multipopulation Spin Models: A View from Large Deviations Theoretic Window. *Hindawi Journal of Mathematics*, Volume 2018.

[SH96] N. J. Savill and P. Hogeweg. Modelling Morphogenesis: From Single Cells to Crawling Slugs. *Journal of Theoretical Biology*, 184(3), 229 – 235, 1996.

[Sha48] C. E. Shannon. A Mathematical Theory of Communication. *Bell System Technical Journal*, 27(4): 623 – 666, 1948.

[Sin93] A. Sinclair. *Algorithms for random generation and counting: a Markov chain approach*. Boston, MA: Birkhäuser, 1993.

[SM13] A. Szabó and R. M. H. Merks. Cellular Potts modeling of tumor growth, tumor invasion, and tumor evolution. *Frontiers in Oncology*, 3, 2013.

[Tsc18] P. Tschisgale. *Einige Eigenschaften des Potts-Modells*. Bachelor thesis (unpublished), Potsdam, 2018.

[Wu82] F. Y. Wu. The Potts model. *Reviews of Modern Physics*, 54(1): 235 – 268, 1982.

Declaration of Originality

I herewith declare that I have written the present Master thesis titled *Introduction to the Glauber Dynamics for the Curie-Weiss Potts Model* independently. No other sources or aids than those stated in the bibliography were used. I marked all passages and sentences in my work that were taken from other sources clearly as such and named the exact source.
Furthermore, I confirm that this work has never been before submitted at this or any other university, nor has it been published.

Kiel, 30th September 2020 (Paul Tschisgale)